THE ROLE OF MIR-218-5P AND TGF-β SIGNALING IN HUMAN PLACENTA FROM NORMAL AND COMPROMISED PREGNANCIES

JELENA BRKIĆ

A DISSERTATION SUBMITTED TO
THE FACULTY OF GRADUATE STUDIES
IN PARTIAL FULFILMENT OF THE REQUIREMENTS
FOR THE DEGREE OF

DOCTOR OF PHILOSOPHY

GRADUATE PROGRAM IN BIOLOGY
YORK UNIVERSITY
TORONTO, ONTARIO

JANUARY 2017

ABSTRACT

Placenta is critical during pregnancy, forming the interface between mother and fetus. A key process in placental development is the differentiation and invasion of extravillous trophoblast cells (EVT). While some EVT invade the uterine interstitial space, a subset upregulates endovascular genes forming the endovascular EVT (enEVT) that invade decidual vessels. EnEVT are critical mediators in spiral artery remodeling (SAR), which is essential for proper placentation. Preeclampsia (PE) is a serious hypertensive disorder that can manifest during pregnancy. The cause of PE is unclear; however shallow EVT invasion, inadequate enEVT differentiation and SAR play crucial roles. The transforming growth factor-β (TGF-β) family is known to regulate placentation and has been implicated in the pathogenesis of PE. Specifically, TGF-βs and Nodal are upregulated in PE placenta and they exert potent inhibitory effects on EVT invasion. MicroRNAs (miRNA) are small non-coding RNAs that regulate most physiological processes and are dysregulated in PE. In this study, we investigated the role of miR-218-5p in modulating TGF-β signaling and placental development and their contribution to the pathogenesis of PE. The models used in our study included a human trophoblast cell line (HTR8/SVneo), first trimester placenta and decidua tissues, and clinical samples. Our findings indicate that the expression of miR-218-5p was downregulated in PE and upregulated during second trimester in healthy tissues. Overexpression of miR-218-5p promoted trophoblast migration and invasion. Furthermore, miR-218-5p upregulated key genes involved in enEVT differentiation and accelerated SAR in vitro. Using a TGF-β signaling reporter, we found that basal and TGF-β-induced transcriptional activities were

strongly inhibited by mir-218-1. TGF-β2, Smad2, and Smad3 are predicted miR-218-5p targets, and their expression was inhibited by miR-218-5p. Both TGF-β2 and Smad2 were able to partly rescue the miR-218-5p phenotype. Interestingly, knockdown of Smad2 promoted, while knockdown of Smad3 inhibited, invasion and enEVT differentiation, suggesting they play differential roles in placentation. Additionally, the level of pSmad3 is strikingly downregulated in PE placentas. In conclusion, our study demonstrates that TGF-β signaling in the maternal-fetal interface is modulated by miR-218-5p and disruption of the balance between miR-218-5p and TGF-β signaling may lead to abnormal placental development and pregnancy complications.

ACKNOWLEDGMENTS

First of all I would like to express my sincere gratitude to my supervisor Dr. Chun Peng for her continued guidance and support. You have provided me with great opportunities over the years that have challenged me, allowed me to present my work internationally, and receive invaluable training to advance my skills and knowledge.

I would also like to give my heartfelt thank you to my supervisory committee. Dr. Tara Haas, you have supported me from my first year at York. Thank you for all of your guidance, feedback, and encouragement. Dr. Vivian Saridakis, thank you for all of our talks, your time, kindness, and support. To my ex-committee member, Dr. Suraj Unniappan, despite the short time you have truly made me feel encouraged and motivated, thank you for all of your time and support.
In addition, I would like to say thank you to my previous mentor, Dr. Heyu Ni, for being instrumental in my early development and guiding me to this wonderful project I have spent a long time investigating.

Next, I would like to thank all of the past and present members of our lab for everything we have been through together and all of their amazing support. I have shared many memories with each of you and I will cherish those times. I would like to further thank several people that have a become my dearest friends:

Michele (RIP), your support and friendship over the years will never be forgotten. I wish I could share this moment with you, I know you would have been truly happy for me.

Stefanie, you have been with me from day one, and we both know how long that is. You have set an example that I aspired to reach, and I am grateful for how much I have grown because of that. Thank you for your guidance, friendship, and especially through the writing of this thesis.

Mohamed, my husband No.2

Marlee, thank you for everything we have been through, you are one of a kind. Thank you for encouraging me all the way and all of your time and effort during editing.

Dayana, what can I say? I don't think I would have seen the end of this without you there by my side. You have been instrumental to me seeing this to the end. I thank you for your kindness, motivation, and genuine friendship. Also, thank you for the many hours of editing and your comments; they have truly been a blessing.

Heyam and Jake, thank you for being great desk neighbors and sweet friends over the years. I hope you take miR-218 to new heights and wish you all the success in the future.

Lubna, thank you for your guidance, especially in my first year, your sweetness and kindness are rare to find.

Gang, thank you for your happy face, and supporting me over the years.

Guodong, thank you for all of your hard work in starting my project.

Xin and Wenyi, thank you for all the things you have taught me, I hope we see eachother again.

Rina, Yara, Adilya, Queenie: thank you for your friendship and all the great memories.

Uzma, Christina, Shahin: thank you for our talks and being great colleagues to me.

A special thanks to the undergrads I shared the most laughs with: Eilyad, Dan, Jackie, Amy, Sarah, and Stefano.

I would like to thank the many friends I have made at the Lye and Kingdom lab through our collaboration. Caroline, your mentorship over these last few years has been vital to my growth and success. I am eternally grateful to your time, attention, and friendship. Mellissa, Ella, Oksana, Zhang, Dora, Jan, and Kristin: thank you for always making me feel welcome and all of our great discussions. Also, thank you to Dragica from the BioBank for all our great talks and her friendship.

Next, I would like to thank my friends and family for their unconditional love and support.

Michelle, thank you for your unwavering support, and your genuine friendship. You never doubt my strength and remind me of it when I need it most.
Ted, thank you for your friendship and support over the years. You are truelly a “djerk”.
Al, thank you to you and your family for always showing me love and support.

To my mom and dad: thank you for never doubting me, for supporting me through every aspect of my life, for being my rock. This entire journey would not be possible if I wasn’t blessed to have you on my side.

To my sister and Vince: thank you for always cheering for me, and supporting me in whatever I set out to achieve.

To Zvezdana, Sonja (mala), Masha: thank you for encouraging me over the years, and celebrating with me all of my little and big wins. Also, I would like to give a special thank you to my aunt that gave me my first steps in Science many years ago.

To Sonja and Dan: although you weren’t always close by, I always felt your love and support. Thank you for always being there for me.

To my in-laws - Milan, Božana, i Draško: kako da vam se zahvalim na vašoj nepokolebljivoj podršci? Bez vašeg strpljenja i bodrenja ovaj posao bi bio nemoguc. Hvala vam na svemu od srca.

Lastly, I would like to thank my husband and best friend. You have been by my side through all the best moments and through the darkest times. With your support and love I know I can achieve whatever my heart desires. You have spent so many late nights and weekends in the lab with me that this degree will forever be partly yours ☺.

Chapter 2 Acknowledgments

We thank Dr. Charles Graham for providing us with HTR8/SVneo cells.
We thank Dr. J. Wrana and Dr. M. Whitman for providing us with the pAR3-Lux and FAST2 constructs, respectively.

We thank the donors, RCWIH BioBank, the Lunenfeld-Tanenbaum Research Institute, and the Mount Sinai Hospital/UHN Department of Obstetrics and Gynecology for the human specimens used in this study.

We also thank Dr. Rosman from York Central Hospital and the donors that provided term umbilical cords for the isolation of HUVEC used in this study.

This work was supported by grants from the Canadian Institutes of Health Research to Dr. Chun Peng, and the Ontario Graduate Scholarships, the Queen Elizabeth II. Graduate Scholarship in Science and Technology, and the Susan Mann Dissertation Scholarship to Jelena Brkic.

Chapter 3 Acknowledgments

We thank Dr. Charles Graham for providing us with HTR8/SVneo cells.
We thank Dr. Yan Chen for providing us with the Smad2 and Smad3 wild type constructs.

We thank the donors, RCWIH BioBank, the Lunenfeld-Tanenbaum Research Institute, and the Mount Sinai Hospital/UHN Department of Obstetrics and Gynecology for the human specimens used in this study.

This work was supported by grants from the Canadian Institutes of Health Research to Dr. Chun Peng, and the Ontario Graduate Scholarships, the Queen Elizabeth II Graduate Scholarship in Science and Technology, and the Susan Mann Dissertation Scholarship to Jelena Brkic.

TABLE OF CONTENTS

LIST OF TABLES

CHAPTER 2:

CHAPTER 3:

LIST OF FIGURES

CHAPTER 1:

CHAPTER 2:

CHAPTER 3:

CHAPTER 4:

LIST OF ABBREVIATIONS

CTB	cytotrophoblast
STB	syncytiotrophoblast
EVT	extravillous trophoblast
hCG	human chorionic gonadotropin
hPL	human placental lactogen
HLA	human leucocyte antigen
cAMP	cyclic adenosine monophosphate
PKA	protein kinase A
GCM-1	glial cells missing-1
iEVT	interstitial extravillous trophoblast
enEVT	endovascular extravillous trophoblast
uPA	urokinase-type plasminogen activator
MMP	matrix metalloproteinase
PAL	plasminogen activator inhibitor
TIMP	tissue inhibitor of metalloproteinase
MHC	major histocompatibility complex
dNK	decidua-specific natural killer
ILIR	inhibitory leukocyte immunoglobulin-like receptor
KIR	immunoglobulin-like receptor
VCSM	vascular smooth muscle cell
VE-Cadherin	vascular endothelial cadherin
PECAM1	Platelet And Endothelial Cell Adhesion Molecule 1
NCAM	Neural cell adhesion molecule
PE	preeclampsia
VEGF	vascular endothelial growth factor
PGF	placental growth factor
sFlt-1	soluble fms-like tyrosine kinase 1
sEng	soluble endoglin
PI	pulsatility index
PP13	placenta protein 13
miRNA	microRNA (Ribonucleic acid)
3'UTR	three prime untranslated region
pri-miRNA	primary miRNA
pre-miRNA	precurosr miRNA
DGCR8	DiGeorge syndrome Critical Region 8
METTL3	methyltransferase-like 3
EXP5	Exportin 5
TRBP	Trans-activation response RNA-binding protein
RISC	RNA-induced silencing complex
AREs	AU-rich elements

NANOG	Nanog Homeobox
Robo	Roundabout
TGF-β	Transforming Growth Factor Beta
Smad	Mothers Against Decapentaplegic homolog
BMP	bone morphogenetic protein
GDF	growth and differentiation factor
MIS	Müllerian inhibitory substance
GS	glycine-serine
TGF-βRII	Transforming Growth Factor Beta Receptor Type 2
ACVRII	Activin Receptor Type 2
ACVRIIB	Activin Receptor Type 2B
BMPRII	bone morphogenetic protein receptor Type 2
AMHRII	Anti-Müllerian hormone receptor Type 2
ALK	Activin receptor-like kinase
R-Smad	Receptor Smad
Co-Smad	Common Smad
I-Smad	Inhibitory Smad
MH	Mad Homology
SSXS	Ser-Ser-X-Ser
LAP	latency-associated protein
LTBP	latent TGF-β-binding protein
LLC	large latent complex
SARA	Smad Anchor for Receptor Activation
NLS	nuclear localizing signal
NES	nuclear export signal
SBE	Smad binding elements
bHLH	basic/helix-loop-helix
bZIP	basic/leucine zipper
FSH	Follicle-Stimulating Hormone
hESC	human embryonic stem cells
Smurf2	Smad ubiquitination regulatory factor 2
HUVEC	Human Umbilical Vein Endothelial Cells
SNP	single nucleotide polymorphism
FBS	Fetal Bovine Serum
GFP	green fluorescent protein
Cyc1	Cytochrome c1
NC	non-targeting control
PBS	Phosphate Buffered Saline
RIPA	radioimmunoprecipitation assay
BSA	Bovine Serum Albumin
PBS-T	Phosphate Buffered Saline with Tween 20
ITGA1	Integrin Alpha 1
ECSCR	Endothelial Cell-Specific Chemotaxis Regulator

IL-8	Interleukin-8
IL1b	Interleukin-1b
CXCL1	Chemokine C-X-C motif ligand 1
IL6	interleukin-6
CCL2	chemokine C-C motif ligand 2
CXCL16	chemokine C-X-C motif ligand 16
CX3CL1	C-X3-C motif chemokine ligand 1
MIF	macrophage migration inhibitory factor
CK-7	cytokeratin-7
SMA	smooth muscle actin
CD45	cluster of differentiation 45
ICAM1	Intercellular Adhesion Molecule-1
QRT-PCR	quantitative real time polymerase chain reaction
GAPDH	Glyceraldehyde 3-phosphate dehydrogenase
cPML	Cytoplasmic promyelocytic leukaemia
DAB-2	disabled-2
ERK	Extracellular signal–regulated kinases
Akt	RAC-alpha serine/threonine-protein kinase
pSmad2	phosphorylated Smad2
pSmad3	phosphorylated Smad3
NF-κB	nuclear factor kappa-light-chain-enhancer of activated B cells
p50	Also known as NFkB1
p65	Also known as Rel1
ACHP	2-Amino-6-[2-(cyclopropylmethoxy)-6-hydroxyphenyl]-4-(4-piperidinyl)-3-pyridinecarbonitrile
WT	Wild Type

CHAPTER 1: LITERATURE REVIEW

I. THE HUMAN PLACENTA

The placenta is a transient organ that has a multitude of critical roles in maintaining and protecting the developing fetus throughout the entire pregnancy. Animal models and human pregnancies alike have shown that the multifaceted nature of the placenta is vital for embryo survival and health [1]. Serving as the interface between fetal and maternal environments, the placenta is involved in the exchange of gases, nutrients, and waste products between the mother and the growing fetus [2]. The human placenta, along with some rodents and higher apes, is characterized as "hemochorial", since maternal blood is in direct contact with the chorion. In fact, the human placenta has the greatest degree of maternal-fetal contact, reducing the thickness of the maternal-fetal barrier to a single cell layer by the third trimester [3]. Moreover, the placenta serves as an endocrine organ producing a number of pregnancy-associated hormones and growth factors, as well as ensuring protection of the fetus from maternal immune attack [4].

1. IMPLANTATION AND THE TROPHECTODERM

Implantation is a complex process that requires coordinated communication between the maturing blastocyst and the transiently receptive uterus [5,6]. In preparation for implantation, the endometrium undergoes a progesterone-induced decidualization process, whereby it thickens and further matures the decidual blood vessels in order to become receptive to the blastocyst [7]. The blastocyst is comprised of two cell lineages: the outer cell layer, the trophectoderm, and an inner cell mass. The trophectoderm gives rise to the chorion, while the inner cell mass develops

into the embryo and other extra-embryonic tissues [8]. Upon blastocyst maturation, the outer covering known as the zona pellucida is shed, exposing the trophectoderm layer and allowing for implantation to begin [6].

The implantation process can be divided into three stages: apposition, attachment, and invasion [9] (Figure 1.1). Apposition describes the initial adhesion of the blastocyst to the decidua, which is very unstable, resembling rolling adhesion in leukocytes [6]. It involves the interaction of the trophoblasts and decidua through a variety of secretory molecules, receptors, and endometrial epithelial protrusions (pinopodes) [3]. These interactions accumulate into a more stable adhesion, leading to the invasion of the extra cellular matrix of the decidua by the proliferating trophectoderm layer, thus embedding the blastocyst deep into the uterine wall. Soon after, the uterine epithelial cells grow over the blastocyst to cover the implantation site. Once the blastocyst is in intimate contact with the decidua, the process of placentation can begin. Cells of the trophectoderm continue to invade until they reach the inner-third of the myometrium, remodeling the maternal vasculature along the way [9].

2. Anatomy of the Human Placenta

The placenta begins to develop at implantation and continues to grow throughout pregnancy. Starting from a single layer of cells on the blastocyst, the placenta expands into a complex organ encompassing extra-embryonic membranes as well as maternal tissues. The full-term placenta is discoid in shape, averaging 22 cm in diameter with a central thickness of 2.5 cm, and weighing approximately 470 g [11].

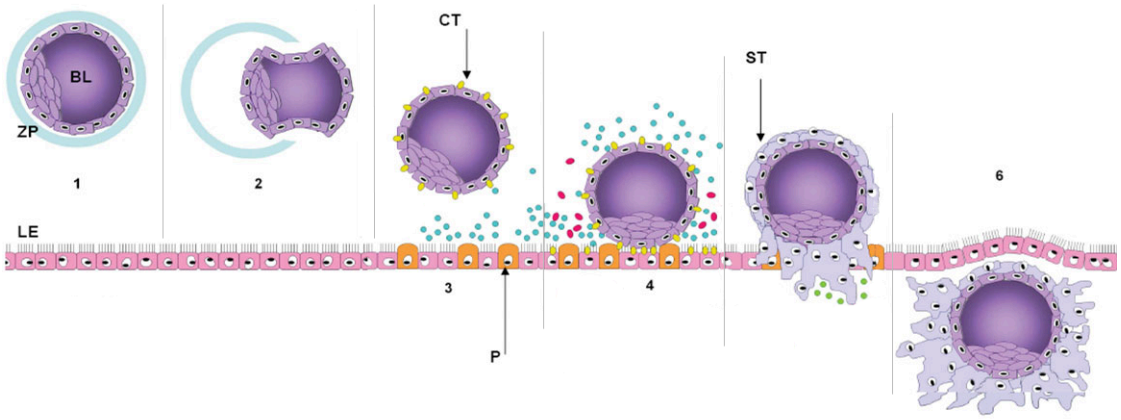

Figure 1.1 Proposed Schematic of Blastocyst Implantation

(1) Free floating blastocyst (BL) composed of trophectoderm layer and inner cell mass, surrounded by zona pellucida (ZP). (2) Hatching of the blastocyst through the shedding of the ZP. (3) Apposition stage of implantation showing secretory molecules, receptors along with transient interactions with pinopods (P) on the surface of the uterine luminal epithelium (LE). (4) Adhesion of the blastocyst to the decidualized endometrium. (5) Invasion stage of implantation characterized by the infiltration of syncytiotrophoblast (ST) cells formed through the proliferation of the underling cytotrophoblast (CT) progenitor cells. (6) Blastocyst fully embedded and covered by uterine epithelium, closing the implantation window. Used with permission from Fitzgerald JS., et al. (2008) [10].

Throughout the entire process of development, the placenta remains functionally active, keeping up with the demands of a growing fetus.

There are three distinct layers of extra-embryonic membranes (Figure 1.2). The amnion, which begins at the base of the umbilical cord, is the inner layer that forms the amniotic sac that encapsulates the fetus. At the fetal-facing side of the placenta, the amnion lies over the chorionic membrane that gives rise to the chorionic villi. Lastly, the decidua capsularis is the maternal component of the membranes composed of the decidualized endometrium, which covers the membranes on the luminal side of the uterus [12].

The chorionic villi make up the main structure of the maternal-facing side of the placenta. The villus "trees" are composed of a cytotrophoblast (CTB) layer covering the villus core, and a syncytiotrophoblast (STB) layer on the villus surface in direct contact with the maternal blood (Figure 1.3). Like the rest of the tissue, these villi go through several stages of development until term. In the first seven weeks, the placenta is composed of primitive villi that lack proper vascularization. Through trophoblast sprouting and proliferation, they elongate and mature forming stem villi that are anchored to the chorionic plate. From stem villi, peripheral branching gives rise to intermediate and tertiary villi that are the primary site of fetal-maternal exchange in the intervillous space. This stage of development is accompanied with rapid formation of villus core fetal capillaries [2]. The stem villi are organized into 15-28 cotyledons that give the maternal side of the placenta its lobular appearance. A subset of chorionic villi attach to the maternal decidua forming the basal plate.

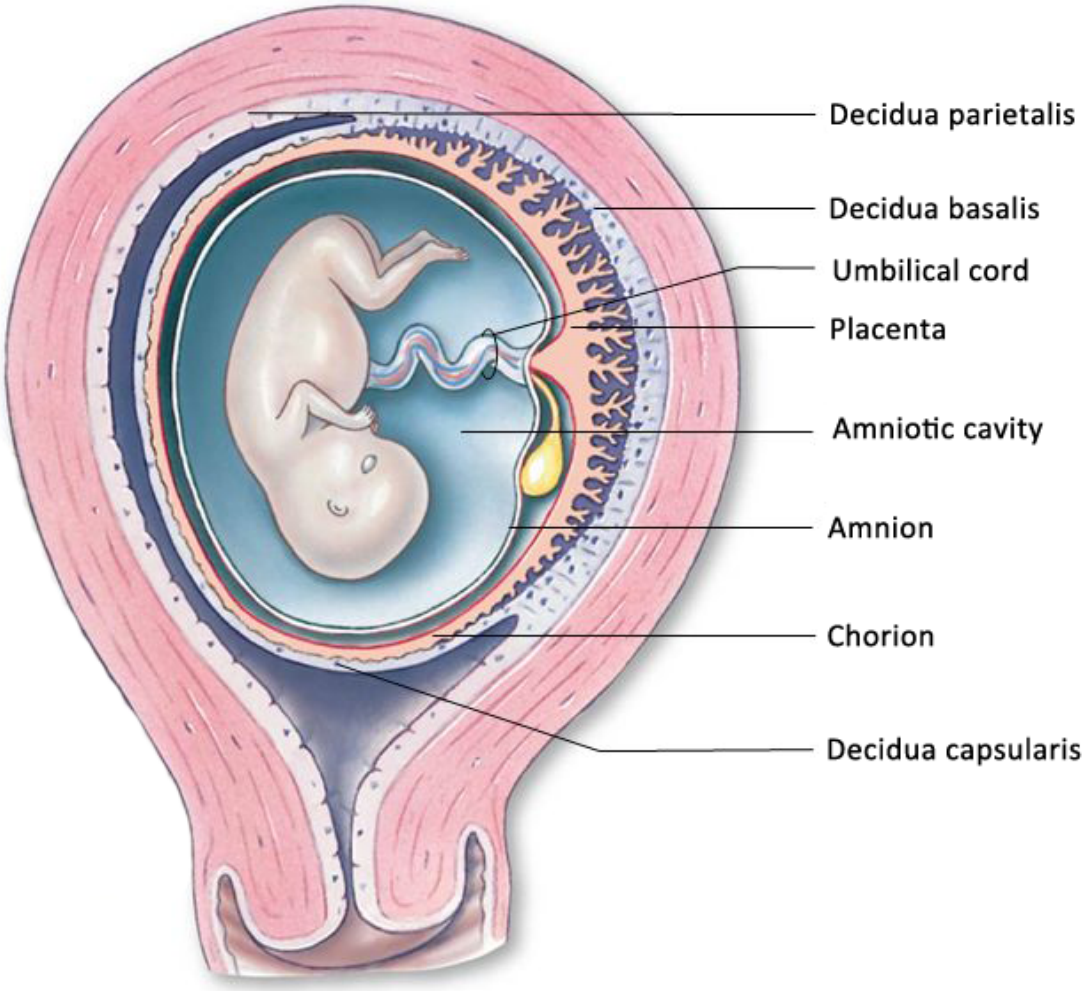

Figure 1.2 Extra-embryonic Membranes and Placenta Formation
In the innermost layer, the amnion stretches from the base of the umbilical cord, forming the fluid-filled amniotic cavity that encapsulates the fetus. The umbilical cord stretches from the fetus and then inserts itself into the chorionic plate. The chorion arises from the trophectoderm layer and develops into the chorionic villi of the placenta. The maternal decidua can be divided into three parts. The decidua capsularis forms the third membrane around the fetus and ends at the placenta margin. The decidua basalis is in intimate contact with the chorionic villi, while the remaining, non-interacting, decidua makes up the decidua parietalis. Used with permission from Martini FH., et al. (2014) [13].

Consisting of cytotrophoblasts, decidua basalis, maternal immune cells, and remodeled vessels, the basal plate forms the extravillous tissue of the placenta. At the basal plate, the establishment of proper placental perfusion is key to a healthy pregnancy.

The placenta is a highly vascularized organ composed of both maternal and embryonic blood vessels. The utero-placental blood flow consists of maternal spiral arteries bringing oxygen-rich blood to the intervillous space, while waste products are drained through the uterine veins. The feto-placental blood flow is comprised of umbilical vessels that feed through the fetal side of the placenta and branch into capillary loops of the chorionic villi. Within the umbilical cord, there is one vein that leads oxygen-rich blood from the intervillous space to the fetus, and two arteries that lead blood from the fetus to the intervillous space [2]. The vascular density of the cotyledons, as well as the uterine and umbilical blood flow, greatly increase in the later part of gestation, coinciding with an exponential increase in fetal growth [16]. Adequate placental vascularization is essential in order to keep pace with the growing fetus. Reduced vascular development can lead to increases in vascular resistance, which can result in compromised pregnancies.

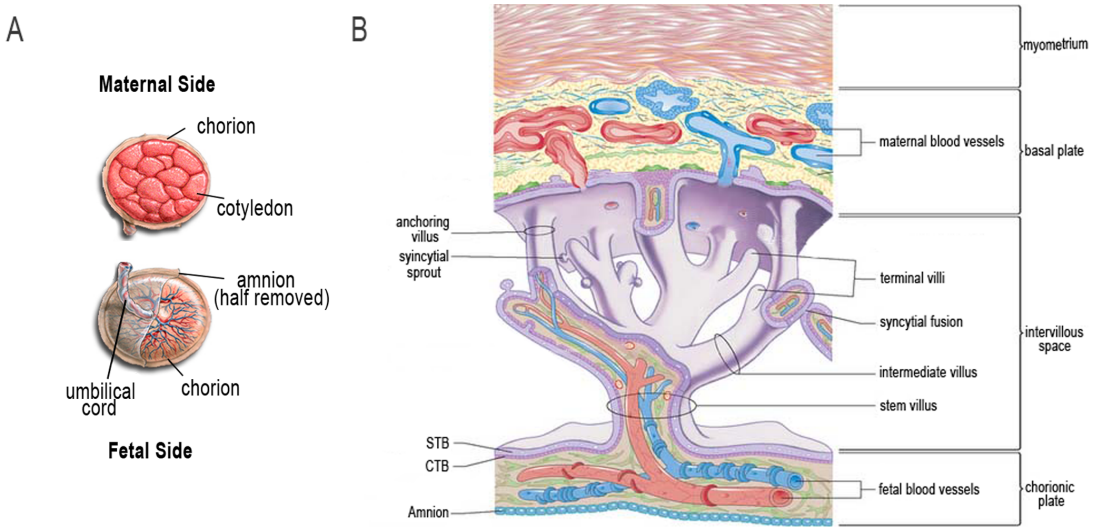

Figure 1.3 The Placenta Unit

(A) Anatomy of placenta and fetal membranes at term. Bottom panel shows the fetal side of the placenta where the umbilical cord is inserted. The smooth membranes are composed of the amnion and chorion. The chorion gives rise to the chorionic villi (top panel) on the maternal side that are organized into lobules or cotyledons. (B) Arrangement of the placenta from the fetal side (chorionic plate) to the maternal side (basal plate). At the chorionic plate the stem villi branch into intermediate and terminal villus that are extensively vascularized with the fetal blood vessels. The villus core is covered with a layer of cytotrophoblast (CTB) progenitor cells that fuse to form the multinucleated syncytiotrophoblast cells (STB). While some villi float in the intervillous space, bathing in maternal blood, a subset become anchoring villi, attaching to the maternal decidua forming the basal plate. From the anchoring cites, trophoblasts invade and remodel the maternal blood vessels up to the inner third of the myometrium. Used with permission from Barcena A., et al. (2011) and Standring S. (2015) [14,15]

3. PATHWAYS OF HUMAN PLACENTAL TROPHOBLAST CELL DIFFERENTIATION

Human cytotrophoblast progenitor cells differentiate toward two general pathways: villous trophoblasts and invasive extravillous trophoblasts (EVT) (Figure 1.4). While the villous pathway is active throughout gestation, the invasive differentiation pathway is indispensible in early placenta development and decreases to term.

3.1. Trophoblast cell fusion: differentiation toward syncytiotrophoblasts (STBs)

In the villous pathway, mononucleated CTBs fuse into multinucleated STBs, forming the syncytial layer that covers the placental villous tree. These cells are intimately involved in the exchange of gases, nutrients and waste across the maternal–fetal interface. The absorptive capabilities of this layer are maximized by the presence of microvilli that considerably increase the surface area [17]. The syncytial layer also plays a major role in the maintenance of pregnancy via the production of pregnancy-related hormones, such as human chorionic gonadotropin (hCG) and human placental lactogen (hPL) [4]. Additionally, STBs are in direct contact with the maternal blood and are therefore required to exhibit a degree of immune tolerance. This tolerance is achieved in large part through the lack of classical class I human leucocyte antigens (HLA) expression [18].

Syncytiotrophoblasts are non-proliferative and are therefore continually replenished throughout pregnancy via the fusion of the underlying CTB cell layer and shedding of the aged portions of the STBs (i.e. syncytial knots) [19]. Interestingly, this cell fusion occurs exclusively between the CTB and the overlaying syncytium; not between neighboring CTBs.

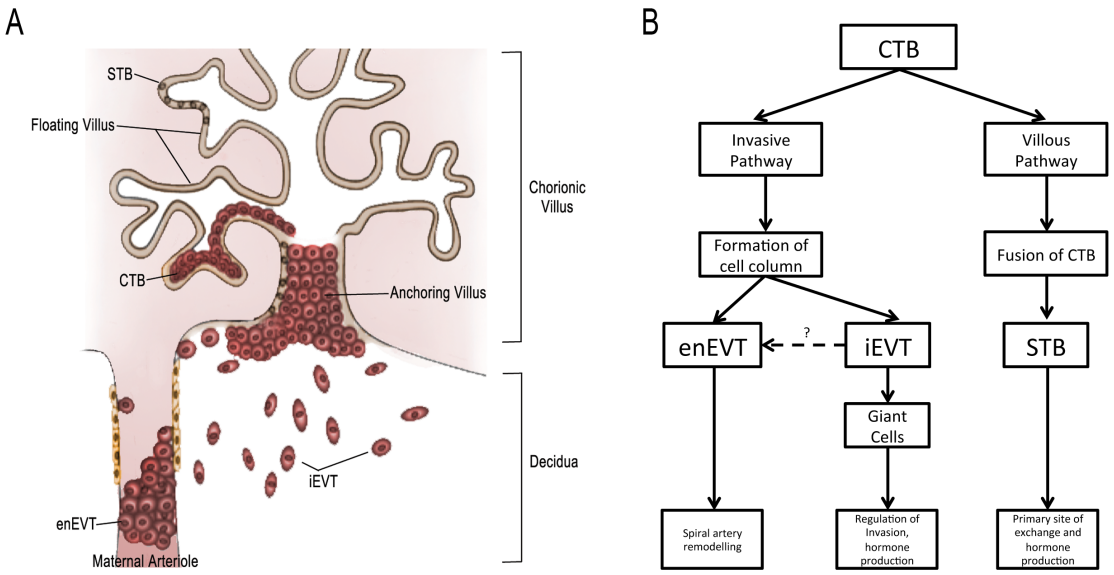

Figure 1.4 Pathways of Human Placenta Trophoblast Differentiation

(A) A single layer of progenitor cytotrophoblast (CTB) cells lines the villus mesenchyme core. CTB fuse down the villus pathway to form multinucleated syncytiotrophoblast (STB) cells. These floating villi are the primary site of exchange with maternal blood and hormone production. In the invasive pathway, proliferative CTB form the anchoring villus that attaches to the decidua. As cells leave the column, they form the interstitial extravillous trophoblasts (iEVT) and endovascular EVT (enEVT). While iEVT form giant cells, the enEVT will actively remodel maternal arterioles. (B) Flowchart of trophoblast differentiation from progenitor cytotrophoblast cells (CTB). Used with permission from Hannan NJ., et al. (2006) [20].

Although the process of trophoblast cell fusion is poorly understood, it is generally accepted that trophoblast differentiation into endocrine STBs is downstream of the fusogenic event. Specifically, the cascade is believed to begin with increased cAMP (cyclic adenosine monophosphate) level, which occurs via the activation of adenylyl cyclase and the consequent activation of protein kinase A (PKA). The downstream activation of transcription factors, such as glial cells missing-1 (GCM-1) and its target genes (for instance, the well-characterized fusion peptide synctytin-1) induces syncytialization and a subsequent increase in hCG production [21]. Syncytin-1 is localized to the syncytiotrophoblast cells and its expression is maintained throughout gestation [22,23]. Evidence from studies in BeWo cells, a well-established human choriocarcinoma cell line and an *in vitro* model of trophoblast fusion, conclusively demonstrates the role of syncytin-1 in triggering cell fusion [24].

Alternatively, there is growing evidence for the hypothesis that the mechanisms that govern the fusogenic and endocrine properties of STBs, although linked, are independently regulated. As demonstrated by Orendi et al., H-89, a selective inhibitor of cAMP-dependent PKA, prevented the cell fusion event in BeWo cells without affecting the production of hCG. This result suggests a second, PKA-independent, pathway in hCG synthesis [25].

The continual fusion of CTBs into a growing syncytial layer raises questions regarding the balance between tissue renewal and tissue loss. Whether the syncytium continues to accumulate nuclei throughout pregnancy or if aging nuclei are selectively shed via apoptosis into the maternal circulation is widely debated, and there is a great deal of evidence to support

both claims. On one side of the argument, there is evidence to support a model where aging nuclei must be shed to maintain the balance between renewal and loss as new CTBs join the STB layer. Studies that have examined the STB layer have indicated that these nuclei become packaged into membrane bound vesicles, termed syncytial knots, and released into maternal circulation [26,27]. It has been suggested that it takes approximately 3–4 weeks following syncytial fusion for one aging nucleus to be removed from the growing cell [28]. Alternatively, another argument states that the nuclei in the STB layer continue to accumulate throughout gestation and that their heterogeneous appearance is primarily a result of their differential ages [29].

3.2. Trophoblast cell invasion: differentiation toward extravillous trophoblasts (EVTs)

The invasive pathway depends on the establishment of anchoring villi that serve to attach the placenta to the uterine wall. The anchoring sites are established as early as the second week of gestation and are composed of a heterogeneous population of CTBs [30]. Trophoblasts invading the decidua from anchoring columns are essential in establishing an adequate perfusion of the placenta to sustain the growing fetus.

A subpopulation of rapidly proliferating CTBs, which participate in the creation of the cell column bridge between the placental villous tip and the maternal decidualized stroma, can be found at the proximal ends of the anchoring sites. Studies of human placental and decidual explant cultures suggest that decidual contact signals the proliferative burst of CTBs to break through the STB layer [30]. The stability of this interaction is in part mediated by the upregulation of integrin α5β1 and a fibronectin-rich matrix on the CTBs that are located in the distal portions

of the trophoblast cell columns [31,32]. There is also evidence that the L-Selectin adhesion system may participate in the formation and maintenance of the anchoring villi early in pregnancy [33]. At the distal ends of the columns, CTBs exit the cell cycle and begin to lose their cell–cell contacts. These CTBs detach from columns and, as they come into contact with the decidual extracellular matrix, they differentiate into interstitial EVTs (iEVTs) and endovascular EVTs (enEVTs), which have distinct roles in maternal decidua [34].

The differentiation process within the heterogeneous trophoblast column population is unclear, however, *in vitro* studies suggest that this process may be intrinsic [35]. A large part of this differentiation process is composed of a switch in adhesion molecule profiles as well as the production and regulation of several proteases.

3.2.1. Interstitial trophoblast cells: invasion into uterine stroma

Interstitial EVTs are described as having two distinct phenotypes: large polygonal iEVTs (or X cells) and small spindle-shaped iEVTs. The large iEVTs are believed to remain around the placental–decidua transition, securing the placenta to the uterus throughout gestation by producing a "trophoblast glue" that is made of a matrix-type firbrinoid [36]. In contrast, it has been demonstrated that the small iEVTs invade deep into the decidua, as far as the inner third of the myometrium [36].

Interstitial EVTs have a distinct adhesion molecule and histocompatibility antigen profile. There is a marked downregulation of integrin α6β4 and an upregulation of the fibronectin integrin, α5β1, within the distal part of the cell column. The collagen integrin, α1β1, is expressed at

higher levels in the iEVTs that invade deeply in the decidua [32,37]. The downregulation of E-cadherin is observed in the distal portion of cell column and is believed to contribute both to the loss of cell–cell contact and to the increase in invasiveness in iEVTs [38]. Consistent with their invasive phenotype, iEVTs have been demonstrated to secrete several proteases that facilitate the breakdown of the decidual extracellular matrix. Specifically, the immunolocalization of urokinase-type plasminogen activator (uPA) and several matrix metalloproteinases (MMPs), most notably the gelatinases MMP-2 and MMP-9, have been reported. Interestingly, the inhibitors of these enzymes, plasminogen activator inhibitor 1/2 (PAI-1/2) and tissue inhibitor of metalloproteinase-1 (TIMP-1), are observed to be co-localized to iEVTs, indicating a certain degree of "fine-tuning" with respect to limiting the invasiveness of these cells [39,40]. Furthermore, unlike the villous CTBs, iEVTs express HLA class I major histocompatibility complex (MHC) antigens. Specifically, these cells express HLA-E, trophoblast specific HLA-G and the polymorphic HLA-C [41-43].

How this movement of iEVTs through the immune cell-dense decidua during the first trimester does not elicit a maternal immune response remains a great topic of discussion [44]. Most notable in this regard is the interaction of iEVTs with decidua-specific natural killer (dNK) cells, which differ from the NK cells that are found in the peripheral blood, and which make up the largest proportion of leukocytes at the implantation site. The receptor profiles on dNK cells allow them to interact with all three of the HLA antigens that are expressed on iEVTs. Likewise, all of these HLA antigens contribute to the immune tolerance that is observed at the maternal-fetal interface. HLA-E binds with higher affinity to the more abundant inhibitor dNK receptor,

suggesting a role in inhibiting cytotoxicity of dNKs [45]. Work by Apps et al. indicates that the inhibitory leukocyte immunoglobulin-like receptor (LILR), LILRB1, has highest affinity for dimerized HLA-G on iEVTs, suggesting that this placenta-specific process modulates the maternal immune response [46]. Lastly, studies of the interaction between HLA-C and corresponding dNK killer cell immunoglobulin-like receptors (KIRs) provides evidence for the importance of this interaction in fetal growth and blood supply [42]. The invading iEVTs finally differentiate into placental bed giant cells. Similar to STBs, these cells have the capacity to produce both hCG and hPL, suggesting their role in the maintenance of normal pregnancy. Furthermore, these giant cells produce protease inhibitors that may be involved in limiting EVT invasion past the myometrium [47].

3.2.2. Endovascular trophoblast cells: remodeling of uterine spiral arteries

Placental circulation is established between 8 and 12 weeks of gestation, with the spiral arteries being fully remodeled by approximately 20 weeks. Endovascular EVTs are believed to play key roles in this remodeling process [48]. Decidual biopsies indicate that enEVTs invade maternal vasculature in the decidua and the inner-third portion of the myometrium [49]. The remodeling of the spiral arteries from high-resistance and low-flow muscular vessels to low-resistance and high-flow sac-like vessels involves cross talk between different cell types, with enEVTs being the key players (Figure 1.5). These events can be divided into five stages: (1) decidua-associated early vascular remodeling, (2) iEVT-associated early vascular remodeling (3) enEVT migration, (4) the incorporation of enEVTs into the vessel wall and (5) the re-endothelization and subintimal thickening [7,50]. During the decidualization process, the maternal vessels are modified to prepare them for EVT invasion. This “priming” process appears to be trophoblast-independent based on

studies of ectopic pregnancies [51]. These alterations include smooth muscle swelling and endothelial cell vacuolation [50]. Leukocytes, specifically dNKs and macrophages, have been implicated in this process. MMP-dependent matrix degradation and apoptosis are the suggested mechanisms by which trophoblast-independent early vascular remodeling occurs [52].

Two possible origins of the enEVTs have been suggested: iEVTs and enEVT plugs. During early pregnancy, spiral arteries in the superficial decidua are surrounded by iEVTs [54]. These iEVTs position themselves along the arteries and begin to disrupt and disorganize the vascular smooth muscle cell layer. As these iEVTs invade the lumen of the arteries, they are believed to switch to the endovascular phenotype. However, it has been suggested that the switch from iEVTs to enEVTs occurs only in regions of the spiral arteries in the superficial zone of the decidua, and that deeper regions of the arteries are remodeled by enEVTs from a second origin, the enEVT plugs [50].

EnEVTs from the initial plugs are believed to travel down the vessel lumen in a retrograde manner [7]. This infiltration by the EVTs results in maternal vascular apoptosis, the detachment of these cells from the surrounding extracellular matrix and their migration away from the vessels. EnEVTs go on to replace the endothelial cells of the maternal vessels through a process that is referred to as pseudovasculogenesis or vascular mimicry [37,38,55]. Endovascular EVTs are able to exist within the maternal vasculature in a manner that is similar to endothelial cells, primarily due to their ability to switch from an epithelial to an endothelial adhesion molecule phenotype[56].

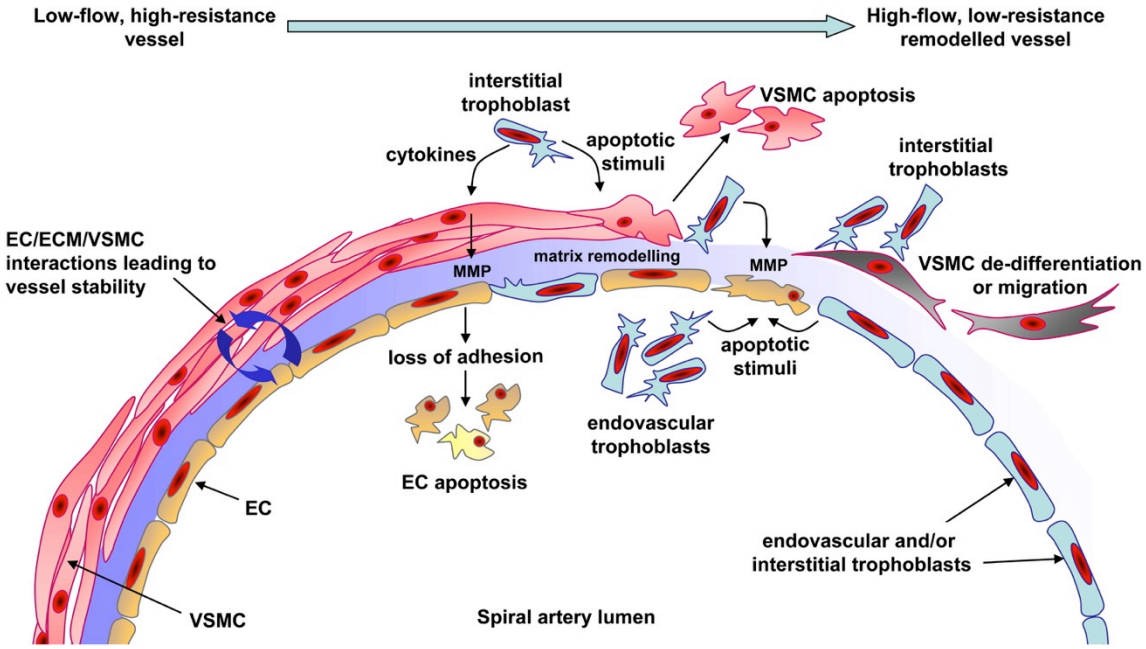

Figure 1.5 Cellular Interactions in Spiral Artery Remodeling

Unremodeled decidua spiral arteries are low-flow, high-resistance vessels. They have tight, circular cross sections, and are made up of a thick vascular smooth muscle cell (VSMC) layer and an endothelial cell (EC) layer embedded in an extra cellular matrix (ECM). The remodeling process begins prior to EVT infiltration. Decidual immune cells (mainly decidual natural killer cells and macrophages) begin priming the vessels starting with the VSMC. EVT are involved in the spiral arteries through their interstitial pool or down the lumen as endovascular EVT. Once the endothelial cells have been removed, the enEVT reline the vessel, completing the remodeling process. As seen in the diagram, the VSMC and EC are removed and replaced with enEVT once remodeled, which consequently produce high-flow, low-resistance vessels supplying blood to to the feto-maternal interface. Used with permission from Whitley G.St.J., et al (2008) [53].

These cells downregulate the epithelial-type markers E-cadherin and α6β4, and upregulate the expression of the adhesion molecules vascular endothelial (VE)-Cadherin, Platelet And Endothelial Cell Adhesion Molecule 1 (PECAM1), and Neural Cell Adhesion Molecule (NCAM), as well as integrins α5β1, α1β1, and αVβ3 [37,38]. Lastly, studies in mice have provided evidence for maternal vascular repair. This process encompasses re-endothelization and the appearance of subintimal thickening between the restored endothelium and fibrinoid layer that surrounds the enEVTs [50].

The remodeling of maternal spiral arteries continues until the mid-second trimester, and can be observed as deeply as the inner-third of the myometrium. This process does not occur uniformly throughout the entire placenta; it is most prominent in the central placental bed and less prominent at the periphery [57]. The remodeled spiral arteries are increased in length, exhibit a several-fold increase in lumen diameter and are unresponsive to vasoconstrictive agents [56,58]. This low-resistance and high-capacity phenotype provides for consistent and low velocity flow of maternal blood into the intervillous spaces, which sustains the growing demands of the fetus throughout gestation.

Mammalian placentation represents a remarkable biological process, during which diverse trophoblast populations are generated. Much work has been performed to identify trophoblast subtypes, especially at early gestational stages, when trophoblasts are actively differentiating. The characterization of enEVTs has been poorly described compared with other trophoblast subtypes. This relative lack of knowledge is most likely due to the difficulty involved in accessing

clinical samples that contain deeper uterine endometrium and the upper one-third of uterine myometrium, where enEVTs are abundant.

4. PREECLAMPSIA (PE)

The establishment of the feto-maternal interface is complex and is tightly regulated by many interactions of a large group of molecules from diverse cell types. Disruption in the pathways involved in placental development, especially during the early stage of gestation, can lead to complications later in pregnancy such as preeclampsia (PE).

4.1 Etiology and Pathophysiology

Preeclampsia is the leading cause of maternal morbidity, mortality, and premature delivery, affecting approximately 2–8% of pregnancies worldwide [59]. While mainly defined as a hypertensive disease of pregnancy, PE is increasingly seen as multisystemic, seriously affecting the liver, kidneys, lungs, and brain. Typically, PE is diagnosed after 20 weeks of gestation by the presence of hallmark symptoms in the mother including non-preexisting hypertension (≥140/90 mmHg) and proteinuria (≥3 g in 24 h). Although PE is considered to be a late-pregnancy disorder based on clinical data, the molecular events leading to its onset have been suggested to occur early in pregnancy. It is generally accepted that the presence of a placenta is a major cause of preeclampsia. Specifically, placental ischemia appears to play a central role in this disease [60].

The pathological changes in the PE placenta have been reported in an increasing number of studies (Figure 1.6). The first stage is poor development of the early placenta and utero-placental blood supply that occurs in the first half of pregnancy, during which no clinical symptoms are presented (Figure 1.6).

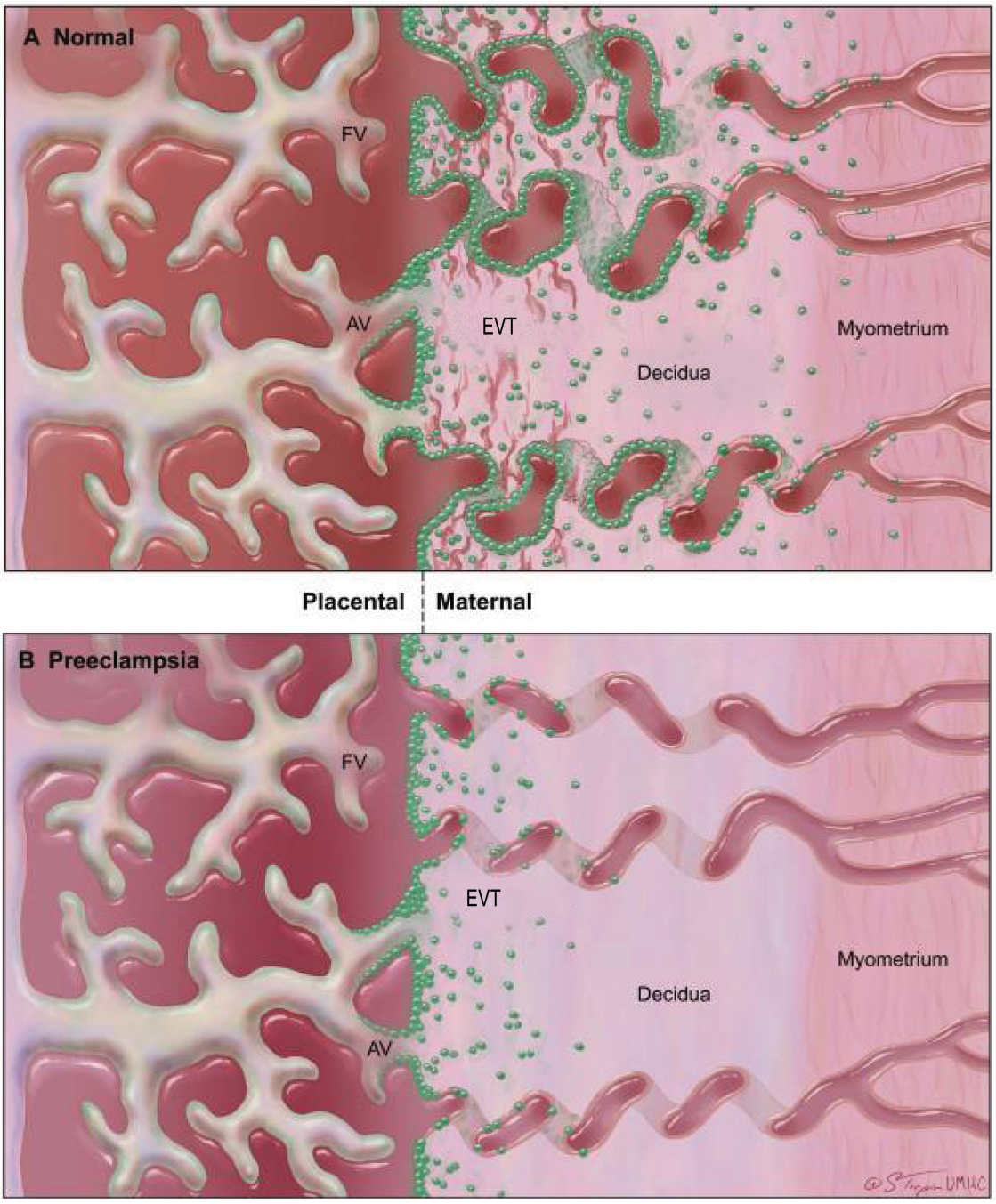

Figure 1.6 Defective Mechanisms of Invasion and Spiral Artery Remodeling in PE
(A) In normal pregnancy, EVT (shown in green) from anchoring villi (AV) invade the decidua and maternal spiral arteries remodelling them up to the inner-third of the myometrium. (B) In pregnancies compromised by PE, the population of EVT is reduced, and remodeling is restricted to the proximal portion of the vessel. Insufficient remodeling in PE is observed as smaller diameter vessels accompanied by variable blood flow with increased velocity to the intervillous space. Used with permission from Pennington KA., et al. (2012) [69].

The second stage is the manifestation of the maternal syndrome that arises, in part, from factors released by the placenta as it is placed under an increasing amount of oxidative stress [70]. It should also be considered that maternal determinants, including genetic, behavioral, and environmental factors, might reciprocally influence and interact with the first stage in multiple ways.

4.2 Classification

Agreement on a clear definition of PE has been understandably difficult. One reason for this is the central belief that PE is a broad classification for a number of diseases with shared pathophysiology.

Two broad categories of PE have been suggested, placental PE and maternal PE [70]. Maternal PE is considered to arise from the interaction between a normal placenta and an abnormal maternal response. In this regard, clinical manifestation is likely to be influenced by the presence of preexisting microvascular or metabolic diseases, as well as environmental and nutritional factors, and usually occurs in late pregnancy. In contrast, placental PE is considered to originate from a malfunctioning placenta under ischemia-reperfusion conditions and oxidative stress. However, the classification of these two types of PE has not been well defined, and the combination of both the maternal and placental contribution has been most commonly presented.

Further classification of PE as early versus late, or mild versus severe have been widely used across literature. The initial classification refers to the gestational age of diagnosis and severity

of symptoms, respectively. Specifically, onset of clinical symptoms prior to 34 weeks of gestation is classified as early-onset PE, while late-onset PE is anything diagnosed at 34 weeks onward. The majority of clinical cases fall in the late-onset group, with only 12 % making up the early-onset cases. It is unclear whether early- or late-onset PE are gradients of the same condition or if they have different pathological mechanisms. While few comparison studies exist, there is evidence for differential risk factors and origins associated with early-PE compared to the late-onset cases [71-74]. The classification of PE based on severity of symptoms at diagnosis has been discouraged in recent years due to PE being a progressive disease. While some cases can progress very slowly from initial diagnosis, others can very quickly escalate into more severe complication [75].

A recent study has brought more insight into the heterogeneity of this condition by classifying PE into three clinical etiologies through unsupervised genome clustering [76]. The first cluster is believed to result from underlying maternal cardiovascular disease–susceptibility and fall into the “maternal PE” classification. It was characterized as late-onset PE, with milder clinical symptoms, appropriate for gestation age babies, and normal placentas. The second cluster exhibited placenta origins of diseases and the canonical definition of PE. It was characterized by severe early-onset cases, fetal complication such as intrauterine growth restriction (IUGR), and systemic maternal pathology. The last group was classified as “immunologic” PE, characterized by a maternal-fetal incompatibility coupled with a poor maternal response. Understanding of PE has greatly progressed in the last decade. However, the search for reliable biomarkers and potential therapies still remains a challenge.

4.3 Biomarkers and Treatment

Currently, the only effective treatment available for PE is termination of pregnancy and premature delivery. If left untreated, PE can result in serious health consequences or even death for both the mother and fetus. The major challenges are to effectively diagnose the condition early, and develop preventive and therapeutic strategies that will minimize the burden of PE. Finding a reliable biomarker that can predict the onset of PE prior to clinical symptoms has proven to be a difficult task, with studies focused on finding predictive biochemical markers proposing several candidates.

Among the first studied serum biomarkers of PE are vascular endothelial growth factor (VEGF) and placental growth factor (PGF), and their antagonists, soluble fms-like tyrosine kinase 1 (sFlt-1), and soluble endoglin (sEng). A significant downregulation of VEGF and PGF was reported in second trimester serum prior to diagnosis of early-onset severe PE [77,78]. Upregulation of sFlt-1 was able to predict onset of PE on average 11.2 weeks prior to the onset of clinical symptoms [79]. Other studies also showed a similar increase of sFlt-1 limited to several weeks prior to the onset of clinical symptoms [78,80]. On the other hand, sEng levels were significantly higher starting at 17 weeks or 25 weeks of gestation in women destined to develop early-onset or late-onset PE, respectively [81]. The ratio of sFlt-1:PGF has shown to increase ability to predict PE compared to either marker alone [81,82]. Another study showed that combining maternal physical parameters (i.e. uterine artery pulsatility index (PI), mean arterial pressure) and serum PGF at 11- 13 weeks gestation was able to predict 75% of early and 47% of late-onset PE cases [83]. The heterogeneity

in patterns of prediction is most likely a result of low detection limits, mixed tissue origins (fetal and/or maternal), and biomolecule reactivity and stability within maternal circulation [84].

Many studies have looked into the usefulness of placenta protein 13 (PP13), an immunoregulatory galectin, as an early biomarker of PE. Unlike the angiogenic biomarkers, PP13 is only produced by the placenta STB cells [85]. Furthermore, patients destined to develop PE had a downregulation of PP13 as early as 7 weeks of gestation [86,87]. However, the downregulation of PP13 in the first trimester did not discriminate between PE and other complications such as pre-term birth and IUGR [88]. Also, in another study that combined maternal characteristics and other serum biomarkers, PP13 proved to be inadequate for screening purposes [89].

Discovery of microRNAs (miRNAs) in maternal plasma has opened up a new area for biomarker discovery [90]. The differential expression of >130 miRNAs between normal and PE placenta has been reported [91]. However, nearly 90% of the dysregulated miRNA have only been reported once. Similar inconsistent findings are true of circulating serum miRNA early in gestation. A study conducted on sera from 12-14 weeks of gestation revealed 19 significantly dysregulated miRNAs in patients destined with severe PE [92]. On the other hand, a similar study on sera from the same gestation period found no circulating miRNA that were useful in predicting PE [93]. The large variation between studies could be the result of many factors, including small sample sizes, differences in classification of tissues, exclusion criteria, and methodologies (RNA processing, miRNA detection etc.). In spite of inconsistencies in literature, miRNAs represent a diverse and stable pool of potential biomarkers for discovery.

II. MICRORNA

MiRNA are a class of small non-coding RNAs that are important regulators of post-transcriptional gene expression. In 1993, landmark papers by Drs. Ambros and Ruvkin introduced the first microRNA, *lin-4*, in *C. elegans* [94,95]. They demonstrated that this gene, essential for controlling the timing of larval development, did not encode a protein, but suppressed the expression of *lin-14* through a RNA-RNA interaction in its 3'UTR (three prime untranslated region). For many years, this phenomenon remained unique to *lin-4* and nematode development. In 2000, the discovery of *let-7* in *C. elegans* demonstrated that one miRNA can target the 3'UTR of several mRNAs, and likewise, that one mRNA 3'UTR can be targeted by many miRNAs [96]. Intense cloning efforts revealed the presence of miRNA in a variety of cell types and across all eukaryotic branches, suggesting that regulation by miRNAs was a more wide-spread phenomenon than previously anticipated [97,98]. Presently, online databases have annotated ~1600 human miRNA genes. While the function of most of these miRNAs is unknown, it is clear they make up an important and large class of molecules involved in gene regulatory networks. MiRNAs have been reported to regulate nearly all cellular processes, including cell proliferation, differentiation, apoptosis, and development [99]. Involvement of miRNAs in human diseases has been demonstrated and the possibility for their use as therapeutic targets shows great potential [100,101].

1. Biogenesis and RISC Assembly

Depending on their genomic location, miRNA can be broadly classified as "intronic" or "intergenic". Approximately half of all annotated human miRNA are found within host genes,

predominantly introns of protein-coding genes or genes of other non-coding RNAs [102]. The biogenesis of all miRNA is generally consistent; however, their genomic location influences the mechanisms of transcriptional regulation. Intronic miRNA are generally transcribed in parallel with their host gene transcripts through the host gene promoter, while intergenic miRNA are governed by their own promoters. However, recent evidence has shown an uncoupling in the expression of certain miRNAs from their host genes through possible independent transcription mechanisms and alternative splicing [103].

For the majority of miRNA, transcription is mediated by RNA polymerase II, generating a primary miRNA (pri-miRNA) transcript of up to several kilobases in length, containing a 5' cap and a 3' poly-A tail (Figure 1.7). The pri-miRNA is processed into mature miRNA through a step-wise process with specific subcellular localization [104]. The first step in processing is cropping of the long pri-miRNA transcript into a ~70nt hairpin precursor miRNA (pre-miRNA) in the nucleus [105]. The cropping is mediated by a microprocessor complex, which consists of an RNase III, Drosha, and the double-stranded-RNA-binding protein, DGCR8 (DiGeorge syndrome Critical Region 8) [106]. Despite the diversity in sequence among pri-miRNA, there are several structural features in common that are essential for processing.

Pri-miRNAs form an imperfect double stranded stem structure of ~3 helical turns, which are flanked at one end by a ssRNA apical loop and long ssRNA base segments on the opposite end [108]. Several models of microprocessor cleavage determination have been proposed; however they all center on the recognition of the ssRNA-dsRNA junctions.

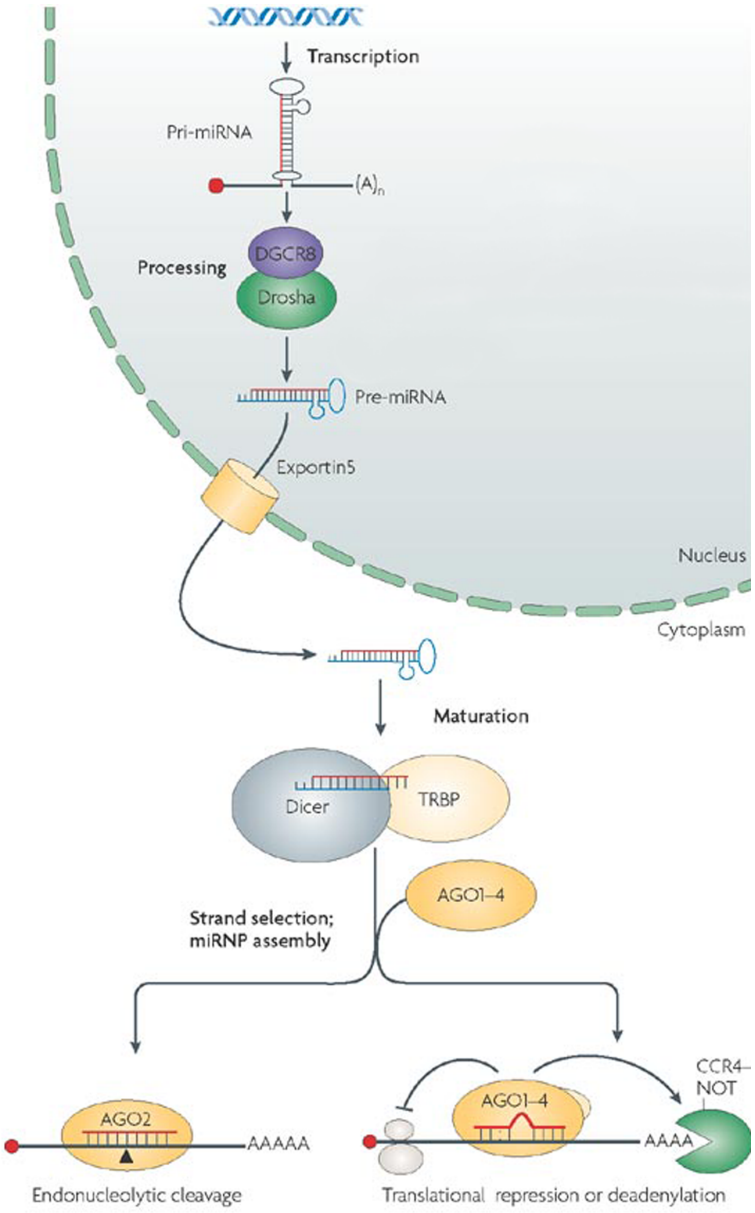

Figure 1.7 Model for microRNA Biogenesis and Mechanism.
First step of biogenesis is the transcription of primary miRNA transcripts (pri-miRNAs) that contain a double stranded stem, a loop, ssRNA tails, a 5' cap and 3' poly-A Tail. Processing by Drosha and DGCR8 leads to the formation of the precursor miRNA (pre-miRNA) that is then exported out of the nucleus by Exportin 5. DICER and TRPB complete the final processing from pre-miRNA to the mature miRNA duplex. The guide strand is loaded into one of the AGO proteins and, along with other accessory proteins, RISC is complete. Target recognition can lead to endonucleolytic cleavage (which only applies to AGO2 loaded miRNA) or translational repression and deadenylation. Used with permission from Filipowicz W., et al. (2008) [107].

Namely, the cleavage occurs approximately one helical turn (~11bp) from the basal segments and two helical turns (~22bp) from the apical loop [109,110]. The binding of the microprocessor complex to the pri-miRNA is mediated through the direct binding of DGCR8, which serves as an anchor. DGCR8 recognition of pri-miRNA over other secondary structures in the transcript is facilitated by the marking of pri-miRNA though methylation, by methyltransferase-like 3 (METTL3), for example [111]. Subsequently, the cleavage by Drosha generates one end of the mature miRNA and therefore determines the final miRNA sequence. Once the pre-miRNA is formed it is exported out of the nucleus by a member of the nuclear transport receptor family, Exportin 5 (EXP5), that is bound to Ran small GTPase [112]. In the cytoplasm, the pre-miRNA binds to a second RNase-III protein, Dicer, which, in combination with Trans-activation response RNA-binding protein (TRBP), cleaves ~22nt from the pre-existing pre-miRNA terminus, forming the miRNA:miRNA* duplex [112-114]. The dsRNA duplex is short lived, and quickly undergoes the coordinated process of RNA-induced silencing complex (RISC) assembly.

At the center of RISC are the ubiquitous post-transcriptional regulators, the AGO family of proteins. There are four main AGO proteins expressed in humans (AGO 1-4) that bind miRNA indiscriminately [115]. The multi-step process of RISC assembly can be generally summarized into: 1) loading of the miRNA duplex and 2) subsequent RISC maturation [116]. With the aid of the HSC70/HSP90 chaperone machinery and ATP, the newly formed miRNA duplex is loaded into AGO [117]. The miRNA duplex consists of a “guide strand” and a “passenger strand”. The guide strand will be incorporated into RISC where it will serve in target transcript recognition, while the passenger strand will be ejected from the AGO protein. The process of strand selection

remains unclear; however thermodynamic stability is a major determining factor [114]. It is generally believed that the less thermodynamically stable 5' end of the miRNA will be anchored by AGO, while the strand with the more stable 5' end will be ejected through RISC maturation. Ultimately, the guide stand is positioned so that its phosphate backbone is interacting with the AGO while both its 5' and 3' ends are anchored, exposing the "seed-region" (nucleotides 2-8, from the 5' end) for target recognition [118].

2. Mechanism

The interaction between the miRNA-containing RISC and its mRNA target is driven by base pair complementarity. In general, miRNA:mRNA binding is largely dependent on a perfect complement at the seed region, which forms a thermodynamically stable interaction for target suppression. However, some miRNA have shown to compensate for mismatches in the seed region through increased complementarity at the 3' end [119]. Several mechanisms for miRNA action have been proposed and yet a unified model remains to be clearly defined. In general, miRNA have shown to exert their repressive action through mRNA cleavage, mRNA decay, and/or translational repression [120].

While target mRNA cleavage is the predominant mechanism seen in siRNAs and plant miRNAs, it is rarely observed in human miRNA:mRNA interactions [107]. Several theories have been proposed to explain this observation. Unlike siRNAs and plant miRNAs, the majority of human miRNAs do not exhibit perfect Watson-Crick complementarity along the entire length of the mRNA target. Since the AGO RNaseH domain prefers perfect complementarity near the cut region (10-11nt from the 5' end), a bulge in the miRNA:mRNA interaction at this site would hinder its

endonuclease activity [120]. Furthermore, while all four human AGO proteins interact with miRNAs, only AGO2 has retained this "slicer" function [121].

The second mechanism of miRNA-guided gene silencing is through the destabilization and degradation of mRNA targets. After target recognition, the AGO-interacting GW182 protein family is essential in mediating the downstream steps of target repression [118]. Apart from interacting with AGO, GW182 is capable of interacting with the poly-A binding protein on the poly-A-tail of the mRNA as well as cellular deadenylases, such as the CCR4/NOT complex [122]. This leads to the deadenylation and decapping of mRNA, and its consequential degradation.

The third mechanism, involving translational repression, stemmed from the initial observation that *lin-4* regulated the LIN-14 protein without affecting mRNA levels [95]. How miRNAs suppress translation is still unclear; however, strong evidence points to their interference with the process of translation initiation [123]. Furthermore, the suppression of translation was suggested to precede mRNA destabilization and degradation, challenging the initial observations with *lin-4* [123].

On the other hand, miRNAs as activators of translation have also been reported, albeit to a much lesser extent. This mechanism involves the recruitment of translation initiation factors to the site of miRNA-RISC binding at AU-rich elements (AREs) in the 3'UTR [124]. To add to the complexity, several miRNA have been reported to switch between their repressive and activating roles depending on the cellular context, specifically in growth-arrest conditions [124,125].

3. Target Prediction

Understanding the biological function of a miRNA relies on identifying its regulatory targets. Considering that miRNAs can target mRNAs through imperfect binding, each miRNA has the potential to target many different mRNAs. Over 30% of the human genome shows potential for miRNA regulation, making predictive algorithms with high signal to noise ratios imperative [126]. Since the initial discovery of miRNAs, the importance of target complementarity to the 5' portion of the guide strand has been evident, and the mechanism of target recognition has proven to be even more complex.

Five canonical "seed" types on mRNA targets have been defined [127] (Figure 1.8). Those with the highest conservation and efficacy in miRNA repression are the 8mer targets that possess contiguous Watson-Crick pairing to 2-8 nucleotides in the seed region and an adenosine across position one. The preference for nucleotide A in the first position is not dependent on miRNA sequence identity. Rather, it proved to increase AGO affinity over all other nucleotides in this position due an adenosine-binding pocket in AGO that mediates target recognition [128]. Slightly less effective are seed types with a 7mer-m8 site (match at position 2-8) or 7mer-A1 site (match as position 2-7 with an A opposite position 1). While the 6mer (match at position 2-7) and offset-6mer (match at position 3-8) show very weak preferential conservation and much lower efficacy.

Basing target prediction on seed-region complementarity alone has not produced predictions with high specificity. Many algorithms today will use a combination of factors to increase the predictive power of functional targets [129,130].

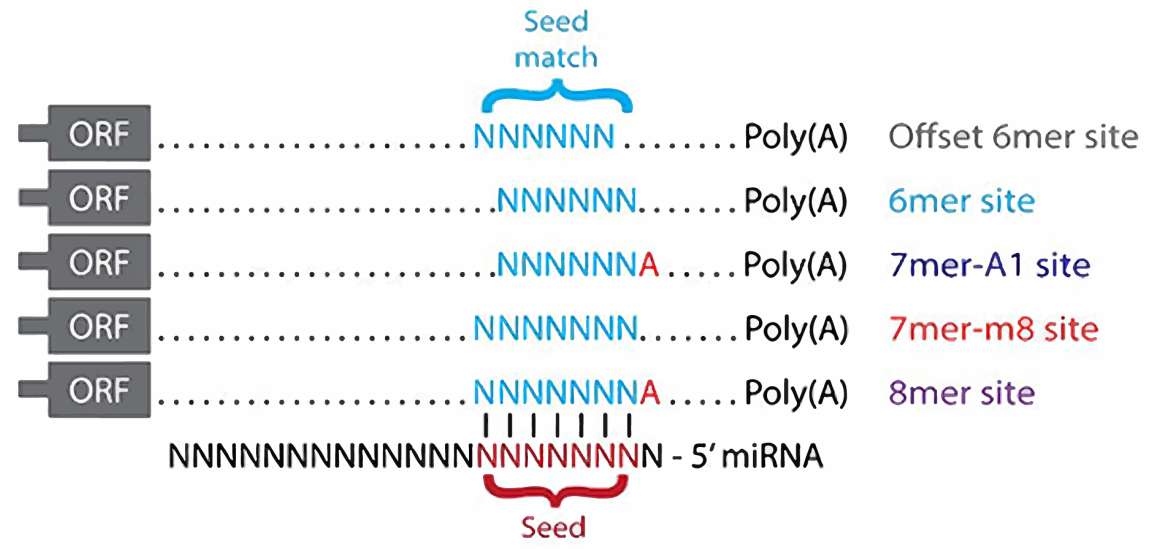

Figure 1.8 Canonical mRNA target site types.
The 8mer targets (match nucleotide 2-8 of miRNA "seed" region and have an adenosine across position one) possess the highest conservation and efficacy in miRNA repression. Slightly less effective are seed types with a 7mer-m8 site (match at position 2-8) or 7mer-A1 site (match as position 2-7 with an A opposite position 1). The 6mer (match at position 2-7) and offset-6mer (match at position 3-8) show very weak preferential conservation and much lower efficacy in target repression. Used with permission from TargetScan Human7.

Most often, thermodynamic stability of the miRNA:mRNA duplex is used. While conservation across species, specifically of the 7nt seed region, can further refine predicted targets that otherwise score well in both complementarity and stability. More recently, RNA secondary structures and RNA binding proteins and their influence on target site accessibility has been another important factor to consider. Likewise, an increase in the number of target sites within the 3'UTR has shown to increase the likelihood of target repression through cooperative action [131].

4. Nomenclature

A consistent naming scheme has been an essential part in facilitating the exponential discovery of novel miRNAs and subsequent database construction [132]. The naming of miRNAs was conducted in a sequential numerical order, independent of biological function. Each miRNA begins with a 3 to 4 letter prefix that designates the species of origin, such as "hsa" for human miRNAs. The precursor hairpins are designated with "mir", while the mature miRNA are labeled with "miR". Paralogous miRNAs that have minor differences in sequence are designated by a letter suffix (eg. Hsa-miR-376**a**, Hsa-miR-376**b**, Hsa-miR-376**c**). In the event that more than one gene gives rise to an identical mature miRNA, the identifier of the hairpin is followed by a numerical suffix (eg. hsa-mir-218**-1** and hsa-mir-218**-2**). Lastly is the naming of the two strands of the miRNA:miRNA* duplex. Initially, the "*" designation was used for the minor duplex product that was considered to be non-functional, and would result in strand ejection and degradation. However, with further investigation many "*" miRNA strands showed similar expression levels to the guide strand, and exhibited unique biological functions [133,134]. In order to avoid confusion in annotating these miRNA species, the miRNA:miRNA* designation was

retired and replaced with the more conventional -5p (processed from the 5' arm) and -3p (processed from the 3' arm) suffix (hsa-mir-218-1 hairpin: hsa-miR-218-5p and hsa-miR-218-1-3p).

5. MiR-218-5p in Development and Disease

MiR-218-5p is a vertebrate specific microRNA with a high degree of evolutionary conservation. In humans, there are two genes encoding miR-218-5p, *mir-218-1* (4p15.31) and *mir-218-2* (5q35.1), located in *Slit2* and *Slit3* introns, respectively. Processing of the *Slit2* and *Slit3* pre-mRNAs generates mir-218-1 and mir-218-2 precursors, which are further processed to produce mature miR-218-5p. The mature miR-218-5p sequence is the same from both 5' arms of miR-218-1 and miR-218-2 precursors; however, the mature mRNAs formed from the 3' arms are different, and are named miR-218-1-3p and miR-218-2-3p, respectively.

MiR-218-5p is not a tissue specific miRNA and has been reported in a variety of systems. First evidence for miR-218-5p function was in the brain, where its expression correlated with the progression of neuronal differentiation specification [135,136]. It suppresses stem cell self-renewal in part through the direct targeting of Nanog Homeobox (NANOG), a transcription factor involved in maintenance of pluripotency [137,138]. On the other hand, it has shown to promote [139,140] and suppress [141] osteogenic differentiation through different mechanisms.

In accordance with its location, miR-218-5p plays an important role in regulating the Slit-Robo pathway. Slit ligands are best known as molecular guidance cues essential in both nervous and

cardiovascular development, through their binding to the Roundabout (Robo) receptor family [142]. Robo-1 and Robo-2 are functional targets of miR-218-5p, which serves to fine-tune this pathway during complex physiological events such as cardiovascular development and vascular patterning [143,144]. Slits also play an important role in inhibiting tumorigenesis, cancer progression, and metastasis [145]. Both *Slit2* and *Slit3* genes are often hypermethylated in breast, lung, colorectal, and glioma tumors [146,147]. Likewise, the hypermethylation of miR-218-5p genes in cancer has been reported [148,149], and its role as a potent tumor suppressor is well established [150]. MiR-218-5p exerts its action by suppressing a variety of cancer phenotypes, including proliferation, invasion, migration, epithelial–mesenchymal transition, and metastasis [151-153]. MiR-218-5p has also shown to suppress markers of cancer "stemness" [154-156] and restore sensitivity in chemoresistant cells [157-159].

Currently, the role of miR-218-5p in placenta development is not known. However, downregulation of miR-218-5p in preeclampsia has been reported [160], and moreover, studies on the Slit-Robo family may provide insight into the function of miR-218-5p in placenta development. For example, both Slit2 and Robo1 were detected in CTB, STB, and EVT in tubal pregnancies [161,162], whereas overexpression of Robo1 in PE tissue has been reported [163]. In a model of trophoblast vascular remodeling, iEVT near the site of active remodeling were strongly positive for Slit2, but weak for Robo1 [162]. Furthermore, enEVT in later stages of remodeling were both Slit2 and Robo1 positive, and their expression slowly decreased with remodeling progression [163]. Together, these data suggest a multifaceted role for miR-218-5p in placenta development, in both early and late stages of pregnancy.

III. TRANSFORMING GROWTH FACTOR–β (TGF-β) SIGNALING

TGF-β was the first polypeptide characterized from the TGF-β family nearly four decades ago. Its name originates from early work that suggested it was a product of transformed (cancer) cells [164]. We now know that the TGF-β family of cytokines consists of a large group of secretory proteins expressed throughout all mammalian tissues. In canonical signaling, these proteins act through serine/threonine receptor complexes, which upon phoshphorylation recruit intracellular signaling molecules from the Smad (Mothers Against Decapentaplegic homolog) family [165]. Activation of Smads propagates the signal to the nucleus and, through interactions with a variety of transcription factors, are known to regulate hundreds of genes [166]. TGF-β signaling plays an important role in embryo development, tissue homeostasis, and most disease states, including cancer. Smad-independent signaling has been reported [167,168]; however the focus of this introduction will be on the canonical, Smad-dependent, pathway.

1. TGF-β Family: Ligands

Since the discovery of TGF-β1, at least 40 additional TGF-β-related proteins have been characterized. They can be broadly grouped into: TGF-βs, BMPs (bone morphogenetic proteins), GDFs (growth and differentiation factors), MIS (Müllerian inhibitory substance), or Activins/Inhibins. In mammals, there are three isoforms of TGF-β (TGF-β1-3) encoded by separate genes [169]. BMPs make up a large part of the TGF-β family, consisting of approximately 20 members [170]. First identified as critical factors in skeletal development, they are now known to have a variety of important functions including embryogenesis. For example, Nodal (BMP-16) is essential for mesoderm formation and axial patterning in early embryonic development [171].

GDFs are often classified within the BMP family and include an additional 11 molecules, such as Myostatin, known to inhibit muscle cell growth and differentiation [172]. MIS, also known as anti-Müllerian hormone, has predominantly been studied for its role in male sex differentiation, but has recently been suggested as a marker for ovary health and function [173]. Activins were first identified as promoters of FSH (follicle-stimulating hormone) biosynthesis and secretion, while Inhibins are predominantly antagonists of Activins, and to a lesser degree, other TGF-β members. Structurally, they are very similar in that they form dimers consisting of two inhibin-β subunits. In mammals, one Inhibin-α and four Inhibin-β polypeptides (β_A, β_B, β_C, and β_E) have been identified. Inhibins form heterodimers, containing the α subunit and one of the four β subunits. For example, Inhibin A is composed of α -β_A subunits. On the other hand, Activin A is the dimer of two β_A subunits [174].

TGF-β family cytokines are secreted proteins that are first synthesized as long precursor molecules with similar organization. In general, their structure consists of an amino-terminal signal peptide (removed in the ER), a large propeptide, and a carboxy-terminal polypeptide that forms the mature ligand upon proteolytic cleavage. It is these carboxy-terminal segments that display the high sequence similarity shared between TGF-β family members [169]. Notably, it is the number and location of cysteine residues in the carboxy-terminal peptide that are conserved. Specifically, it is an odd number of cysteines (nine or seven) that allows for the intermolecular disulfide-linked dimer formation required for signaling [175]. A few members (such as GFP-3, -9, BMP-15, and Lefty/BMP-17) possess an even six residues, suggesting that these members do not transduce signaling as dimers [169].

2. TGF-β Signal Transduction and Regulation

Initiation of cell signaling begins with the binding of dimerized and active TGF-β family ligands to their receptors (Figure 1.9). Most TGF-β family members exist as both homodimers and heterodimers [169]. While Activins and BMPs are secreted in their active form, TGF-βs remain inactive. Mature TGF-β is formed after the processing of the prodomain from precursor TGF-β polypeptides in the trans-Golgi [176]. However, this propeptide has high affinity for mature TGF-β and remains non-covalently associated upon the secretion of the C-terminal dimer [177]. Since the TGF-β-associated propeptide prevents its interaction with receptors, it is also referred to as the "latency-associated protein" (LAP). Moreover, TGF-βs are known to complex with "latent TGF-β-binding proteins" (LTBPs) that are structurally similar to fibrillins [178]. In this capacity, LTBPs regulate the deposition of TGF-βs into the extracellular matrix, where they can be stored until they are activated. The large latent complex (LLC) consisting of the TGF-β dimer, TGF-β propeptide dimer (or LAP), and the LTBP, provides extensive regulation of the TGF-βs at the ligand level compared to other cytokines in this family [179]. Liberation of the active TGF-β dimer can be achieved through a variety of mechanisms that largely depend on cellular context. These activation mechanisms involve proteases (i.e. plasmin, etc.), thrombospondin-1, integrin binding, extreme pH, and free radicals [176].

This large group of ligands elicits their biological function through a family of structurally related transmembrane receptor kinases with specificity towards serine and threonine residues. In general, the receptors have a short extracellular cysteine-rich domain, a single transmembrane domain, and an intracellular kinase domain [180].

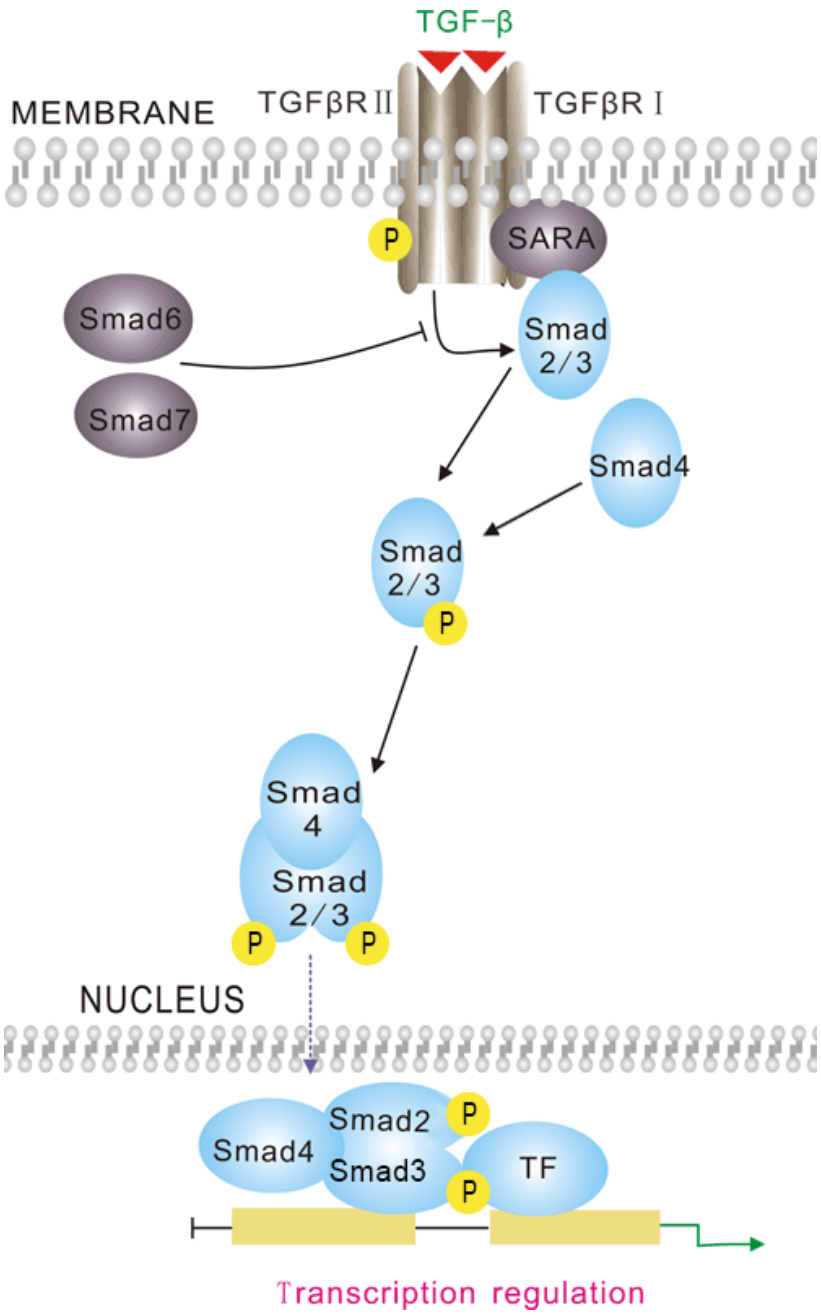

Figure 1.9 Canonical TGF-β Signaling.
Active TGF-β dimers bind to the constitutively active type II receptor **(TGFβRII)**, which subsequently recruits the type I receptor **(TGFβRI)** into the complex. TGFβRI is phosphorylated by interaction with the TGFβRII. Receptor smads (eg. **Smad2/3**) are recruited by **S**mad **A**nchor for **R**eceptor **A**ctivation (**SARA)** to the TGFβRI for phosphorylation. R-Smads oligomerize with other phosphorylated R-Smads and the common smad, Smad4. The Smad complex is translocated to the nucleus where it can then regulate target gene expression or repression. Inhibitory Smads (**Smad6/7**) inhibit the interaction of R-Smads with their Type I receptor. Used with permission from SAB Signaling Antibody www.sabbiotech.com.

The receptor family can be divided into two classes, type II and type I, which differ predominantly with the presence of a glycine-serine (GS) repeat domain in the latter [181]. In spite of the large size of the ligand family, only five type II (TGF-βRII, ACVRII/IIB, BMPRII, and AMHRII) and seven type I (Activin receptor-like kinase (ALK) 1-7) receptors have been identified in mammals.

At the cell surface, the TGF-β receptor family exists as type I and type II homodimers which assemble into heterotetramers at close proximity [181] (Figure 1.9). In general, TGF-β family ligands are known to initiate signaling by binding first to their type II receptors [165] (Figure 1.9). The type II receptors are considered constitutively active and have a characteristic cysteine-rich fold in their extracellular region that is important for ligand binding [182]. Binding of the ligand facilitates their interaction, allowing the type II receptor kinase domain to phosphorylate the GS domain of the type I receptor. Expression of both the type I and type II receptors is required for signal transduction [183]. Alternatively, the inherent affinity between the receptor pair is ligand-independent [184]. This is evident in receptor over-expression experiments where signal transduction was observed even in the absence of ligand [185,186]. However, in most cells, the relatively low number of receptor complexes necessitates the ligand's role in stabilizing the heterotetrameric complex [187].

After receptor activation, the signal is propagated to the nucleus through downstream effectors from the Smad family of proteins (Figure 1.9). The Smad family can be divided into three groups: Receptor Smads (R-Smads), Common Smad (co-Smad), and Inhibitory Smads (I-Smads) [188]. In

general, the six R-Smads (Smad- 1, 2, 3, 5, 8, and 9) consists of an MH1 (Mad homology I) and an MH2 domain that are connected by a linker region. The MH2 domain is required for interaction with the type I receptor, complexing with Smad molecules, and interacting with other regulatory proteins [165]. The MH1 domain is responsible for facilitating DNA binding, as well as interactions with other transcription factors. However, the Smad2 MH1 domain contains an insert that perturbs its DNA binding ability [189]. Unlike the MH1 and MH2 domains, the linker region is poorly conserved between R-Smads and is primarily involved in regulation. One co-Smad (Smad4) has been identified, and has the ability to complex with all R-Smads. Like R-Smads, it contains a MH1 and MH2 domain, but its MH2 domain lacks the C-terminal SSXS (Ser-Ser-X-Ser) motif required for phosphorylation by the type I receptor [190]. Furthermore, the I-Smads (Smad 6 and 7) have no distinct MH1 domain, but do contain MH2, allowing them to interact with the type I receptor and block activation of R-Smads [191].

TGF-β signaling has the capacity to elicit a vast number of unique biological responses through a limited number of mediators. This can be explained in part through receptor promiscuity. Transduced signals are broadly grouped into either BMP-like or TGF-β/Activin-like transcriptional responses. While the type II receptors often cross between these two classes, type I receptors tend to be more specific [180]. In general, BMP-like signals activate Alk-1, Alk-2, Alk-3, and Alk-6, whereas TGF-β/Activin-like signals engage Alk-4, Alk-5, or Alk-7 type I receptors. Similarly, R-Smads activated by the type I receptors can typically be classified as downstream of the BMP-like pathways (Smad1/5/8) or TGF-β/Activin pathways (Smad2/3) (Figure 1.10).

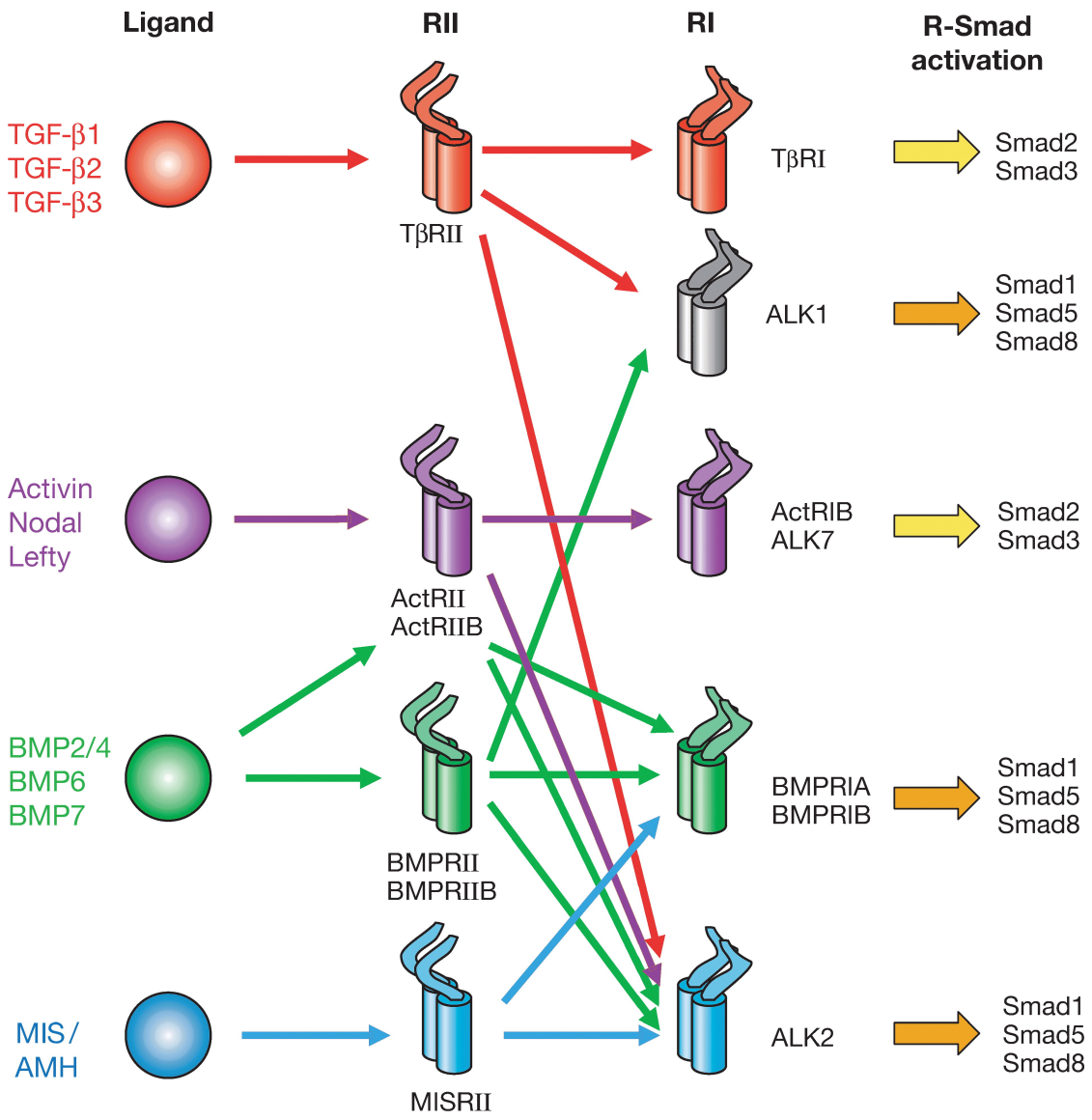

Figure 1.10 Combinatorial interactions of serine-threonine kinase receptors and their downstream effectors.

Five type II**/RII** (TGF-βRII, ACVRII/IIB, BMPRII, and AMHRII) and seven type I/**RI** [Activin receptor-like kinase (Alk) 1-7] receptors have been identified in mammals. In general, BMP-like signals activate Alk-1, Alk-2, Alk-3, and Alk-6, whereas TGF-β/Activin-like signals engage Alk-4, Alk-5, or Alk-7 type I receptors. Likewise, the R-Smads activated by the type I receptors can typically be classified as downstream of BMP-like pathways (Smad1/5/8) or TGF-β/Activin pathways (Smad2/3)**.** Used with permission from Feng X-H, et al. (2005) [196].

Cofactors, such as SARA (Smad Anchor for Receptor Activation), are required to present the R-Smads to the phosphorylated GS domain of type I receptors [192]. The R-Smads are consequently phosphorylated by type I receptors and become available for Smad4 oligomerization [165]. R-Smads are often found in trimeric complexes with co-Smad4 as either homodimers or heterodimers. Discordant with previous studies, Smad4 is not required for nuclear translocation as observed in Smad4-null cells [193]. Several mechanisms mediate nuclear translocation depending on which Smads are involved, such as the Importin-β1/Ran system or CAN/Nup214 [194,195]. In general, shuttling of Smads into the nucleus involves release from cytoplasmic anchors, exposure of their nuclear localizing signal (NLS), or the blocking of their nuclear export signal (NES) [165].

Once in the nucleus, the R-Smad/Co-Smad complex can bind to DNA and promote or repress gene transcription. On their own, Smads have a low affinity for DNA and their binding-activity is not highly selective [197]. Although they are known to bind Smad binding elements (SBE) with a CAGA motif as well as GC-rich sites, no TGF-β- or BMP-responsive promoter sequence common to all target genes has been identified [198]. Hence, the regulation of Smad target genes depends heavily on their partnered DNA-binding transcription factors and transcription co-repressors or co-activators. Smads have been reported to interact with a variety of transcription factor families including: bHLH (basic/helix-loop-helix), bZIP (basic/leucine zipper), forkhead, zinc-finger, and Runx [198].

The TGF-β pathway is regulated at all levels of signal transduction in order to fine tune cellular

responses. As previously mentioned, the first level of control is the activity and availability of ligands. Unlike the TGF-βs, other cytokines in the family are secreted in their active form and rely largely on accessory proteins for regulation [199]. Follistatin, discovered as an inhibitor of Follicle-stimulating hormone (FSH) release, has high affinity for Activin and blocks its action through masking the type I and type II receptor binding sites [200]. Similarly, Noggin binds BMPs, preventing receptor interaction, which is essential for proper neural, somite, and skeletal development [201]. Decorin, an extracellular protein from the small Leucine-rich proteoglycan family, is also known to attenuate TGF-β signaling pathways [202]. Like Inhibins, other TGF-β members can also negatively regulate ligand availability. For example, Lefty proteins are important negative regulators of Nodal signaling, as demonstrated during left-right axis determination during embryonic development [203,204].

The composition of the activated receptor complex heavily defines the resulting transcriptional response. Furthermore, the availability of co-receptors also greatly influences possible signaling outcomes. TGF-β type III receptor (Betaglycan) is required for efficient TGF-β2 binding to its type II receptor [205]. It also serves as an Inhibin co-receptor which lowers the concentration of Inhibin needed to disrupt Activin signaling [206]. Endoglin has been reported to participate in a variety of TGF-β receptor complexes, and is known to promote or suppress both TGF-β responses, depending on cellular context [207-209]. Cripto is another important co-receptor that facilitates Nodal signaling through Alk-4, while antagonizing Activin [210].

Apart from activation of the receptor complex, ligand binding induces receptor internalization

into endosomes [211]. Endocytic regulation of TGF-β signaling is important in order to determine if the signal will be enhanced through clathrin-coated pits, or turned off through lipid raft-mediated endocytosis [212]. From the receptor complex, the signal is further modulated intracellularly through the availability and activity of R-Smads. As previously mentioned, proteins such as SARA facilitate access of Smads to their cognate receptors, while I-Smads have the opposite effect [213]. Smad activity can further be regulated through a variety of modifications, including phosphorylation of the linker region, dephosphorylation by phosphatases, and ubiquitin-mediated degradation [198].

3. Role of TGF-β Signaling in Placenta Development and PE

Placental development is a complex process involving a number of specialized cell types that require specific spatial and temporal regulation for a successful pregnancy. Expression of TGF-β family molecules has been reported on both the fetal and maternal sides of the placenta. They are important players at the maternofetal interface, regulating a variety of processes including decidualization, formation of the trophectoderm, implantation, differentiation down the fusion or invasive pathway, and maintenance of pregnancy. Furthermore, many TGF-β family members are dysregulated in PE and a few have been identified as potential clinical biomarkers.

On the maternal side, the process of endometrial decidualization is vital to embryo implantation. The expression of both type I and type II Activin receptors in endometrial stroma and endothelial cells suggest they are capable of responding to Activin signals [214]. Co-expression of the Activin regulators Follistatin, Betaglycan, and Inhibin, suggest that Activin action during

this process is tightly regulated. Furthermore, Activin A was shown to directly promote decidualization of endometrial stroma *in vitro* [215]. TGF-β signaling through ALK-5 promotes the decidual enrichment of pregnancy-associated growth factors, cytokines, and the maturation of dNK needed for maternal immune tolerance and spiral artery remodeling [216]. Whereas BMP signalling through Alk-3 is essential for the attachment of the blastocyst to the decidua during implantation [217].

In early placentation, BMP-2 and BMP-4 promote the differentiation of human embryonic stem cells (hESC) into the trophoblastic lineage [218]. Nodal/Activin signaling can further dictate the terminal differentiation of hESC-derived trophoblasts. Inhibition of Activin/Nodal signaling leads to formation of EVTs, while the loss of inhibitors associated with this pathway promote fusion into STBs [219]. Conversely, in proliferating CTBs Activin A promotes the differentiation of EVTs along with invasive markers such as MMP-2 and MMP-9 [220]. Activin A also has a positive role on trophoblast proliferation, while Nodal acting through Alk-7 inhibits trophoblast proliferation and promotes apoptosis [221]. TGF-β, Nodal and their receptors, Alk-5 and Alk-7, also have an inhibitory role on trophoblast proliferation [222,223].

TGF-β signaling further regulates the functions of both STB and EVT lineages. Activin A stimulates, while TGF-β1 inhibits the production and secretion of pregnancy maintenance hormones hCG, Progesterone, and Estradiol [224-227]. However, the effect of TGF-βs on STB fusion [222,228] and the role of TGF-βs and Nodal on trophoblast invasion have been inconsistent. In general, TGF-β1-3 inhibit differentiation towards the invasive EVT pathway in part by

upregulating TIMPs and E-Cadherin, while downregulating urokinase plasminogen activator (uPA) and MMP-9 [229-233]. On the other hand, the TGF-β suppressive effects are lost in choriocarcinoma cell lines, possibly due to Smad3 deficiency [229]. Furthermore, Smad ubiquitination regulatory factor 2 (Smurf2) exhibits highest expression in first trimester placenta, and promotes trophoblast invasion and migration *in vitro* via Alk-5 degradation [234]. Nodal inhibits trophoblast invasion through ALK-7, and not through ALK-4 signaling [235]. Conversely, Nodal was shown to promote trophoblast invasion possibly via a Smad-independent mechanism involving β-arrestin/Ral and Erk1/2 [236]. Activins promote trophoblast invasion through several mechanisms, including MMP-2 upregulation through ALK-4, and Smad2/3/4-dependent upregulation of N-cadherin [237,238]. Furthermore, Myostatin expression was localized to the EVT population and promoted trophoblast proliferation and migration *in vitro* [239]. Studies investigating the role of TGF-β in spiral artery remodeling are limited. However, Activin A has shown to promote trophoblast endothelial-like tube formation *in vitro* through Smad2/3/4-dependent upregulation of VEGF-A [240].

The dysregulation of TGF-β signaling in PE is well supported. The soluble form of the co-receptor Endoglin is one of the most upregulated anti-angiogenic markers in serum of PE patients [241]. Similarly, serum Activin A levels in women affected with PE were greatly increased even prior to onset of clinical symptoms [242,243]. Furthermore, Activin A mirrored PE serum-induced oxidative stress, and endothelial activation and dysfunction in Human Umbilical Vein Endothelial Cells (HUVEC) [244,245]. Nodal and ALK-7 immunoreactivity were also strongly upregulated in PE placenta tissues [235]. Interestingly, pathological levels of Activin A were shown to induce

trophoblast apoptosis through the upregulation of Nodal [246]. Activin Receptor Type II (ACVRII) has been implicated as a genetic risk factor for PE, due to a single nucleotide polymorphism (SNP) in its promoter region [247,248]. A recent study proposed that the downregulation of ACVRII due to this SNP, in combination with pathological levels of Activin A, resulted in the increase of Nodal in PE cases [249]. SNPs in *TGFB1* have also been reported in several small case studies [250-252]. Serum TGF-β1 and TGF-β2 levels were also elevated in PE cases [253,254], while inhibition of TGF-β3 in PE tissues restored their invasive capacity *in vitro* [255].

IV. RATIONALE, HYPOTHESIS, AND OBJECTIVES

During normal pregnancy, EVTs invade the uterus and differentiate into interstitial and endovascular trophoblasts. The enEVTs go on to remodel maternal spiral arteries by replacing the endothelial cells and some portion of the smooth muscle wall [7]. In PE, shallow invasion of EVTs results in insufficient remodeling of the maternal vasculature, reducing placental perfusion for adequate nutrition and oxygen exchange. Furthermore, EVTs in PE fail to acquire the endovascular phenotype suggesting that upregulation of endovascular genes is required for successful placentation [65].

The role of TGF-β signaling in reproduction has been the primary focus of our lab. In previous studies we have demonstrated that Nodal inhibits trophoblast cell proliferation, migration, and invasion while promoting apoptosis [221,235]. Furthermore, we have reported that Nodal and its receptor ALK-7 were overexpressed in PE placentas [235]. TGFD-1, -2 or -3 have also been reported as negative regulators in trophoblast migration and invasion [231,233]. Likewise, miRNA suppression of Smad2 was shown to have pro-invasive effects on first trimester trophoblasts [160].

Reports of miRNAs regulation in development and disease are increasing. However, the function of miRNA in placental development and pathology is still poorly understood. A microarray study from our collaborators revealed that there are a number of miRNAs aberrantly expressed in PE placentas compared to their gestation-age matched controls. We were interested in selecting a dysregulated miRNA that has potential in regulating TGF-β family members. We identified the specific down-regulation of miR-218-5p in PE, consistent with previous microarray-based

screening studies [160,256]. *In silico* analysis of potential miR-218-5p gene targets revealed an enrichment of many TGF-β signaling molecule targets including TGF-β2, Nodal, Smad2, and Smad3.

Since dysregulation of EVT invasion into the uterus and the subsequent failure in the remodeling of the maternal spiral arteries are the key mechanisms that underlie the development of PE, we investigated the role of miR-218-5p in these processes. Our preliminary findings indicated the miR-218-5p promoted trophoblast invasion and suppressed TGFβ signaling. Therefore, we hypothesize that miR-218-5p is involved in the pathogenesis of PE in part by regulating TGFβ signaling. It is postulated that a down-regulation of miR-218-5p may lead to upregulated TGFβ signaling, which in turn, results in shallow invasion of trophoblast cells into the decidua and poor remodeling of spiral arteries.

The overall objectives of my study were to 1) Determine miR-218-5p function in differentiation of the EVT pathway. 2) Investigate the TGFβ mechanism responsible for miR-218-5p action in EVT differentiation. 3) Further characterize the TGFβ pathway in enEVT differentiation.

CHAPTER 2: MIR-218-5P PROMOTES ENDOVASCULAR TROPHOBLAST DIFFERENTIATION THROUGH SUPPRESSION OF TGF-β SIGNALING

Brkić J., Dunk C., O'Brien J., Fu G., Nadeem L., Yang P., Lye S., Peng C.[1]

SUMMARY

MicroRNAs (miRNA) are small non-coding RNAs that play important roles in developmental and physiological processes. In this study, we examined the expression and function of miR-218-5p in the human placenta. We show that miR-218-5p was highly expressed in second trimester and its level was significantly downregulated in placentas obtained from patients with preeclampsia (PE). Since dysregulation in the invasion of extravillous trophoblasts (EVTs) into the uterus and the subsequent failure in the remodeling of the maternal spiral arteries are the key mechanisms that underlie the development of PE, we investigated the role of miR-218-5p in these processes. The functional role of miR-218-5p was assessed using the immortalized first trimester trophoblast cell line HTR8/SVneo and first trimester human tissues. Overexpression of miR-218-5p promoted, while anti-miR-218-5p suppressed, trophoblast migration, invasion, EVT outgrowth, and markers of enEVT differentiation. Furthermore, miR-218-5p accelerated spiral artery remodeling in a first trimester decidua-placenta co-culture. The promoting effect of miR-218-5p in enEVT pathway differentiation was mediated by the suppression of TGFβ signaling.

[1] Dr. Dunk performed the bioplex assay in Supplementary Figure 2.2 with samples I provided. In addition, the analysis of the *in vitro* trophoblast mediated decidua vessel remodelling experiments (Figure 2.5) greatly relied on her expertise. Jake O'Brien performed the experiments in Supplementary Figure 2.3. Dr. Fu generated the Mir-218 hairpin-containing construct that I used to generate stable cells. He also performed one invasion experiment on HTR8/SVneo cells that was pooled into Figure 2.4A (left panel) with my other trials. He also processed the tissues for RNA from clinical samples that I used in this study. Dr. Nadeem performed one EVT outgrowth experiment with first trimester placenta tissues that was pooled into Figure 2.4C with my other trials. Dr. Yang performed one of the TGF-β2 invasion assays that was pooled into Figure 2. 6F with my other trials.

Specifically, miR-218-5p suppressed TGF-β2 and supplementing TGF-β2 back into the cell culture reversed some of the effects of miR-218-5p. Taken together, our data suggest that miR-218-5p promotes trophoblast migration, invasion and differentiation into enEVTs in part through a novel miR-218-5p-TGF-β2 pathway. This study is first to elucidate the role and mechanism of a miRNA in enEVT differentiation that is required for spiral artery remodeling and proper placentation.

INTRODUCTION

A successful pregnancy is dependent on the health and functionality of the placenta, which requires the precise and coordinated differentiation of cytotrophoblast cells (CTBs) into both syncytiotrophoblast (STB), which cover the villous tree, and the extravillous trophoblasts (EVTs) that invade the decidua, reaching as far as the inner third of the myometrium. A subset of EVTs further differentiates into endovascular EVTs (enEVTs) that are directly involved in the process of maternal uterine spiral artery remodeling. The remodeling of the uterine spiral arteries into large dilated sinusoids is essential for the adequate perfusion of the placenta to support and sustain the increasing requirements of the growing fetus [257]. The molecular mechanisms governing the development of these two distinct EVT subtypes are now a major focus of the placental research field [258].

Great Obstetrical Syndromes are associated with disorders of deep placentation, collectively affecting 15% of pregnancies worldwide [259,260]. The greatest proportion is attributed to preeclampsia (PE), the leading direct cause of maternal and neonatal morbidity and mortality [59]. Currently, PE is described as a two-stage disorder. In the first stage, shallow EVT invasion into the decidua along with poor enEVT mediated remodeling of spiral arteries remains a key precursor to stage two, the oxidative stress and ischemia-reperfussion injury, leading to increased shedding of necrotic placental debris and systemic maternal endothelial dysfunction [261]. The diagnosis of PE is currently limited to late second trimester at the onset of clinical maternal symptoms, and predictive markers remain unreliable to date [262].

Most recently much interest has focused on the pool of RNA regulatory factors including the miRNAs; many of which have been identified in the placenta and are thought to play an active role in the regulation of trophoblast and endothelial cell turnover and fate [263,264]. Furthermore the recent discovery of miRNAs in the maternal serum has suggested their potential use in noninvasive prenatal diagnostics [91].

MiR-218-5p is processed from two precursor genes, *mir-218-1* and *mir-218-2*, encoded in introns of *Slit2* and *Slit3*, respectively. Initial studies investigating the Slit-Robo pathway focused on its role as a guidance cue important for proper neuronal and vascular development [143,265-268]. The Slit-Robo pathway has been investigated at the feto-placental interface suggesting its involvement in STB function and angiogenesis in the placental bed [163,269], and Slit-2, Robo-1 and Robo-4 are reported to be lower in PE placentas [270]. Interestingly, a recent study on human tubal pregnancies reported that migratory iEVT and actively remodeling enEVT were both strongly positive for Slit2 [162]. More recent studies suggest that miR218-5p is a tumor suppressor and a potential prognostic and predictive biomarker in a variety of cancers [271-274]. MiR-218-5p is expressed in human placenta and its levels are also down-regulated in PE placental tissues [160,275]. However, the functional role of miR-218-5p in the placenta has not been reported.

The transforming Growth Factor (TGF)-β family is a large group of multifunctional peptide growth factors that play fundamental roles in many cellular processes, such as cellular proliferation, differentiation, apoptosis, and angiogenesis [276]. They signal through a complex of type-I and type-II serine/threonine receptors. Upon phosphorylation of the type I receptor by

the type II receptor, a family of intracellular signaling molecules, Smads, are activated propagating the signal to the nucleus. Many studies, including those from our lab, have demonstrated that the TGFβ signaling pathway plays important roles in regulating trophoblast survival, proliferation, and invasion [223,277,278].

In this study, we investigated the expression and function of miR-218-5p in human placenta. We confirmed that miR-218-5p was decreased in PE placental tissues as has previously been shown [160,275]. Using both established cell lines and human tissues, we demonstrate that miR-218-5p promotes enEVT differentiation and accelerates the spiral artery remodeling process *ex vivo*. We also identify TGF-β2 as a gene inhibited by miR-218-5p and observed that treatment with recombinant human TGF-β2 suppresses differentiation into enEVT. Our study reveals a novel miR-218-5p mediated mechanism regulating enEVT differentiation that may contribute to the uteroplacental pathology associated with PE.

MATERIALS AND METHODS

Patients and Tissue Collection

All fresh and frozen human tissues used in this study were collected through the BioBank program at the Research Centre for Women's and Infants' Health at Mount Sinai Hospital (Toronto, ON, Canada), and approved by the Mount Sinai Hospital Research Ethics Board. Placental and decidual tissue samples from first and second trimester were collected with informed consent from healthy patients undergoing elective termination of pregnancy at the Morgentaler Clinic, Toronto. At the point of collection the research nurse excluded all samples with known HIV or Hepatitis infection and any that have been classified as a missed miscarriage. Third-trimester placentas were from vaginal delivery or cesarean section with Appropriate for Gestation Age babies. For the evaluation of miR-218-5p expression across gestation, 72 placentas were used. Specifically, 13 from first-trimester (5-12 weeks), 12 from second-trimester (13-25 weeks), 23 from pre-term (26-36 weeks), and 24 from term (37-40 weeks) were analyzed. To assess if there is dysregulation of miR-218-5p in preeclampsia, we used 16 placentas from PE patients delivered pre-term, and 11 placentas from PE patients delivered at term. Control preterm tissues were collected from laboring cesarean deliveries after fetal distress or from premature rupture of membrane spontaneous labor. Examination by a placental pathologist determined that all control preterm placenta lacked gross abnormalities or signs of chorioamnionitis. Clinical data for PE patients and the controls are summarized in Table 2.1.

Table 2.1 Clinical Data for PE patients and Controls

	Pre-Term Control	Pre-Term PE	Term Control	Term PE
Gestational age (week)	29.83±0.51	30.27±0.36	38.32±0.14	36.55±0.41
Maternal age	31.95±1.15	30.8±1.85	33.36±0.73	34.8±2.21
Systolic blood pressure (mmHg)	120.56±2.9	165.13±2.93	118.88±2.11	166.8±6.05
Diastolic blood pressure (mmHg)	73.83±2.27	106.67±1.9	77.04±1.79	101.2±1.46
Proteinuria	–	3.46±0.13	–	2.41±0.25

Mean ± SEM, PE: preeclampsia

Cell culture

An immortalized human first trimester trophoblast cell line, HTR8/SVneo, was obtained from Dr. Charles Graham (Queen's University, Kingston, ON, Canada), and was cultured as previously described [279]. Briefly, cells were maintained in HyClone™ Classical Liquid Media RPMI 1640 - With L-Glutamine (Fisher Scientific) supplemented with 10% Fetal Bovine Serum (FBS) (GIBCO), Streptomycin (100μg/ml), and Penicillin (100 IU/ml), in an atmosphere of 5% CO_2 at 37°C. Cells were periodically checked for mycoplasma contamination using a Mycoplasma Detection Kit-QuickTest (BioTools), and when needed, treated with MycoSmash Mycoplasm Removal Kit (BioTools) following the manufacturers directions. All experiments were carried out on cells in between passage 73 and 85.

Transfections and Recombinant Protein Treatment

Transient transfection of miRNA or siRNA oligomers (100nM) was carried out using Lipofectamine RNAiMax (Invitrogen). All plasmid transfection were carried out using Lipofectamine 2000 (Invitrogen). A modified protocol was used to optimize for transfection efficiency and cell survival. Transfections were carried out in 6-well plates on 70% confluent cultures. For each transfection reaction, 2μl of lipofectamine reagent was used and incubated with nucleotides for 15min at room temperature in Opti-MEM media (GIBCO). Transfections were carried out for 5h, then allowed to recover with 10% FBS containing media for 16hr. Cells used for marker analysis were allowed to recover for an additional 24h in serum-free media. MiR-218-5p, siTGFβ2, siSmad2 and non-targeting negative controls were purchased from GenePharma Co. (Shanghai, China) (Table 2.2). MirVana™ anti-miR-218-5p and a negative control were purchased from Ambion. Recombinant human TGF-β2 protein (R&D) was used at

10ng/mL in serum-free media. Cells for marker experiments were treated for 24h, while cells for functional assays were pre-treated overnight prior to seeding for downstream assays.

Generation of Mir-218 stable cells

A portion of the Slit2 intron (NG_047105; 281231 to 281568 bp) bracketing the Mir-218-1 stem-loop sequence was cloned into a GFP expressing pEGP-miR vector in the NheI/BamHI cut site using FP: TCGGTAGTAATACTCTTACTGTGGTC and RP: CAAGG-CAAATAGATATACTCAGGC. HTR8/SVneo cells were subsequently transfected with the empty pEGP-miR vector (referred to as EV) or Mir-218-1 construct, followed by addition of 2µg/ml Puromycin treatment for two weeks. All viable colonies were assessed for overexpression by detecting green fluorescent protein (GFP) signal and by measuring miR-218-5p levels.

RNA Extraction, Reverse Transcription and qRT-PCR

Total RNA from cells and tissues was extracted using TRIzol reagent (Invitrogen) as per manufacturer's protocol. Reverse transcription was performed on 1.5µg total RNA with M-MuLV Reverse Transcriptase (New England Biolabs). All miRNA quantification was performed with the NCode™ miRNA First-Strand cDNA Synthesis Kit (Thermo Fisher), following the manufacturer directions. Quantitative Real Time PCR (qRT-PCR) was carried out with EvaGreen qPCR Master Mix (ABM), following manufacturer directions, on a RotorGene Q thermocycler (QIAGEN). MiR-218-5p levels were normalized to U6 snRNA levels, and all other genes were normalized to Cytochrome c1 (Cyc1). The relative mRNA level was calculated using the $2^{-\Delta\Delta ct}$ method. All primers (Table 2.2) used in this study were validated for specificity with primer-BLAST (NCBI), and amplified products were run on an agarose gel to ensure a single band product.

Microarray

A gene expression analysis was conducted at the Princess Margaret Genomics Centre on a mir-218-1 overexpressing cell line and a control EV cell line (n=3), using the Human HT-12 V4 BeadChip, which comprises a total of 47323 probes. Data were checked for overall quality using R (v3.0.2) with the Bioconductor framework and the LUMI package installed. Data were imported in GeneSpring v12.6 for analysis. During import, the data were normalized using a standard (for Illumina arrays) quantile normalization followed by a "per probe" median centred normalization. Only probes that were above the 20th percentile of the distribution of intensities in 100% of any of the groups were allowed to pass through the filtering. A one-way ANOVA with a Benjamini-Hochberg FDR corrected $p<0.05$ showed 4106 significantly varying probes. Heat maps were created using the MultiExperiment Viewer (MeV) Microarray Software Suite.

EVT Column Markers

First-trimester placentas were collected as described above. Tissues between 8-10 weeks of gestation were dissected for EVT-containing villi. To assess changes in desired gene markers, the tips of villi were carefully dissected with curved scissors and incubated with 200nM of miR-218-5p, anti-miR-218-5p, or non-targeting control oligomers, in serum-free DMEM-F12 phenol-red free media (Life Technologies) at 37°C with 3% O_2 and 5% CO_2. For each treatment group within the experiment, approximately 50 villi tips were used. After 48hr, tissues were collected, snap frozen in liquid nitrogen and stored at -80°C until further processing for RNA extraction. Due to tissue size, only one to two replicates were used per trial, and each experiment was repeated on at least five unique tissues.

Table 2.2 Primers and Oligomers

Name	Sequence: 5' → 3'	NCBI BLAST
Cyc1	**F:** CAGATAGCCAAGGATGTGTG **R:** CATCATCAACATCTTGAGCC	Cytochrome c1
VE-cad	**F:** GCCAGTTCTTCCGAGTCACA **R:** TTTCCTGTGGGGGTTCCAGT	Cadherin 5
PECAM1	**F:** ATTGCAGTGGTTATCATCGGAGTG **R:** CTCGTTGTTGGAGTTCAGAAGTGG	Platelet and Endothelial Cell Adhesion Molecule 1
MMP1	**F:** GTCTCACAGCTTCCCAGCGA **R:** ATGGCATGGTCCACATCTGC	Matrix Metallopeptidase 1
IL1b	**F:** AATCTGTACCTGTCCTGCGTGTT **R:** TGGGTAATTTTTGGGATCTACACTCT	Interleukin 1 beta
IL8	**F:** CAGAGACAGCAGAGCACACA **R:** GGCAAAACTGCACCTTCACA	C-X-C motif chemokine ligand 8
ECSCR	**F:** ACAACTCCCAGCCCACAATG **R:** GTGGTCAGACTTAGACCGCC	Endothelial Cell-Specific Chemotaxis Regulator
CXCL1	**F:** CAGGGAATTCACCCCAAGAACA **R:** GGATGCAGGATTGAGGCAAGC	C-X-C motif chemokine ligand 1
ITGA1	**F:** GCTGGCTCCTCACTGTTGTT **R:** CACCTCTCCCAACTGGACAC	Integrin subunit alpha 1
TGFβ2	**F:** ATTGATGGCACCTCCACATATA **R:** ACGTAGGCAGCAATTATCCTG	Transforming Growth Factor beta 2
miR-218-5p	**F:** TTGTGCTTGATCTAACCATGT **R:** N-Code Universal Primer	N/A
U6 snRNA	**F:** CGCAAGGATGACACGCAAATTC **R:** N-Code universal primer	N/A
siTGFβ2	**Sense:** ACCAAATACTTTGCCAGAAACTAT **Anti-sense:** ATAGTTTCTGGCAAAGTATTTGGT	Transforming Growth Factor beta 2
siSmad2	**Sense:** GUCCCAUGAAAAGACUUAAtt **Anti-sense:** UUAAGUCUUUUCAUGGGACtt	SMAD family member 2
NC	UUCUCCGAACGUGUCACGUtt ACGUGACACGUUCGGAGAAtt	No match
hsa-miR-218-5p	**Sense:** UUGUGCUUGAUCUAACCAUGU **Anti-sense:** ACAUGGUUAGAUCAAGCACAA	
Anti-NC	mirVana™ miRNA Inhibitor, Negative Control #1	
Anti-hsa-miR-218-5p	hsa-miR-218-5p mirVana™ Inhibitor	

Transwell Migration and Invasion Assay

Transwell inserts with 8 µm pores (Costar, Corning Inc) were coated with 150 µg/ml Matrigel in serum free media (Cultrex Reduced Growth Factor BM extract-PathClear, Trevigen) and allowed to polymerize overnight at 37°C. Cells were gently removed from culture plates using Accutase (Innovative Cell Technologies), and seeded at a density of 20,000 cells per well in serum-free RMPI-1640 media. As a chemotactic agent, 10% serum containing medium was seeded on the outside of the transwell. After 24h, membranes were fixed for 2 min in 100% methanol and stained using Harleco Hemacolor Staining Kit (EMD Chemicals). Similarly, for migration assays 10,000 cells per well were seeded on 8 µm pore transwell membranes without any matrigel coating. Invaded or migrated cells were counted with ImageJ [280] and the invasion/migration index was calculated as a fold of invaded/migrated cells in the treated groups compared to the control group. Each experiment was repeated in a minimum of three independent trials.

First-Trimester Human Placental Explant Culture

Explant cultures were performed as previously described [277,281]. Briefly, villous explants with potential EVT columns were carefully dissected and positioned on Transwell inserts (Millipore) pre-coated with 200µL of undiluted phenol red-free Matrigel (BD Biosciences). Explants were left overnight to attach to the matrigel, at 37°C with 3% O_2 and 5% CO_2, before adding serum-free DMEM-F12 media supplemented with 100 U/ml of penicillin, 100 U/ml of streptomycin, 100 µg/ml Normacin™. After two days of culture, villous tips were examined under the dissecting microscope for successful EVT outgrowths. All successfully attached explants were selected for treatment with 200nM oligomers (Table 2.2). Explants were photographed immediately after adding treatment, and subsequently at 24 and 48hr, using a Leica DFC400

camera attached to a dissecting microscope. ImageJ was used to measure the area of EVT outgrowth. Specifically, total outgrowth area was calculated by subtracting the area at the end of the treatment with the initial area before treatment. Each experiment was designed with a minimum of four replicates, and was repeated on at least three unique placenta samples.

First-Trimester Placenta-Decidua Explant Co-culture

Placenta-decidua co-culture was performed as previously described [282]. Briefly, small sections of decidua parietalis and placental villi with EVT columns from the same patient were carefully dissected from tissues collected as described. Decidua were carefully placed at a 45° angle, epithelial side facing up, on Transwell inserts (Millipore) pre-coated with 120µL of undiluted phenol red-free Matrigel (BD Biosciences). Placental explants were placed in serum-free medium containing 200nM miR-218-5p or non-targeting control (NC). Tissues were incubated at 37°C with 3% O_2 and 5% CO_2 for 24h. Treated placenta explants were carefully washed five times in 1X Phosphate Buffered Saline to remove residual oligomers. Villi were gently placed on the exposed epithelial surface of decidua and anchored with 50ul of matrigel. Tissues were covered with serum-free DMEM-F12 media supplemented with estradiol (0.3ng/mL) and progesterone (20ng/mL), and allowed to incubate for an additional six days, at which point the tissues were fixed in 4% paraformaldehyde (Electron Microscopy Sciences) for 1hr. Tissues were dehydrated in ascending concentration of ethanol, cleared in xylene, and embedded in paraffin. Blocks were sectioned to 5 µm thickness, and every tenth slide was histologically assessed by standard Haematoxylin and Eosin staining. Decidua alone samples served as a control to ensure selected tissue was not decidua basalis in origin. Experiment was performed on three individual placenta-decidua matched tissues with similar findings.

Immunohistochemical analysis

Immunohistochemical analysis was performed using the streptavidin peroxidase method as previously described [282]. Paraffin-embedded tissues were baked overnight, de-waxed in xylene, and rehydrated in descending grades of ethanol, and incubated in 3% hydrogen peroxide in methanol for 50 min to quench any endogenous peroxidase activity. Antigen retrieval for all antibodies used was performed by briefly boiling slides in 10mM sodium citrate. A blocking buffer of 10% goat serum and 2% rabbit serum (Dako X0909) was used in a humidified chamber for 1h at room temperature following an overnight incubation at 4°C in primary antibody (Table 2.3). Incubation with mouse IgG (1:100, Dako, X0931) in place of primary antibody served as a negative control. Excess antibody was washed off and subsequent incubations with anti-mouse or anti-rabbit biotinylated secondary antibody (1:300, Dako E0464 and E0432) and the streptavidin-HRP conjugated tertiary reagent (Invitrogen SA1007) were performed for 1h each at room temperature. Specific signals were detected using a Dako DAB staining kit containing 0.02% H_2O_2 and 0.075% 3,3′-diaminobenzidine in 1×PBS. Slides were counterstaining using Harris hematoxylin (1:2; Sigma-Aldrich Corp.), and dehydrated in ascending series of ethanol, cleared in xylene, and mounted with Cytoseal (Fisher Scientific). Photographs were taken with an Olympus DP72 camera mounted on a BX61 Olympus microscope using the cellSens standard program.

Reporter Constructs and Luciferase Assay

Luciferase 3'UTR reporter constructs were generated by cloning a portion of the 3'UTR, containing the proposed miR-218-5p seeding sequence, into pMIR REPORT™ miRNA Expression Reporter (Ambion), downstream of a luciferase gene. Specifically, TGFB2 3'UTR was amplified

from nucleotide 178 to 813 with primers TGFB2 3'UTR1 FP: AGGACTAGTAGTATGCA-AGTGGGCAGCAA and TGFB2 3'UTR1 RP: ACTACGCGTACAAC-CAACCCCAGAAAGCA. Both constructs were cloned using the SPEI and MLUI restriction enzyme cut sites. Luciferase assays were performed using the Dual-Luciferase® Reporter assay system as per manufacturer's direction (Promega). Renilla construct (10ng/mL) was co-transfected with all experiments as a normalization control. TGF-β signaling was assessed using the PAR3-Lux reporter and FAST2 as previously described [283].

Primary HUVEC isolation

Umbilical cords of term placentas were collected from Mackenzie Richmond Hill Hospital after caesarean delivery. The use of tissues was approved by the research ethics committee at Mackenzie Health and patients provided informed consent. Human Umbilical Vein Endothelial cells (HUVEC) were isolated as previously published [284]. In brief, umbilical veins were washed with 1x Hank's Buffered Salt Solution (CellGro 21-021CV), and injected with 0.1% Collagenase Type I (Worthington) prepared in 1x Dulbecco's PBS (GIBCO 14287). The cells were allowed to dissociate for 15 min at 37°C. Cells were plated in M199 media (GIBCO) supplemented with 10% FBS, streptomycin (100µg/ml) and penicillin (100 IU/ml), and 5mg/mL Endothelial Cell Growth Supplement (BD BioScience). Validation of HUVEC isolation was performed each time by examining morphology and positive staining for VEGF-A and PECAM-1, and discarded after ten passages.

Network Formation Assay and HUVEC Co-culture

On ice, 96-well plates were quickly coated with 50µl of matrigel (Celtrex Reduced Growth Factor BM extract-PathClear, Trevigen), and allowed to polymerize at 37°C for 30min. For network

formation assays, 25,000 HTR8/SVneo cells were seeded per well in 100ul of 10% FBS containing RPMI1640. After 16-20h of culture, cells were stained with 1µM Calcein AM (Corning) for 15min, and pictures were taken at 20X magnification on a fluorescence microscope. For co-culture assays, HUVEC and HTR8/SVneo cells were stained for 45min with 1µM CellTracker™ Red CMTPX (Invitrogen) or CellTracker™ Green CMFDA (Sigma-Aldrich), respectively. Once stained, cells were seeded in a one to one ratio with a total of 25,000 cells per well. Total network length was quantified in ImageJ using the NeuronJ plugin [285]. Each experimental group had a minimum of 3 replicates, and was repeated at least three individual trials.

Protein Extraction and Immunoblot Analysis

Cells were lysed using HEPES lysis buffer (10mM HEPES, 10mM NaCl, 0.1mM EDTA, 0.1mM EGTA, 1.0mM DTT, 0.1% NP-40, pH7.9) freshly supplemented with a Pierce Protease and Phosphatase inhibitor (Thermo Scientific). Equal amounts of protein were separated by SDS-polyacrylamide gel electrophoresis and were transferred to a polyvinylidene difluoride membrane (Immobilon-P, Millipore Corp.). Membranes were blocked in 5% blocking buffer (5% skim milk in 1x Tris-buffered Saline and Tween-20) for 1h at room temperature, then incubated overnight in primary antibody at 4°C (Table 2.3). Membranes were subsequently probed using horseradish peroxidase–conjugated secondary antibodies at room temperature for 2h. Signals were detected using the ECL Plus Kit (Amersham Biosciences).

Table 2.3 Primary Antibodies and Staining Reagents

Antibody	Company	Cat No.	Species	Dilution/ Concen-tration	Diluent
Cytokeratin-7	Dako	M7018	Mouse	1:100	PBS
PECAM1	Dako	M0823	Mouse	1:100	PBS
SMA	Dako	M0851	Mouse	1:100	PBS
CD45	Dako	M0701	Mouse	1:100	PBS
HLA-G	ExBio	11-499	Mouse	1:300	PBS
Ac-α-tubulin	Sigma-Aldrich	T6793	Mouse	1:500	1% BSA-PBST
TGFβ2	Santa Cruz	sc-90	Rabbit	1:100	5%Milk-TBST
Smad2/3	Cell Signaling	3102S	Rabbit	1:1000	5%BSA-TBST
GAPDH	Santa Cruz	sc-47724	Mouse	1:5000	5%Milk-TBST
Calcein AM	Corning	354217	N/A	1μM	Serum-free media
CellTracker™ Green CMFDA	Sigma-Aldrich	C2925	N/A	1μM	Serum-free media
CellTracker™ Red CMTPX	Invitrogen	C34552	N/A	1μM	Serum-free media

ELISA

Mir-218-1 overexpressing stable cells were seeded on 12-well plates at 100,000 cells/well in 10% FBS containing 1640 RPMI media. Conditioned medium was collected after 72h and spun down at 500g for 5min. TGF-β2 was measured using the Human TGF-beta 2 Quantikine ELISA Kit (R&D Systems) following the manufacturer's directions. Briefly, samples were activated with 1N HCl and subsequently neutralized with 1.2N NaOH/0.5M HEPES. Neutralized samples were not further diluted, and were immediately assayed for total active TGF-β2 levels. The color reaction was quantified on the BioTek Synergy H4 Plate Reader at 450nm and background detected at 540nm was subtracted. Quantification of total TGF-β2 levels in conditioned media was calculated from the standard curve generated during each assay.

Cell Growth Assay

Mir-218-1 and EV stable cells were seeded at 50,000 cells per 6-well plate in 10% FBS containing RPMI1640 media. Cells were detached and counted on a hemocytometer at 24h, 48h and 72h post-seeding. Each time point was done in triplicate and repeated three independent times. To account for possible differences in apoptosis, dead cells were counted at each time point.

Immunofluorescence

EV control and Mir-218-1 overexpressing cells were seeded in a monolayer on glass coverslips and allowed to attach overnight. Cells were wounded down the middle with a tip, and covered in serum-free medium for 16h. Cells were fixed in ice cold Acetone:Methanol (1:1 solution) for 20min then washed three times in 1xPBS. Cells were permeabilized with 0.2% Tween for 15min then blocked in 1% BSA-PBS-T for 1h. Cells were probed for acetylated alpha tubulin (Table 2.3)

for 2h at room temperature, followed by secondary anti-mouse antibody for 1h. Coverslips were mounted on slides, and pictures were taken on the Zeiss LSM 700 Confocal Microscope.

Statistical Analysis

Statistical analysis was performed using Graphpad Prism 7 ($p<0.05$, 95% CI). One-way ANOVA followed by a Tukey's multiple comparisons test determined differences among several groups. Unpaired, two-tailed, Student's *t* test was used for comparison between two groups. When necessary, alternative statistical tests were used and specified in corresponding figure legends.

RESULTS

Expression of miR-218-5p in placentas from healthy and PE pregnancies

MiR-218-5p is a highly conserved miRNA. A closer comparison across several hemochorial placenta species (human, chimpanzee, mouse and rat) showed complete conservation of the entire 21 nucleotide sequence (Figure 2.1A). To assess the possible role of miR-218-5p in placenta function, we analyzed a total of 72 healthy placenta samples across gestation. Second trimester tissues (13-25 weeks) showed a significantly higher ($p<0.0001$) expression of miR-218-5p compared to all other stages of gestation (Figure 2.1B). A set of placenta tissues from pregnancies diagnosed with preeclampsia (PE) delivered preterm (25-36 weeks) and term (37-40 weeks) were analyzed for miR-218-5p level, and compared to placenta from healthy patients during the same gestation period. Only placenta from PE patients delivered at term had a significantly lower ($p<0.0005$) expression of miR-218-5p compared to their gestational age matched controls (Figure 2.1C).

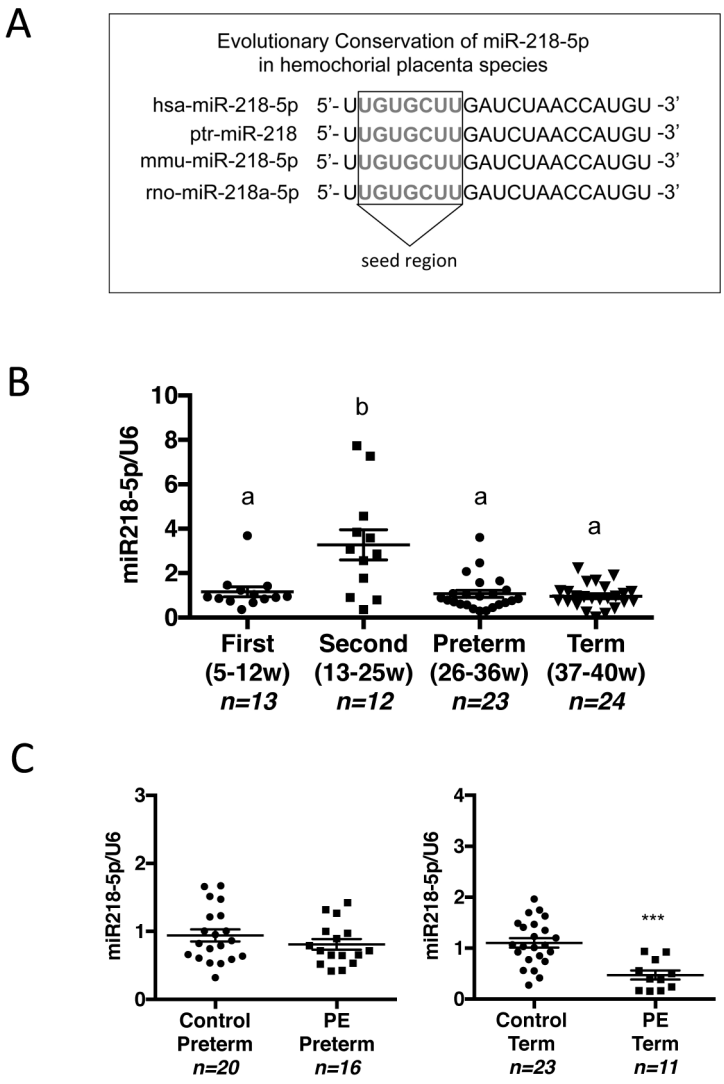

Figure 2.1 Expression pattern of miR-218-5p in human healthy and PE placentas.
(A) miR-218-5p across hemochorial placenta species (ptr: chimpanzee, mmu: mouse, rno: rat) shows complete conservation, including the full seeding region responsible for target complementarity. **(B)** Healthy placenta from patients at Mount Sinai Hospital undergoing elective termination or Caesarean section were assessed for miR-218-5p level by qRT-PCR and normalized to endogenous U6 snRNA. A significant increase ($p<0.0001$) in miR-218-5p levels occurred during second trimester (13-25 weeks gestation) was observed compared to all other gestational periods. **(C)** Placenta from patients diagnosed with preeclampsia (PE) delivered preterm (26-36 weeks) or at term (37-40 weeks) were assessed for miR-218-5p levels as in B, and compared to pregnancies that were found to have no placental abnormalities. A significant decrease ($p<0.0005$) of miR-218-5p was observed in the PE-Term placenta group when compared to its gestational age matched control. Error bars represent SEM.

Overexpression of mir-218 induced differentiation towards the enEVT pathway

To investigate the role of miR-218-5p in placental development, we generated a stable HTR8/SVneo trophoblast cell line stably overexpressing mir-218-1. The mir-218-1 stem-loop sequence was cloned into the miRNASelect™ pEGP-miR expression vector (Figure 2.2A, top panel). After transfection into the immortalized first trimester trophoblast cell line, HTR8/SVneo, positive clones were selected with Puromycin treatment. Twenty-two single-cell colonies were assessed for miR-218-5p level (Figure S2.1). HTR8/SVneo, positive clones were selected with Puromycin treatment. For simplicity, we present the findings from a single representative over-expressing clone (mir-218-1). It is important to note that we independently re-created these stable cells three times and observed similar key functional findings (data not shown). The chosen miR-218-5p clone was shown to significantly overexpress ($p<0.05$) mature miR-218-5p six fold over the endogenous level (Figure 2.2B). The rate of mir-218-1 overexpressing cell growth was significantly ($p<0.05$) slower as compared to the control cells, and this decrease was not due to increase in dead cells (Figure 2.2C). When seeded at equal cell density, the mir-218-1 overexpressing cells displayed clear morphological differences in that they were smaller and more spindle-shaped, and grew in a more diffuse pattern lacking the characteristic epithelial cell-cell contact normally observed in the parental and EV cells (Figure 2.2D). Confocal microscopy revealed more disorganized microtubules with asymmetric distribution in the Mir-218-1 overexpressing cells as compared to the control cells (Figure 2.2E). Finally, using an *in vitro* endothelial-like network formation assay we showed that the mir-218-1 overexpressing cells formed more richly branched and extensive networks as compared to the control cells. (Figure 2.2F).

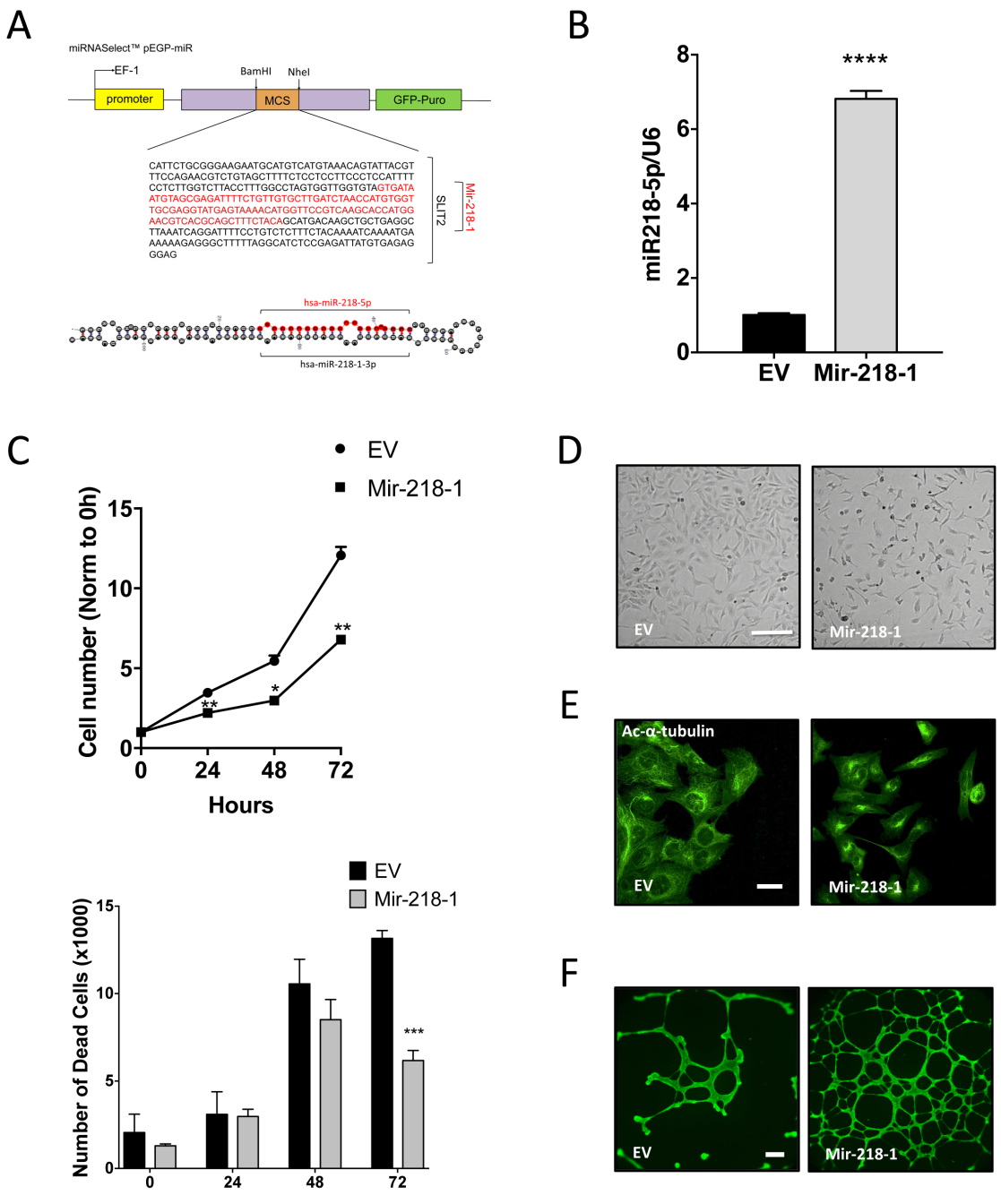

Figure 2.2 Legend found on next page

Figure 2.2 Generation and Initial Characterization of mir-218-1 stable cells.

(A) A portion of the Slit2 intron (primers underlined), bracketing the Mir-218-1 stem-loop sequence, was cloned into the miRNASelect™ pEGP-miR expression vector. An immortalized human first trimester trophoblast cell line, HTR8/SVneo, was used to create stably expressing clones through Puromycin selection. **(B)** MiR-218-5p was significantly increased ($p<0.05$) in the Mir-218-1 stable cells when normalized to the endogenous control, U6 snRNA. **(C)** Over three days, cells were counted and Mir-218-1 overexpressing cells showed an overall decreased rate of growth that was not explained by cell death. Stable Mir-218-1 and control cells were seeded in equal number under normal growing conditions. Multiple t-tests ($\alpha=0.05$) were performed and corrected for multiple comparisons with the Holm-Sidak method using Graphpad Prism. **(D)** Morphological examination with bright field microscopy showed that Mir-218-1 cells were smaller and spindle shaped, growing with less cell-cell contact compared to the empty vector (EV) cells. Scale bar: 200 µm **(E)** Mir-218-1 cells stained for acetylated-alpha-tubulin show a more disorganized microtubule network and asymmetric organization. Scale bar: 10 µm **(F)** When seeded on matrigel-coated wells, mir-218-1 cells displayed an increased ability to align into network structures compared to the control cells. Scale bar: 500 µm. Data are representative of three independent experiments. Error bars represent SEM.

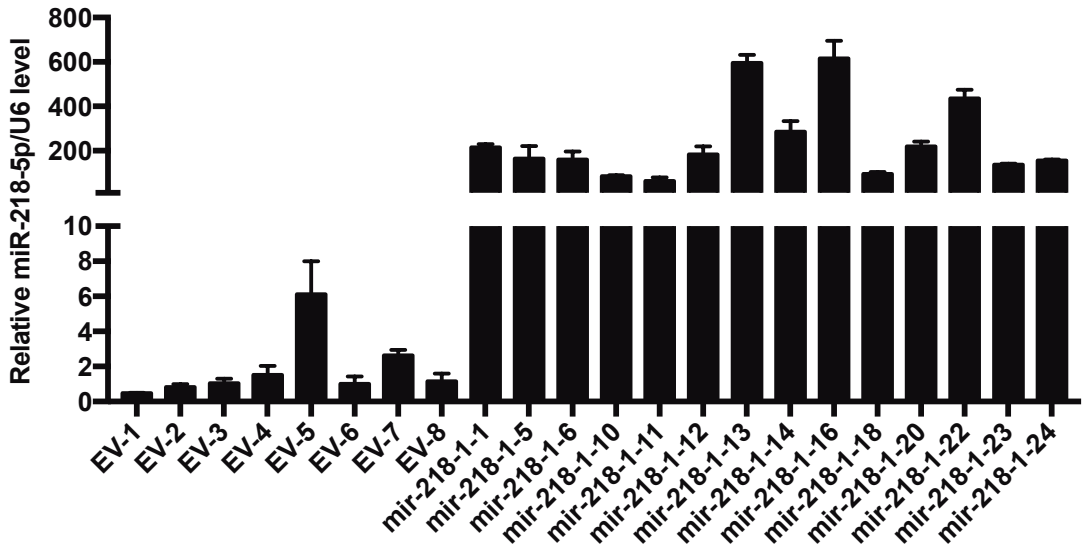

Figure S 2.1 Mir-218 stable cell single colony screening.
First trimester trophoblast cell line, HTR8/SVneo, was stably transfected with empty vector (EV) or mir-218-1 stem-loop construct. Single colonies were selected with Puromycin treatment for two weeks. Mir-218-5p levels were quantified using hsa-miR-218 TaqMan MicroRNA Assay. All future experiments were performed on EV-6 and mir-218-1-14 clones.

MiR-218-5p upregulated key markers of invasion and pseudovasuclarization

To determine which genes are regulated by mir-218-1, a cDNA microarray was performed to identify differentially expressed genes between control and mir-218-1 stable cells. Interestingly, markers associated with trophoblast invasion and the enEVT pseudo-vascularization process that is needed for proper spiral artery remodeling were among the top upregulated genes (Figure 2.3A). To confirm these results, we assessed mRNA levels of several key markers from the microarray using qRT-PCR. Matrix Metallopeptidase-1 (MMP1), Integrin α 1 (ITGA1), Platelet and Endothelial Cell Adhesion Molecule 1 (PECAM1), Vascular Endothelial Cadherin (VE-cadherin), Endothelial Cell-Specific Chemotaxis Regulator (ECSCR), Interleukin-8 (IL8), Interleukin-1b (IL1b), and Chemokine C-X-C motif ligand 1 (CXCL1) were all significantly upregulated in the mir-218-1 overexpressing cells (Figure 2.3B). Similar results were seen using primary 1st trimester EVT, collected via dissection of anchoring EVT cell columns (8-10 weeks), and treated with control, miR-218-5p, or anti-miR-218-5p oligomers, prior to processing for EVT RNA. Compared to the non-targeting control (NC), miR-218-5p oligomer treatment upregulated MMP1, ITGA1, PECAM1, CHD5, IL8, and IL1b mRNA levels (Figure 2.3C). In contrast, treatment with anti-miR-218-5p, downregulated these markers as compared to the anti-scramble control (Figure 2.3D).

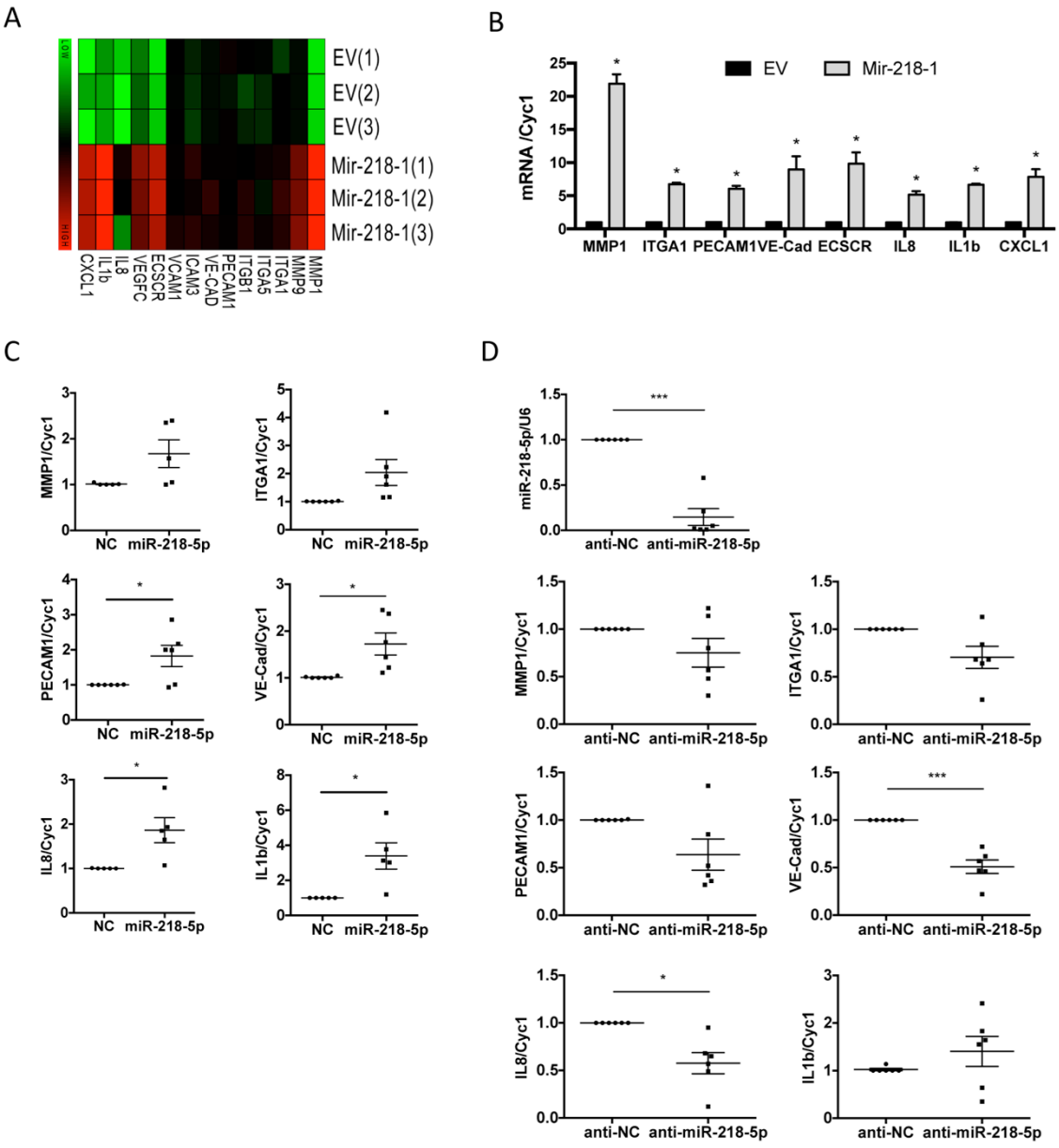

Figure 2.3 Legend found on next page

Figure 2.3 MiR-218-5p promotes key markers of trophoblast invasion and endovascular differentiation.

(A) A gene expression analysis report was conducted at the Princess Margaret Genomics Centre on control and mir-218-1 overexpressing cells using the Human HT-12 V4 BeadChip. Markers of trophoblast differentiation were greatly upregulated in mir-218-1 cells. **(B)** Several key markers were validated with qRT-PCR and the trend was consistent with initial microarray findings. All markers were significantly upregulated in mir-218-1 cells. Results represent three independent trials. **(C)** First trimester placental tissues were dissected to enrich extravillous trophoblasts (EVT) columns and treated with miR-218-5p or a scrambled non-targeting control (NC) for 48 hrs prior to RNA isolation. MiR-218-5p upregulated key markers of trophoblast differentiation. Results represent six independent placentas. **(D)** Similar to C, tissues were incubated with anti-miR-218-5p for 48 hrs and assessed for marker mRNA levels. All markers were downregulated by anti-miR-218-5p compared to the scramble control. Transfection efficiency was validated (top panel) by quantifying miR-218-5p levels. Results represent six independent tissue samples. Statistical analysis was performed using (A) multiple t-tests (α=0.05) and corrected for multiple comparisons with the Holm-Sidak method and (C and D) a two-tailed paired t-test ($p<0.05$, 95% CI) using Graphpad Prism. Error bars represent SEM.

Secreted proteins in the conditioned media collected from control- or miR-218-5p-treated explants were measured using a Bio-Plex assay. The conditioned medium from the miR-218-5p treatment group showed a marked upregulation of many secretory proteins important in the establishment of the feto-placental interface (Figure S2.2). In agreement with our earlier findings both IL8 and CXCL1 were increased in the miR-218-5p conditioned media (Figure S2.2 A and B). Other secretory proteins enriched in our miR-218-5p treatment group were interleukin-6 (IL6), chemokine C-C motif ligand 2 (CCL2), chemokine C-X-C motif ligand 16 (CXCL16), C-X3-C motif chemokine ligand 1 (CX3CL1), and macrophage migration inhibitory factor (MIF) (Figure S2.2 C-G).

MiR-218-5p promoted first trimester trophoblast migration and invasion.

To assess the effect of miR-218-5p on the invasive function of first trimester trophoblasts we transfected the parental HTR8/SVneo cell line with NC, miR-218-5p, or anti-miR-218-5p oligomers. Transfection of mir-218-5p significantly increased the number of trophoblast cells that crossed the matrigel barriers compared to control ($p<0.0001$ Figure 2.4A left panel). In contrast, anti-miR-218-5p significantly decreased invasion ($p<0.0005$, Figure 2.4A right panel). As expected, the mir-218-1 overexpressing cells also had significantly higher invasive capacity compared to control, and this effect was reversed with transient anti-miR-218-5p transfection ($p<0.0001$, Figure 2.4B). To confirm the miR-218-5p effect on invasion, we used a more recently established immortalized first trimester trophoblast cell line, Swan71. As in the HTR8/SVneo, we observed a marked upregulation of invasion in the miR-218-5p treated cells (Figure S2.3A).

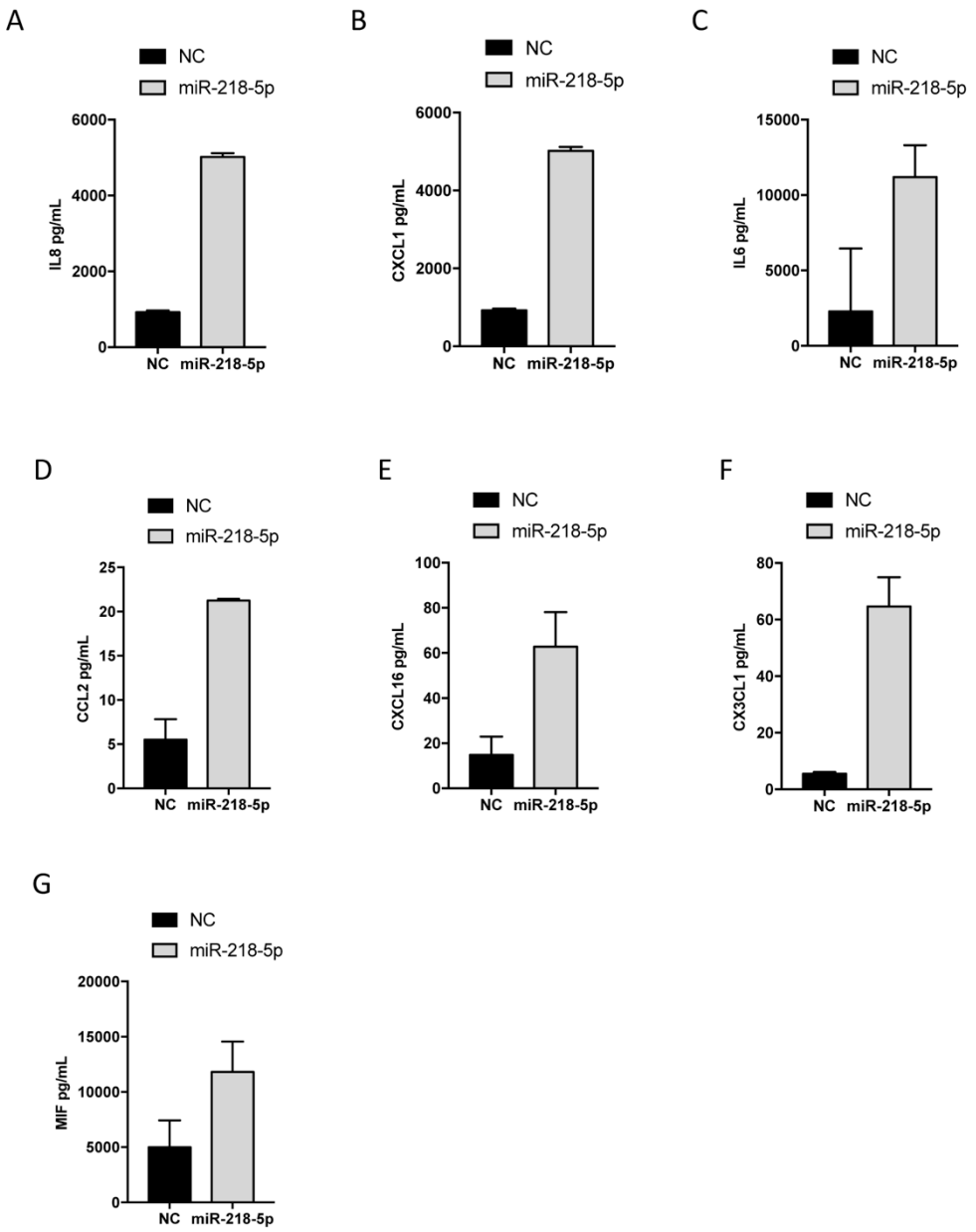

Figure S 2.2 miR-218-5p upregulates the secretion of pro-invasive pro-angiogenic factors.
First trimester placenta was treated with negative control or miR-218-5p (200 nM) for 48 hrs. The condition media was collected and used to assess the abundance of secretory proteins in the Bio-Plex assay. Upregulation of **(A)** Interleukin-8 (IL8), **(B)** Chemokine ligand 1 (CXCL1), **(C)** Interleukin-6 (IL6), **(D)** Chemokine C-C motif ligand 2 (CCL2), **(E)** Chemokine C-X-C motif ligand 16 (CXCL16) **(F)** C-X3-C motif chemokine ligand 1 (CX3CL1) and **(G)** Macrophage migration Inhibitory Factor (MIF) were observed in conditioned media of miR-218-5p treated tissues. Error bars represent SD.

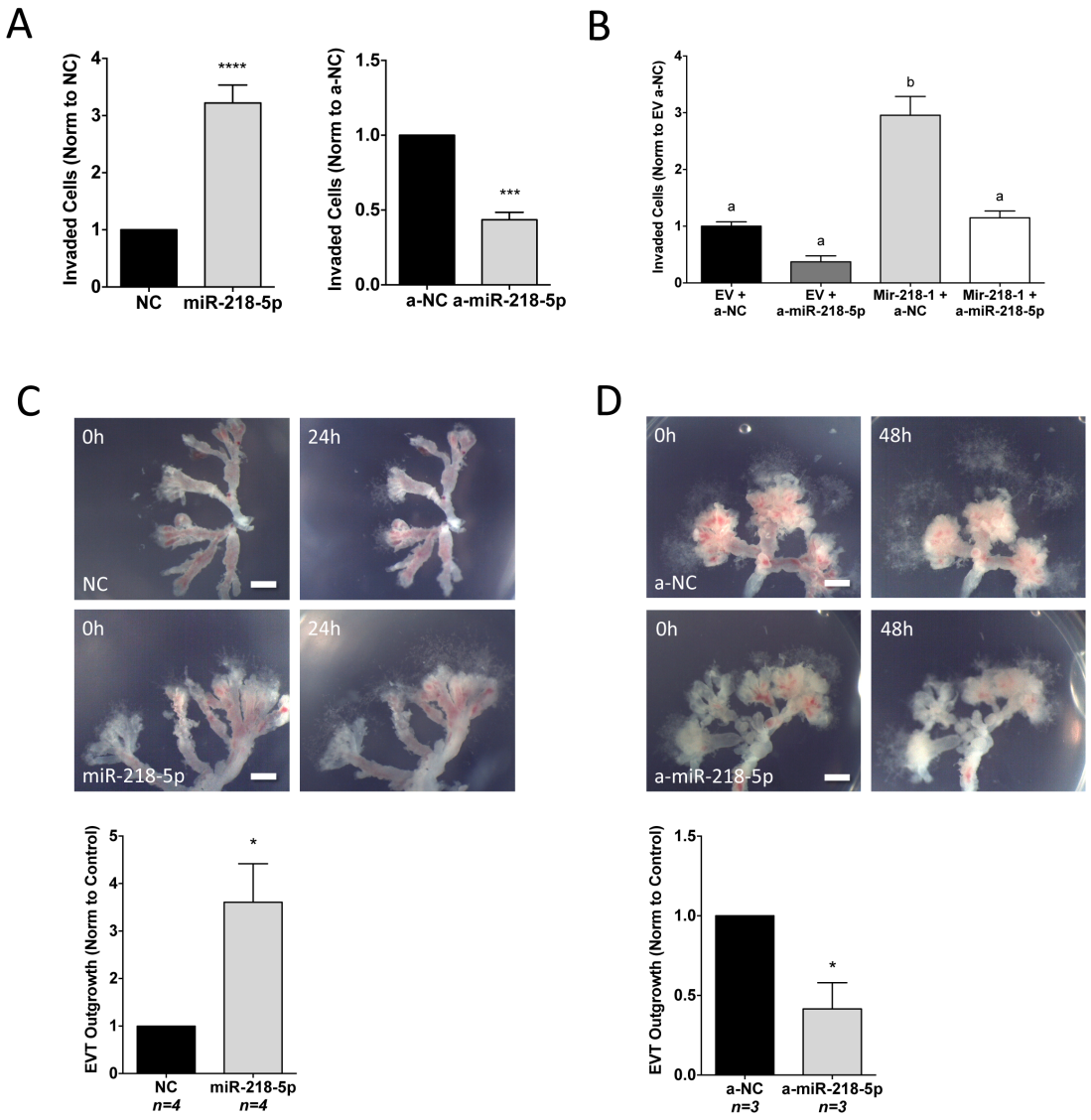

Figure 2.4 Legend found on next page

Figure 2.4 MiR-218-5p promotes trophoblast invasion and EVT outgrowth.
(A) Parental HTR8/SVneo cells were transfected with miR-218-5p (100 nM) or control (NC, left panel), anti-miR-218-5p (100 nM) or control (a-NC, right panel) and seeded on matrigel-coated membranes. MiR-218-5p significantly increased ($p<0.0001$), while anti-miR-218-5p significantly decreased ($p<0.0005$) the invasive ability of these cells. Results represent six (left panel) and three (right panel) independent experiments. **(B)** Mir-218-1 stable cells were used in a matrigel invasion assay as in A and were found to significantly increase ($p<0.0001$) their invasive ability. Transient anti-miR-218-5p transfection completely reversed this effect. A representative graph is shown from three independent experiments. **(C)** Explants from first trimester placenta were placed on matrigel and treated with miR-218-5p or control (200 nM) for 24h. EVT outgrowth was measured in ImageJ at treatment time (0 hr) and termination of experiment (24 hr). Difference of EVT outgrowth was calculated relative to 0 hr. A significant increase ($p<0.05$) in EVT outgrowth was observed in miR-218-5p treated tissues. Results represent four independent tissues with each experiment having a minimum of N= 4 replicates. A representative image is shown. **(D)** Similar to C, tissues were treated with anti-miR-218-5p or the control (200 nM) for 48 hrs. A significant decrease ($p<0.05$) in EVT outgrowth was observed with anti-miR-218-5p treatment. Results represent three independent tissues, with each experiment having a minimum of N= 4 replicates. A representative image is shown. Statistical analysis for (A, C, D) using a two-tailed unpaired t-test ($p<0.05$, 95% CI) and (B) a one-way ANOVA with a Dunnett's multiple comparisons test ($p<0.05$, 95% CI) using GraphPad Prism was performed. Error bars represent SEM. Scale bars: 500 μM.

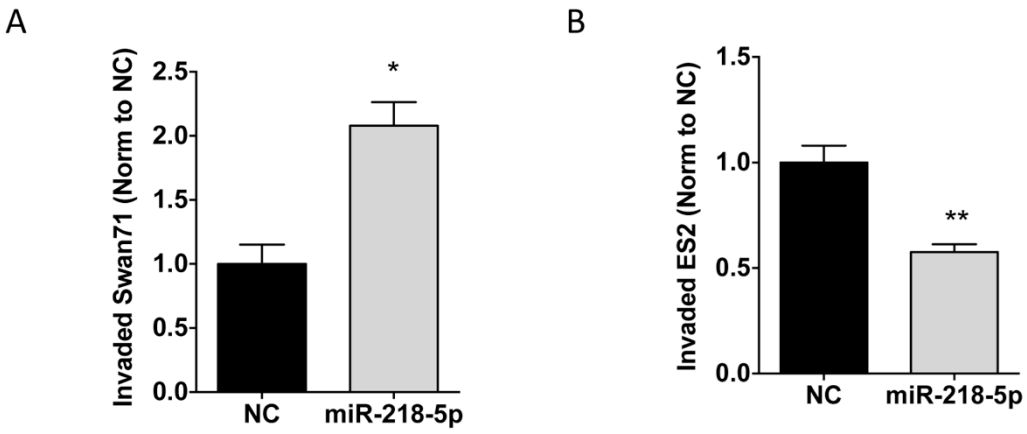

Figure S 2.3 miR-218-5p has anti-invasive effect in cancer cells.

(A) A first trimester immortalized cell line, Swan71**,** was transfected with miR-218-5p (100 nM) and seeded on matrigel-coated transwells. Mir-218-5p had a greater number of cells invade over 24 hrs compared to control **(B)** miR-218-5p was transfected into ovarian cancer cells, ES2, and seeded on matrigel coated transwells. MiR-218-5p downregulated the invasive ability of these cancer cells. Error bars represent SEM.

MiR-218-5p has been reported to inhibit cancer cell invasion [151,153,286], we therefore repeated the matrigel transwell invasion assay in an ovarian cancer cell line, ES2. We found that similar to studies on other cancer cells, miR-218-5p had the opposite effect in cancer cells, decreasing invasion compared to control (Figure S2.3B).

Uncoated transwells were used to assess the migratory ability of HTR8/SVneo transfected with control or miR-218-5p oligomers. MiR-218-5p significantly upregulated ($p<0.05$) the number of migrated cells across the transwell membrane compared to control (Figure S2.4A). Similarly, Mir-218-1 stable cells significantly increased the migratory ability of the trophoblast cells ($p<0.0005$) (Figure S2.4B). Transient transfection with anti-miR-218-5p significantly downregulated ($p<0.05$) the number of migrated cells (Figure S2.4C). To investigate the invasive and migratory effect of miR-218-5p further, we used a first trimester EVT outgrowth model. Established EVT outgrowths were treated with control, miR-218-5p or anti-miR-218-5p oligomers. We found that miR-218-5p significantly promoted ($p<0.05$) the outgrowth of EVT columns as quantified by outgrowth area, while anti-miR-218-5p significantly impeded ($p<0.05$) this process (Figure 2.4C and D, respectively).

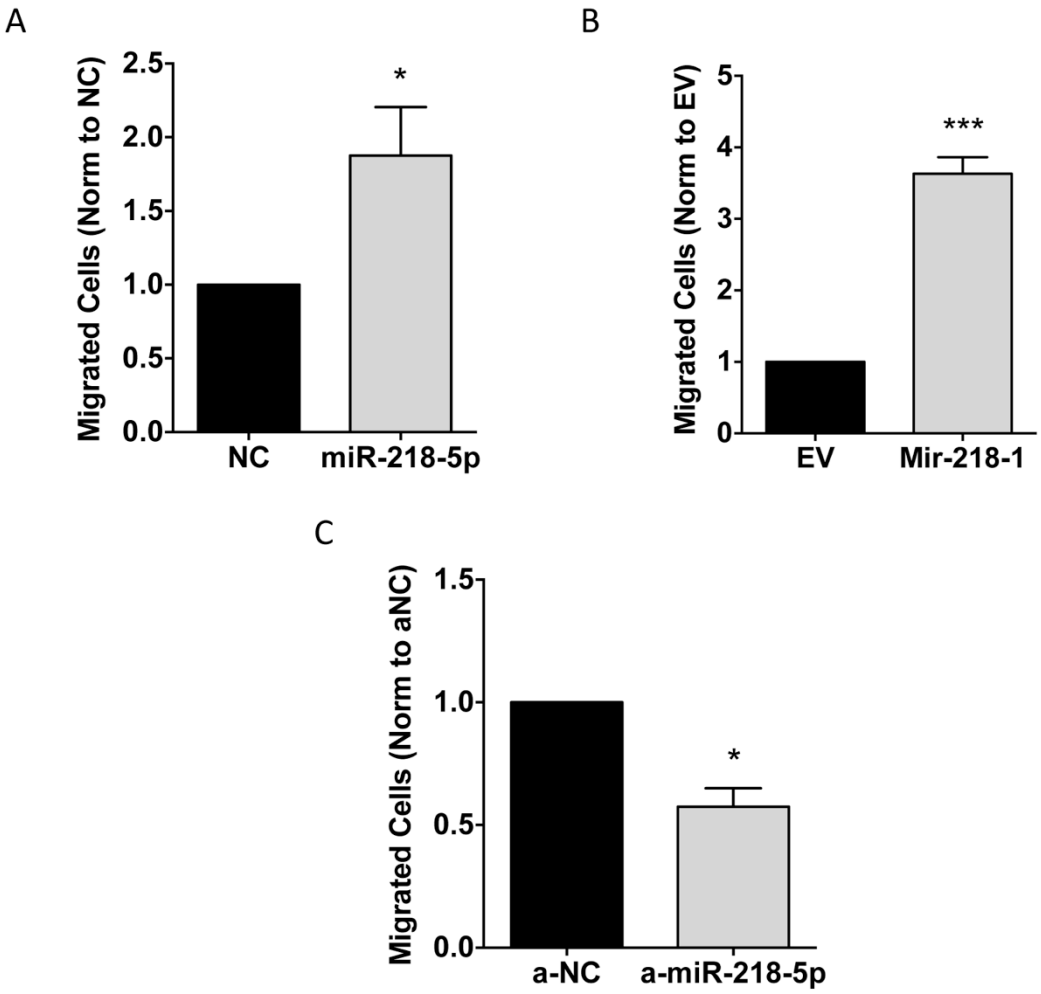

Figure S 2.4 miR-218-5p promotes migration in first trimester trophoblast cells.
(A) NC or miR-218-5p (100 nM) were transfected into HTR8/SVneo cells and seeded on uncoated transwells. MiR-218-5p significantly upregulated ($p<0.05$) the number of migrated cells compared to the scramble control. **(B)** Mir-218-1 stable cells seeded on uncoated transwells showed a significant increase ($p<0.0005$) in cell migration compared to control cells. **(C)** HTR8/SVneo cells transfected with anti-miR-218-5p showed a significant downregulation ($p<0.05$) of migration compared to the control.
Error bars represent SEM.

MiR-218-5p accelerates spiral arteriole remodeling.

As EVT invade and reline the uterine spiral arteries they acquire endothelial-like properties. An established three-dimensional dual cell co-culture assay was used to assess the effect of miR-218-5p on trophoblast ability to interact with endothelial cells. Specifically, control or mir-218-1 stable trophoblast cells were co-cultured on matrigel in a one-to-one ration with freshly isolated human umbilical vein endothelial cells (HUVEC). In order to differentiate the two cell types, staining with cell tracker green and red dye, respectively, was done prior to seeding. As expected, both control and mir-218-1 trophoblast cells co-localized with HUVEC. Mir-218-1-HUVEC co-culture, however, had a more complex network and overall larger total network length (Figure S2.5B). Interestingly, in co-culture with control cells, HUVEC formed intact networks. However, in co-culture with mir-218-1-overexpressing cells, trophoblasts displaced the HUVEC to form the network branches, suggesting that the mir-218-1 enhances the integration of trophoblasts into the endothelial network (Figure S2.5C). To confirm the overall push into enEVT differentiation by miR-218-5p, we used a novel tissue *ex vivo* model of trophoblast-mediated decidual blood vessel remodeling. First trimester (9-10 week) placenta and decidua paretalis from the same patients were used. Placental explants with intact EVT columns were pre-incubated with control or miR-218-5p oligomers prior to placement onto the decidua epithelial surface (Figure S2.6). All decidual tissue used was negative for the cytotrophoblast (epithelial) marker cytokeratin-7 (CK-7) and histocompatibility antigen, class I, G (HLA-G) (Figure 2.5 A and B, black arrows) confirming no prior *in utero* invasion.

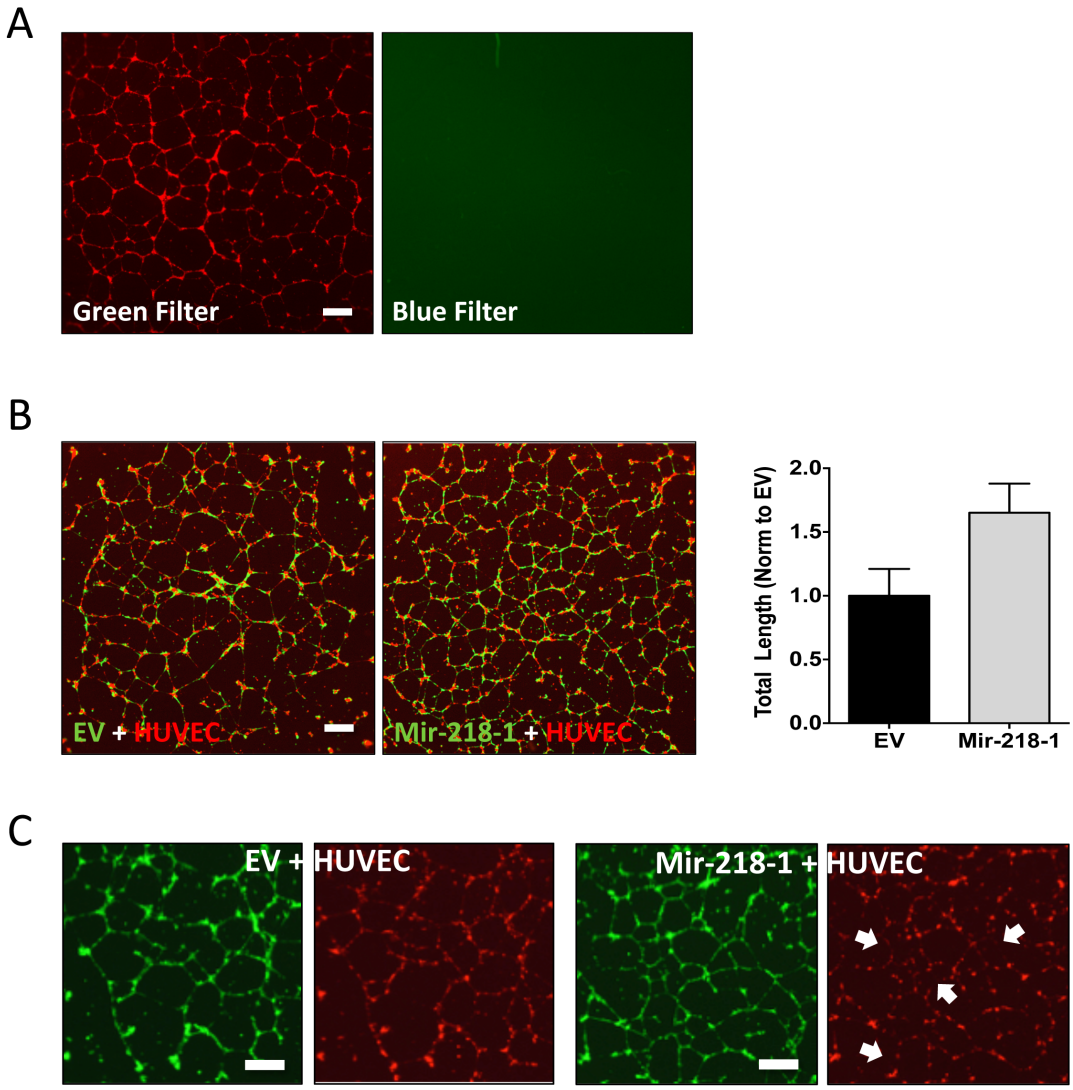

Figure S 2.5 Mir-218 promotes network formation and endothelial replacement.
(A) To verify the specificity of stains, HUVEC were stained with CellTracker™ Red CMTPX and photos were taken with blue filter (left panel) or green filter (right panel). **(B)** Control or Mir-218-1 stable trophoblasts were pre-stained green and seeded on matrigel in a one-to-one ratio with human umbilical vein endothelial cells (HUVEC) pre-stained red. Cells were allowed to co-localize and form networks for 24 hrs prior to imaging. Mir-218-1 trophoblast-HUVEC co-culture showed a more complex network with an overall larger total length. **(C)** In co-culture with control cells, HUVEC formed intact networks. However, in co-culture with mir-218-1-overexpressing cells, trophoblasts displaced the HUVEC to form the branches (white arrow heads), suggesting that the mir-218-1 enhances the integration of trophoblasts into the endothelial network. Scale bar: 500 µm.

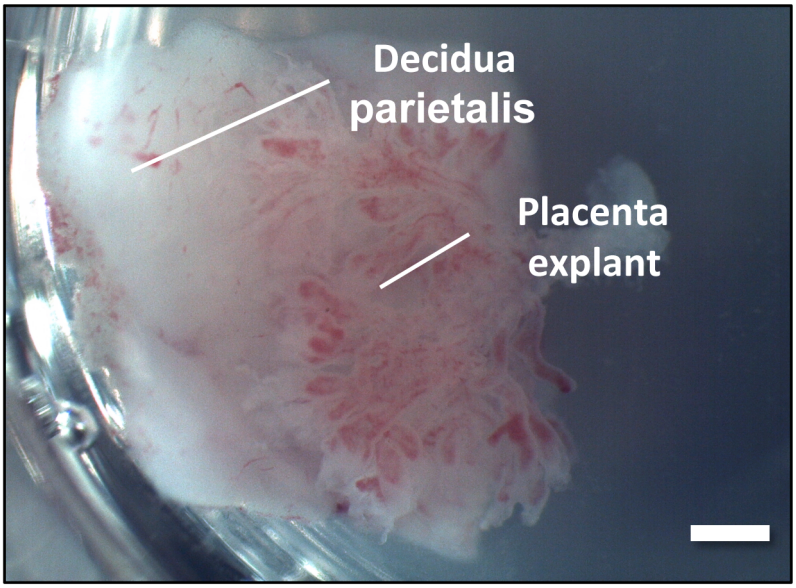

Figure S 2.6 *In vitro* model of decidua spiral artery remodeling.
Labeled representative image of the *in vitro* model used for first trimester placenta-decidua co-culture. Scale bars: 500 µM.

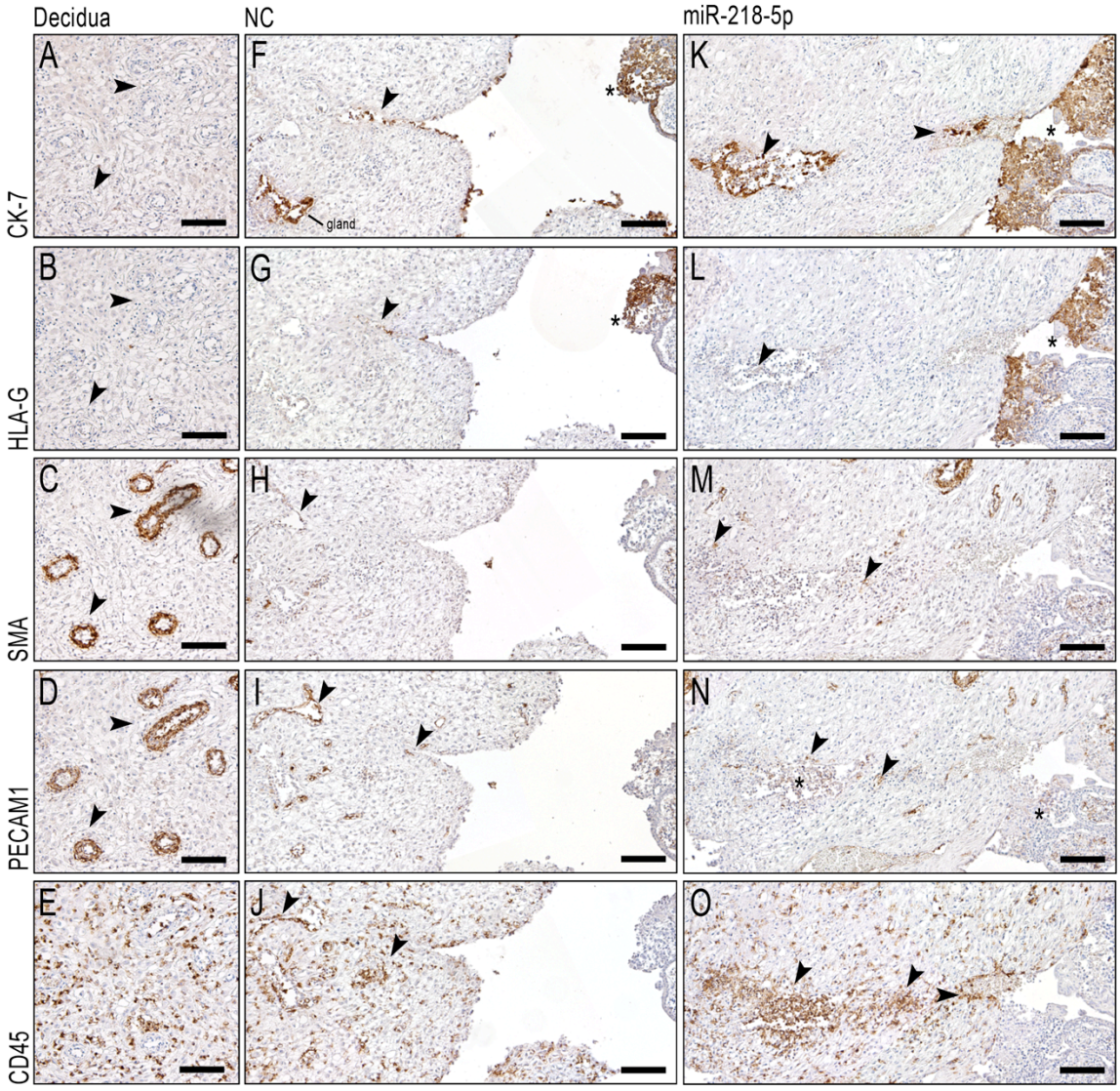

Figure 2.5 Legend found on next page

Figure 2.5 MiR-218-5p accelerates spiral artery remodeling.
(A-E) Decidua parietalis was assessed for *in utero* trophoblast remodeling. Tissue was negative for Cytokeratin-7 (CK-7) and histocompatibility antigen, class I, G (HLA-G) **(A and B, black arrows)**. Tight, non-invaded arterioles stained positive for smooth muscle actin (SMA) and Platelet and Endothelial Cell Adhesion Molecule 1 (PECAM1) **(C and D, black arrows)**. Lymphocyte common antigen, CD45, was spread evenly throughout the tissue **(E)**. **(F-J)** Placenta tissue pre-treated with scrambled sequence was assessed for degree of vessel remodeling. **(F and G)** EVT cells positive for CK-7 and HLA-G (black asterisk) entered the proximal arteriole (black arrows). **(H)** Distal portion of the spiral arteriole stained positive for an intact smooth muscle layer, (black arrow). **(I)** Black arrows point to intact endothelial cells stained positive for PECAM1. **(J)** CD45 positive, Leukocyte recruitment at site of remodeling is indicated by black arrows. **(K-O)** Placenta tissue pre-treated with miR-218-5p was assessed for degree of vessel remodeling. **(K and L)** CK7 and HLA-G positive EVT (black asterisk) entered the distal portion of the arteriole (black arrows). **(M)** Several cells positive for SMA (black arrows) remain at the distal portion of the arteriole. **(N)** PECAM1 positive endothelial cells (black arrow) remain at distal portion of arteriole. EVT are weakly positive for PECAM1 in the placenta column and at the site of remodeling (black asterisk). **(O)** Abundant recruitment of leukocytes at site of remodeling (black arrows) and clearing of leukocytes from surrounding tissue was observed. Similar trend is observed in three unique tissue samples, where representative images are shown. Scale bar: 100 μM

As expected, we observed many intact tight, un-remodeled arterioles that stained positive for the smooth muscle marker, smooth muscle actin (SMA), and the endothelial cell marker, PECAM1 (Figure 2.5 C and D, black arrows). As expected in non-invaded tissues, the leukocytes that stained for lymphocyte common antigen (CD45) were spread evenly throughout the tissue and were not found to be associated with any observed vessels (Figure 2.5E). Placenta tissue pre-treated with NC had a large EVT invasive column, as shown by the CK-7 and HLA-G positive staining (Figure 2.5F and G, asterisk). EVT cells are seen entering the lumen of a cross-sectioned arteriole at the proximal end (Figure 2.5F and G, black arrow). As shown by SMA and PECAM1 staining, the distal portion of the arteriole is still intact and un-invaded by the trophoblasts (Figure 2.5 I and J, black arrows). Surrounding CD45 positive leukocytes were found to be associated with the vessel throughout the entire observable length (Figure 2.5J, black arrows). Placenta pre-treated with miR-218-5p showed an accelerated process of vessel remodeling compared to the scramble control. The placenta of miR-218-5p, like the control, had healthy large EVT columns positive for both CK-7 and HLA-G (Figure 2.5 K and L, asterisk). The CK-7 positive cells entered the proximal portion of the vessel and had invaded to the end of the observable vessel, where they were seen lining the walls and interacting in the lumen (Figure 2.5K, black arrows). The HLA-G marker was lightly positive in the deep invaded trophoblasts (Figure 2.5L, black arrow). Staining for smooth muscle cells showed that nearly all were removed during remodeling (Figure 2.5M, black arrows). Likewise, endothelial cell marker PECAM1 was only observed on a few cells in the vessels (Figure 2.5N, black arrows). Interestingly, the EVT in the distal portion of the vessel were weakly stained for the endovascular marker, PECAM1 (Figure 2.5N, asterisk). Similar to the control tissue, in the

miR218-5p cocultures the leukocyte recruitment to the site of vascular remodeling was observed, however higher numbers of leukocytes were directly associated with the wall and in the lumen with the transformed vessel (Figure 2.5O, black arrows).

Mir-218-5p promotes trophoblast invasion and differentiation into enEVT though suppression of TGFβ2 signaling.

For this study, we used the miRanda algorithm that calculates a prediction score based on 3'UTR complementarity, position within the 3'UTR, energy of formed duplex, and the evolutionary conservation of the target. Based on these parameters, a good score (miRSVR:-0.7857) was assigned to the seeding region within the TGFβ2 3'UTR (Figure 2.6A, top panel). In order to confirm miR-218-5p binding, we constructed a luciferase reporter by cloning a portion of the TGFβ2 3'UTR bracketing the miR-218-5p seeding region downstream of the luciferase gene in the pMir-Report miRNA expression reporter vector (Figure 2.6A, bottom panel). Preliminary findings suggest that miR-218-5p transient transfection significantly downregulated Luciferase activity compared to cell transfected with the non-targeting control, while no change was observed in the empty vector-transfected cells ($p<0.5$, Figure 2.6 B). Mir-218-1 overexpressing cells significant downregulated expression of TGFβ2 mRNA and secretion of TGFβ2 compared to control cells ($p<0.05$, Figure 2.6C and D). Treatment of parental HTR8/SVneo trophoblast cells with recombinant human TGFβ2 significantly decreased ($p<0.05$) differentiation markers VE-cadherin, MMP1, IL1b and IL8 while PECAM1 was unaffected (Figure 2.6E). Treatment with recombinant human TGFβ2 also significantly decreased ($p<0.001$) invasion of HTR8/SVneo cells across the matrigel-coated membrane (Figure 2.6F).

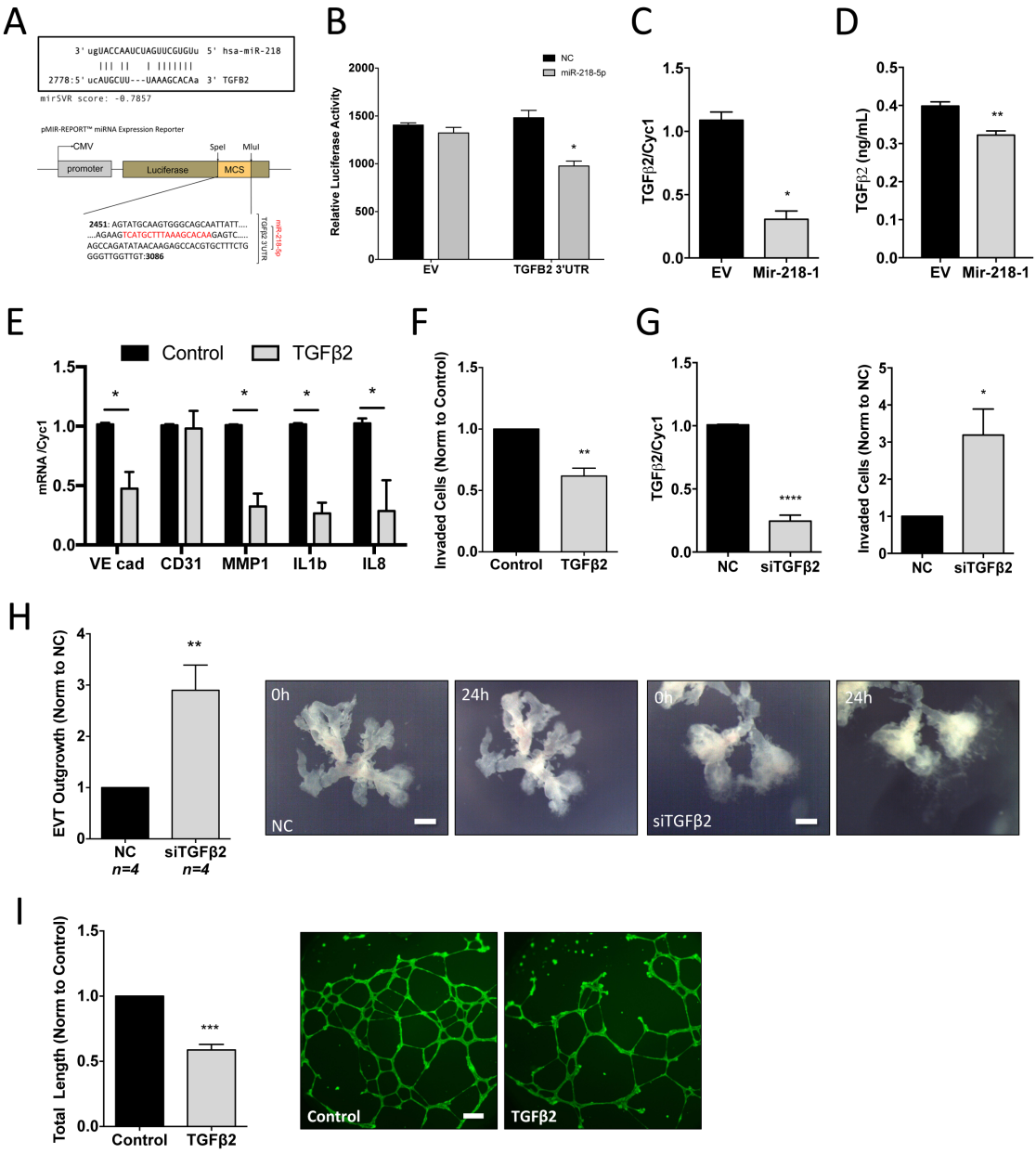

Figure 2.6 Legend found on next page

Figure 2.6 MiR-218-5p predicted target, TGF-β2, suppresses EVT invasion and enEVT differentiation.

(A) miRNA target prediction algorithm, MiRanda, shows a notable miRSVR score (<-0.1) for miR-218-5p and TGFβ2 mRNA (top panel). A portion of the TGFβ2 mRNA containing the miR-218-5p seeding region was cloned into the pMIR-REPORT™ miRNA Expression Reporter, downstream of the Luciferase gene. **(B)** Transient transfection of miR-218-5p significantly downregulated ($p<0.05$) Luciferase activity through the TGFβ2 3'UTR compared to control cells. A representative experiment is shown. **(C)** TGFβ2 mRNA is significantly downregulated ($p<0.05$) in Mir-218-1 cells compared to the control. Results represent three independent experiments. **(D)** ELISA quantification of TGFβ2 showed a significant downregulation in mir-218-1 stable cells compared to EV. **(E)** Parental HTR8/SVneo cells treated with recombinant human TGFβ2 (10 ng/mL) significantly downregulated key markers of invasion and endovascular EVT differentiation. Results represent six independent experiments. **(F)** Cells pre-treated with recombinant human TGFβ2 (10 ng/mL) invaded the matrigel covered membranes significantly less ($p<0.001$) than vehicle treated control cells. Results represent four independent experiments. **(G)** siTGFβ2 significantly suppressed ($p<0.0001$) TGFβ2 mRNA level and significantly increased ($p<0.05$) HTR8/SVneo cell invasion. Results represent three independent experiments. **(H)** Tissues were treated with siTGFβ2 or the non-targeting control (200 μM) for 24 hrs. A significant increase ($p<0.01$) in EVT outgrowth was observed with siTGFβ2 treatment. Results represent four independent tissues, with each experiment having a minimum of N= 4 replicates. Scale bars: 500 μM. **(I)** Cells pre-treated with recombinant human TGFβ2 (10 ng/mL) showed a significantly decreased ($p<0.001$) ability to form network structures on matrigel compared to the vehicle treated control. Scale bar: 500 μM. Results represent three independent experiments. A two-tailed unpaired t-test ($p<0.05$, 95% CI) (for C,D F-I) or a multiple t-tests ($\alpha=0.05$) corrected for multiple comparisons with the Holm-Sidak method (for B and E) was performed, using Graphpad Prism. Error bars represent SEM.

Conversely, transfection with validated siTGFβ2 siRNA resulted in a significant increase ($p<0.05$) in invasion compared to scrambled control (Figure 2.6G).

While first trimester EVT outgrowths mimicked the miR-218-5p phenotype, significantly increasing ($p<0.01$) the EVT outgrowth area in response to siTGFβ2 siRNA (Figure 2.6H). Lastly in the *in vitro* endothelial-like network formation assay, recombinant human TGFβ2 significantly decreased ($p<0.001$) total network length and overall network size in the parental HTR8/SVneo cell line (Figure 2.6I). Healthy placenta tissues collected from the Mount Sinai Bio Bank were randomly selected based on gestational age to represent a spectrum across the entire gestational period. Findings, based on a small sample size, showed that mature TGFβ2 protein was expressed in placenta tissues throughout pregnancy (Figure S2.7). To substantiate our findings, we turned to the mir-218-1 stable cell model to rescue the miR-218-5p effect by reintroducing TGFβ2 without the 3'UTR regulatory region. For this purpose, we used the recombinant human TGFβ2 protein. As observed in the parental cells, TGFβ2 treatment significantly suppressed ($p<0.05$) VE-cadherin, MMP1, IL1b, and IL8 mRNA levels, compared to mir-218-1 treated with vehicle only (Figure 2.7A). Mir-218-1 cells treated with TGFβ2 reversed the pro-invasive phenotype observed in control mir-218-1 cells (Figure 2.7B). As previously reported, mir-218-1 cells seeded on matrigel formed a network with significantly larger ($p<0.05$) total length compared to control cells. This effect was lost after TGFβ2 treatment (Figure 2.7C).

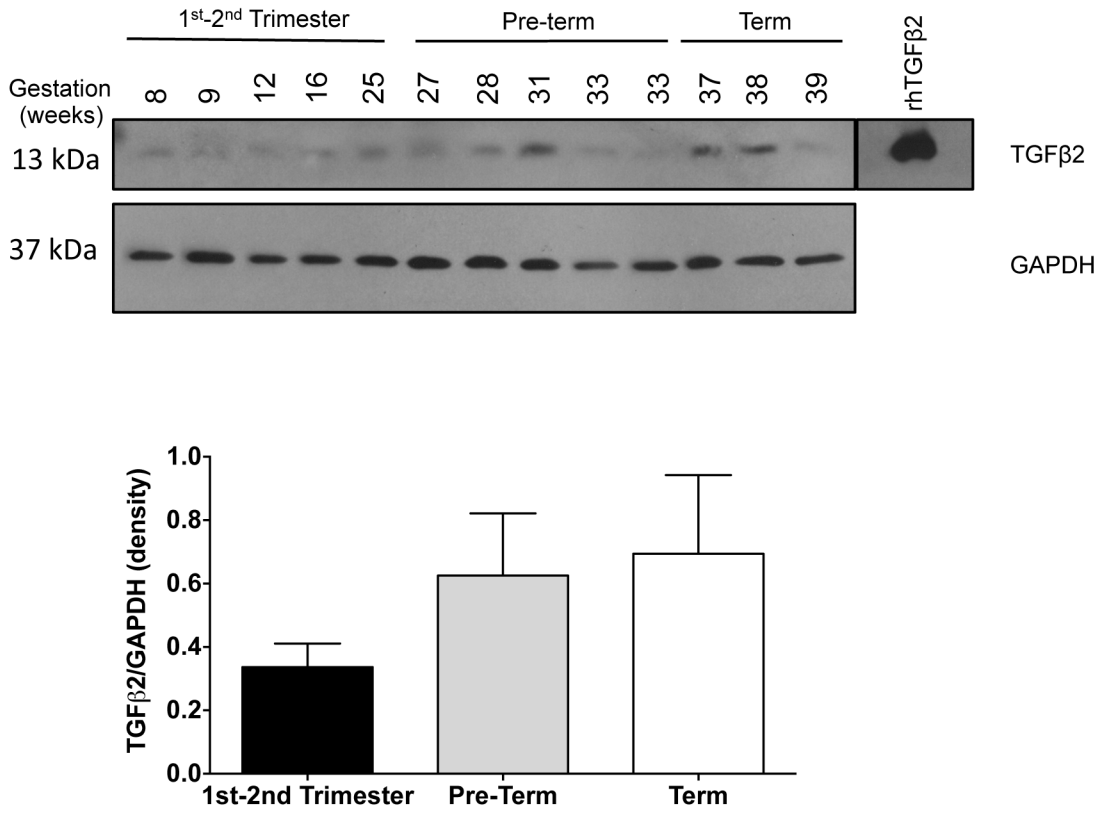

Figure S 2.7 Placental TGFβ2 expression across gestation.
Healthy snap frozen placenta tissues collected from the Mount Sinai Bio Bank were homogenized in RIPA protein lysis buffer and loaded in equal quantities on a 15% SDS-PAGE gel. Probing for TGFβ2 showed a variable expression of the mature protein across gestation. Recombinant human TGFβ2 protein was loaded on a separate gel as a positive antibody control. GAPDH was used as a loading control. Relative Protein Density was measured using the Gel Analyzer plugin in ImageJ, relative to GAPDH.

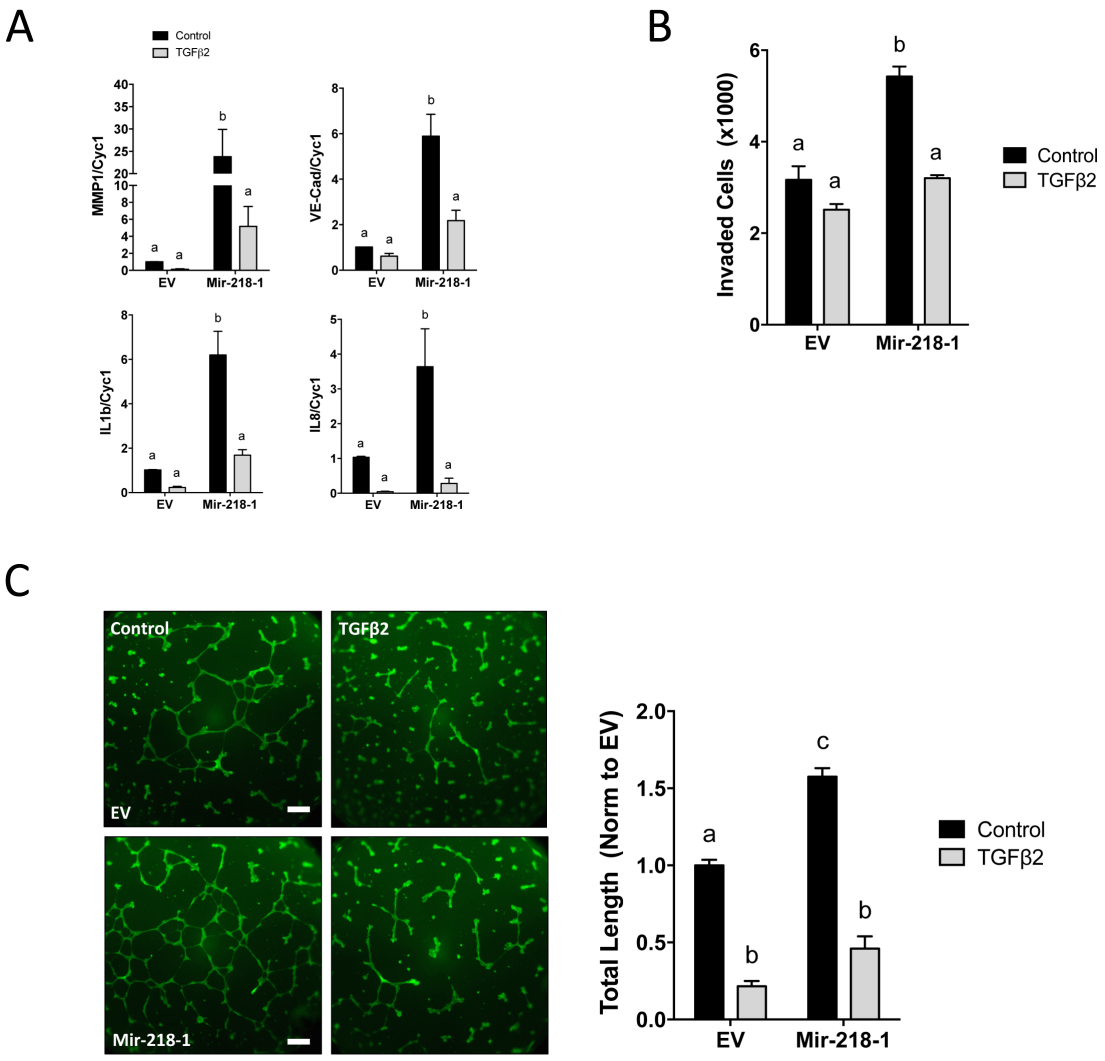

Figure 2.7 MiR-218-5p exerts its effect through the suppression of TGF-β2.
(A) EV control and mir-218-1 overexpressing stable cells were treated with recombinant human TGFβ2 (10 ng/mL). TGFβ2 treatment significantly decreased key trophoblast differentiation markers in both EV and mir-218-1 cells. Results represent three independent experiments. **(B)** Recombinant human TGFβ2 (10 ng/mL) treated stable mir-218-1 cells reversed the pro-invasive effect. A representative experiment is shown. **(C)** Recombinant human TGFβ2 (10 ng/mL) treated stable mir-218-1 cells significantly reversed ($p<0.05$) the network forming ability of the cells on matrigel. A representative experiment is shown. Two-way ANOVA with Tukey's multiple comparison test ($p<0.05$, 95% CI) was performed using Graphpad Prism. Scale bar: 500 µM. Error bars represent SEM.

It is important to note that in addition to TGFβ2, our microarray data indicated that other signaling molecules of the TGFβ pathway were also downregulated (Figure S2.8A). To verify the overall effect of miR-218-5p on TGFβ signaling, we used the activin response element reporter, pAR3-Lux, co-transfected with FAST-2. Both miR-218-5p transient and mir-218-1 stable first trimester trophoblast cell lines showed a downregulation of TGFβ signaling (Figure S2.8B). Interestingly, treatment with recombinant human TGFβ2 was only partially able to rescue suppression by mir-218-1 (Figure S2.8C). As indicated by our microarray findings, Smad2 protein was downregulated in both miR-218-5p transient and Mir-218-1 stable overexpressing cells (Figure S2.8D). To test if suppression of Smad2 is involved in miR-218-5p action, we co-transfected anti-miR-218-5p and siSmad2 into parental HTR8/SVneo trophoblast cells. SiSmad2 siRNA mimicked both the pro-invasive and pro-angiogenic phenotype of miR-218-5p. Furthermore, co-transfection of siSmad2 reversed the inhibitory effect of anti-miR-218-5p in both invasion (Figure S2.8E) and network formation (Figure S2.8F).

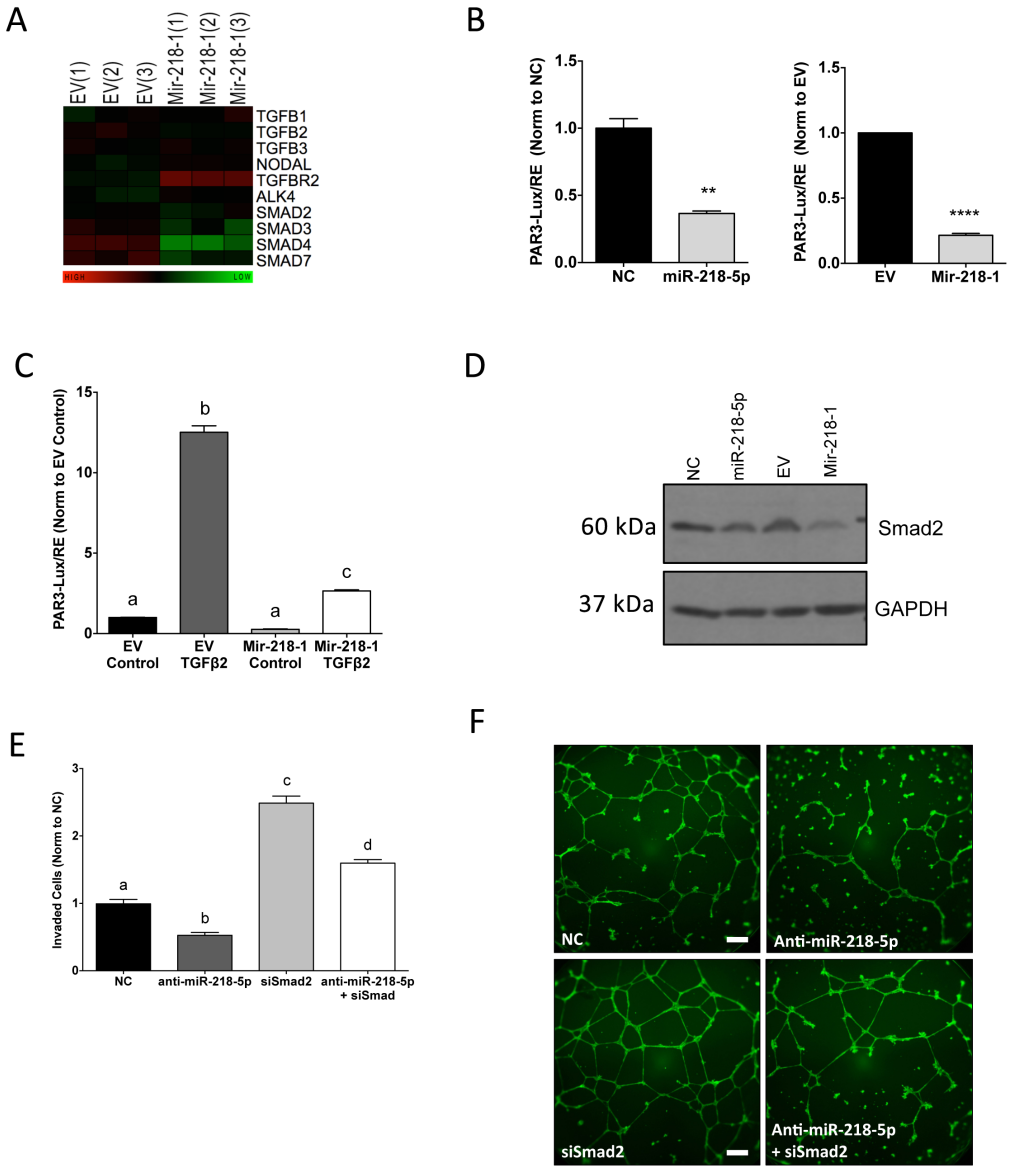

Figure S 2.8 miR-218-5p suppresses TGFβ2 signaling components.

(A) Microarray finding shows an overall downregulation of several TGFβ ligands and downstream signaling molecules (SMADs). (B) A TGFβ response reporter, PAR3-Lux, was used to measure activity of the TGFβ pathway. Both transient miR-218-5p and stable Mir-218-1 overexpression downregulated TGFβ signaling in first trimester trophoblast cells. (C) Treatment with recombinant human TGFβ2 protein only partially reversed the suppressed TGFβ signaling. (D) Total Smad2 protein level was decreased by both miR-218-5p transient and Mir-218-1 stable overexpression in HTR8/Svneo cells. Transfection with anti-miR-218-5p and siSmad2 siRNA was able to rescue the anti invasive (E) and anti-angiogenic (F) effect of anti-miR-218-5p. Statistical analysis for (B) using a two-tailed unpaired t-test ($p<0.05$, 95% CI) and (C and D) a one-way ANOVA with a Tukey's multiple comparisons test ($p<0.05$, 95% CI) using GraphPad Prism was performed. Scale bar: 500 µM. Error bars represent SEM.

DISCUSSION

The precise mechanisms underlying the development of preeclampsia (PE) are still illusive. While it is clear there is a complex interplay of both placental and maternal factors, there is a consensus that a disruption in the invasive trophoblast pathway is part of the etiology. Histological studies of PE tissues have consistently shown superficial cytotrophoblast invasion, absence of the epithelial-to-endovascular switch, and consequent insufficient remodeling of maternal spiral arteries [287-289]. The process of vascular mimicry that takes place in first trimester trophoblasts has not been well studied. In this study, we demonstrate that miR-218-5p, downregulated in PE placentas, promotes enEVT differentiation and induces trophoblast invasion and spiral artery remodeling. To the best of our knowledge, this is the first report that a miRNA is implicated in enEVT differentiation and spiral artery remodeling.

We found that miR-218-5p is downregulated in placenta tissues from patients diagnosed with PE. These findings align with previous microarray and tissue studies [160,275]. While studying the dysregulation of miRNA in PE is a valid approach to tackling this question, it does pose the problem of interpreting whether the findings are contributors to the causation of the disorder or are a response to the clinical condition itself. This is why examining the miRNA expression profile across gestation in healthy tissues is an important mirror into the biological relevance of miRNA function. The period of deep placental invasion and spiral artery remodeling in early second trimester is of particular importance in the onset of PE [290]. Our findings indicate that miR-218-5p expression spikes during this period suggesting it may play a role in regulating the establishment of proper placental perfusion.

In an effort to better understand the function of miR-218-5p in these processes, we first analyzed the consequence of mir-218-1 overexpression in the well-established immortalized first trimester trophoblast cell line, HTR8/SVneo [279]. The changes in cell morphology, cytoskeletal structure, increase in matrigel network-formation, as well as a reduction in proliferation rate, all suggest a switch from a plastic phenotype to a differentiated state [291,292].These findings align with the Highet et al. 2016 gene-expression microarray study comparing HTR8/SVneo cells cultured on and off matrigel. Interestingly, they reported that while the network-forming cells expressed genes associated with cytoskeleton organization, cell migration and blood vessel development, the latter group was enriched for mitotic genes associated with proliferation. Strikingly, *Slit2*, which houses the intronic gene of mir-218-1, was among the pro-angiogenic genes upregulated [293].

The miR-218-5p upregulated markers of differentiation in our study are well documented in previous work as promoters of trophoblast invasiveness and endovascular differentiation. VE-cadherin and IL-8 were the most congruent genes regulated by miR-218-5p in both our cell and tissue models. Studies of feto-maternal interface sections showed that the upregulation of VE-cadherin in healthy tissue cytotrophoblasts was absent in PE affected tissues. They further demonstrated that VE-cadherin promoted primary CTB invasiveness in culture [288]. Likewise, IL-8 promoted primary CTB and HTR8/SVneo cell migration and invasion in a dose-dependent manner through the upregulation of gelatinases, matrix metalloproteinase (MMP)-2 and -9 [294]. MMP-1 is one of the top upregulated genes in the mir-218-1 cells. As a collagenase, MMP-1 is responsible for the degradation of fibrillar collagen-rich extracellular matrices, such as those

found in the distal part of the decidua and the myometrium. A study of MMP profile in decidua basalis reported MMP-1 as the highest down-regulated MMP between healthy and PE cases. Specifically, there was a clear reduction in the MMP-1^{+} EVT population, suggesting its involvement in the reduced invasiveness observed in the pathophysiology of PE [295]. Zymography studies have shown an upregulation of MMP2/9 and MT-MMP1/2 by IL1b treatment [296]. Interestingly, trophoblasts have been shown to regulate the degree of their invasiveness through IL1b secretion and the subsequent downregulation of Metalloproteinase inhibitor, TIMP3, in human decidualized endometrial stromal fibroblasts [297]. Macrophage migration inhibitory factor (MIF) was detected in EVT, and shown to promote trophoblast invasion and migration through upregulation of ITGA1 and MMP2/9 [298].

Placental explants pre-treated with miR-218-5p accelerated the spiral artery remodeling process *in vitro*. The remodeling of maternal spiral arteries is a complex, multi-step process, involving the priming of the vessels by decidual immune cells and the subsequent infiltration of endovascular EVTs [299-301]. One mechanism of miR-218-5p action may be through the upregulation of genes involved in the epithelial-to-endovascular switch resulting in an increased pool of enEVT available for remodeling. Both PECAM1 and VE-cadherin were identified in cytotrophoblasts at the decidual-endothelial junctions, while VE-cadherin was shown to be essential in the trans-endothelial migration of enEVTs during spiral artery remodeling [302]. Similarly, both PECAM1 and VE-cadherin were critical in endothelial cell network formation on matrigel [303]. Strong ECSCR immunoreactivity was detected in enEVT of decidua basalis and within the enEVT of the myometrial microvessels [304]. Interestingly, while CX3CL1 has been

detected in several trophoblast cell lines, its receptor, CX3CR1, has been specifically detected in enEVT, while absent in iEVT, suggesting a possible paracrine role in enEVT function [305].

The second mechanism responsible for the acceleration of spiral artery remodeling by miR-218-5p may lie in the upregulation of immune-responsive chemokines. Crosstalk between trophoblasts and the decidualized uterus are vital to the establishment of a healthy feto-maternal interface. Paracrine signals from the invading trophoblasts have been shown to contribute to the enriched cytokine milieu at the implantation site responsible for immune modulation and angiogenesis. In decidual endometrial stromal cells cultured in conditioned media from primary first trimester trophoblasts, CXCL1, IL6, IL8, and Intercellular Adhesion Molecule-1 (ICAM1), are among the most highly upregulated genes [297]. Closer examination of our miR-218-5p co-culture tissues shows an abundant recruitment of CD45 positive leukocytes along the entire length of the visible vessel compared to the control. These data support a leukocyte chemotaxis effect of miR-218-5p-treated trophoblasts on the surrounding maternal tissue. During the invasive period of gestation, dNK and monocytes are predominant CD45+ leukocytes in the decidua basalis. Trophoblast-derived CCL2 in the promotion of monocyte migration has previously been reported, although not in the context of spiral artery remodeling [306,307]. CCL2 has also been shown to promote the pro-anigogenic dNK phenotype important in spiral artery remodeling; however the CCL2 was dNK in origin [308]. Likewise, trophoblast secreted CXCL16 has been implicated in the recruitment of monocytes and T-cells in the first-trimester decidua [309].

While the TGFβ pathway has been implicated in placental development, its role in enEVT differentiation and spiral artery remodeling has not been reported. In this study, we observed that the TGFβ signaling pathway is downregulated in the mir-218-1 cells. First, microarray analysis revealed that TGF-β2 and several downstream Smads, such as Smad2, 3, and 4, were significantly lower in mir-218-1 stable cells when compared to the cells expressing an empty vector conrol. The downregulation of these signaling molecules were confirmed with qRT-PCR in mir-218-1 cells. Second, mir-218-1 significantly repressed TGFβ signaling as indicated by the PAR-3Lux luciferase reporter assay. Finally, silencing of TGF-β2 mimicked some of the miR-218-5p phenotype. Specifically, in both HTR-8/SVneo cells and placental explants, we found that TGF-β2 inhibited invasion and explant outgrowth and incubation with TGF-β2 resulted in the down-regulation of enEVT markers in the trophoblast cell line. The TGF-β2 treatment also partially reversed the effect of mir-218-1. These findings suggest that the TGFβ pathway may be involved in the miR-218-5p-regulated enEVT differentiation and invasion. Mir-218-1 was shown to suppress TGF-β2 mRNA and protein levels. These findings suggest that TGF-β2 exerts a negative effect on enEVT differentiation and its down-regulation by miR-218-5p is in part responsible for the promotion of enEVT differentiation and spiral artery remodeling. The direct downregulation of TGF-β2 by miR-218-5p through its 3'UTR is suggested, although further validation is needed to ensure this is a specific ineraction. The three TGFβ isoforms and their downstream regulatory molecules have been located at the feto-maternal interface. Most studies suggest that the TGFβ pathway is a negative regulator of trophoblast invasion. An early study of integrin regulation showed that TGFβ-2 treated first trimester primary cytotrophoblasts decreased both migration and invasion by promoting cell attachment [310]. Primary EVT cells

treated with TGFβ-1, -2 or -3 had a dose-dependent inhibition of invasion. Likewise, neutralization of all three endogenous isoforms promoted the EVT invasive ability [311]. In addition, another study reported that TGFβ-2 treated first trimester explants had a reduction in EVT outgrowth area; however TGFβ-1 or -3 had no effect [233]. Suppression of Smad2 by miR-18a was also shown to promote trophoblast invasion [160]. While the effect of TGFβ-2 on the endovascular EVT pathway has not been previously reported, primary trophoblast treatment with TGFβ-1 has been shown to reduce trophoblast invasion through suppression of VE-cadherin [312]. On the contrary, a pro-invasive effect of TGFβ2 in HTR8/SVneo cells has been recently reported [313]. It is important to mention that interpretation of findings from an immortalized cell line alone should be approached with caution. A study examining the role of TGFβ-1 on HTR8/SVneo cells reported that after passage 90, the cell line no longer accurately represented the parental trophoblasts [314]. Likewise, an earlier study on MMP secretion in HTR8/SVneo cells showed a TGFβ-1 upregulation of MMP-2 activity, however this was through a Smad2-independent mechanism [315].

In summary, this study provides the first evidence that miR-218-5p plays important roles in healthy placentation and may be involved in the pathogenesis of PE. Using a combination of cell and human tissue models, we showed that miR-218-5p promoted the pro-invasive and pro-angiogenic phenotype seen in the differentiation of endovascular EVTs. While miR-218-5p was upregulated during the peak period of deep trophoblast invasion and spiral artery remodeling, it was down in tissues affected by PE. We further showed that suppression of TGFβ-2 was partially responsible for the effect of miR-218-5p in trophoblast differentiation and invasion. The use of

microRNAs as potential plasma biomarkers has been investigated [223,316], and the utility of miR-218-5p as both a predictive and prognostic marker in cancer has been suggested by others [272,274]. A significant increase in serum TGFβ-2 was reported in cases of severe PE and eclampsia compared to control [254]. These data, taken together with our findings, suggest great potential of miR-218-5p as a biomarker of PE and possibly other hypertensive disorders of pregnancy.

CHAPTER 3: DIFFERENTIAL ROLE OF SMAD2 AND SMAD3 IN ENDOVASCULAR EVT DIFFERENTIATION AND PREECLAMPSIA

Brkić J. and Peng C.

SUMMARY

Proper placental development is key for healthy pregnancy outcomes. In the first 20 weeks of gestation the placenta needs to invade the uterus, remodel maternal spiral arteries, and establish proper placental perfusion to sustain the needs of the growing fetus. Dysfunction in the precise regulation of these processes can lead to the development of pregnancy complications, such as preeclampsia (PE). TGF-β/Nodal/Activin signaling components have been reported at the feto-maternal interface and are known to both promote and inhibit the invasive extravillous trophoblast (EVT) pathway. These ligands signal through serine/threonine receptor complexes to activate receptor Smads, Smad2 and Smad3. Using first trimester trophoblast cell line, HTR8/SVneo, and first trimester tissues we show that silencing of Smad2 and Smad3 produced opposite effects. Smad2 suppressed, while Smad3 promoted, trophoblast invasion and enEVT marker gene expression. Furthermore, we found that while total Smad2/3 levels are relatively constant across gestation, phosphorylated Smad2 (pSmad2) levels are significantly lower, while pSmad3 are significantly higher, in the first 20 weeks of pregnancy when invasion and spiral artery remodeling occur. Additionally, pSmad3 was significantly downregulated, while pSmad2 was upregulated, in placentas from PE patients. These findings suggest that Smad2 and Smad3 have distinct functions in trophoblasts and that their dysregulation may contribute to events that lead to PE.

INTRODUCTION

Serving as the interface between the fetal and maternal environments, the placenta plays critical roles in maintaining and protecting the developing fetus throughout pregnancy. The polarized outer cells of the blastocyst differentiate into cells of the trophoblast lineage that make up the placenta. Once the trophectoderm is in intimate contact with the decidua the process of placentation can begin. The cytotrophoblast progenitor cells (CTBs), located at the basement membrane of the placental villi, differentiate in two general pathways [257]. In the fusion pathway, CTBs form multinucleated syncytial cells that line the placental villi. In the invasive pathway, proliferative CTB form anchoring columns that attach to the uterine epithelium and differentiate into two populations of extravillous cytotrophoblasts (EVTs). Interstitial EVTs (iEVTs) invade the decidua and differentiate into giant cells. Endovascular EVTs (enEVTs) acquire endothelial-like characteristics and remodel maternal spiral arteries, which provide the steady, low-velocity blood flow to the placenta in order to meet the requirements of the growing fetus. While syncytial cell turnover continues throughout pregnancy, the invasive pathway is mainly restricted to the first and second trimester [290,317]. Disruption in the pathways involved in placental development in this invasive period has been linked to hypertensive diseases of pregnancy, such as preeclampsia (PE) [259].

PE is a multifactorial disorder that can manifest during pregnancy posing a major risk to both the mother and fetus. It is typically diagnosed after 20 weeks of gestation as a maternal syndrome defined by the sudden onset of hypertension (≥140/90 mmHg) and proteinuria (≥300mg in 24h) [318]. Prior to the onset of the clinical condition, characterizations of poor

trophoblast migration and invasion into the decidua, along with inadequate placental perfusion due to shallow invasion of spiral arteries are reported [319]. These histological findings are accompanied by elevated anti-angiogenic factors, namely soluble fms-like tyrosine kinase 1 receptor (sFlt-1) and soluble Endoglin (sEng), and the downregulation of pro-angiogenic factors such as placenta growth factor, PGF [320,321]. These intricate events involved in placental development are tightly regulated by a large group of molecules, including the transforming growth factor (TGF)-β pathway [322].

The TGF-β superfamily is a large group of growth factors implicated in a number of cellular processes during vertebrate development including stem cell renewal and commitment, tissue homeostasis, proliferation, and regulation of invasion. The signaling molecules include the TGF-βs, Activins, Nodal, and bone morphogenetic proteins (BMPs). Acting through the Type I and Type II serine/threonine receptor complexes they activate the downstream receptor Smads (R-Smads). In general, R-Smads, Smad2 and Smad3, are activated by TGFβ, Activin, and Nodal signals. Subsequently, they complex with the common Smad4 and translocate to the nucleus where they act to promote or repress gene transcription. While sharing 96% of sequence identity in their MH2 domain, Smad2 differs from Smad3 mainly in the N-terminal MH1 domain where an additional sequence insertion perturbs its ability for direct DNA binding [189,323]. Studies on knockout mice have shown that while Smad2 knockout mice are embryonically lethal, while Smad3 deficient mice are viable. A great deal of investigation into the exact phenotypes of these mouse models has revealed both distinct and overlapping roles of Smad2 and Smad3 [324-329].

The TGF-β pathway is involved in many aspects of placental development. While Activin A promotes trophoblast differentiation down the invasive pathway, TGFβ-1 and -3 inhibit this pathway [330]. Many studies have confirmed the inhibiting role of all three TGFβ isoforms in trophoblast cell invasion and EVT outgrowth [233,311,331]. However, the pro-migratory and pro-invasive effects of TGFβ have also been recently reported [313,332]. Likewise, Nodal has been shown to both inhibit [223,277,278] and promote [236] trophoblast cell invasion. The mechanisms responsible for different TGF-β signaling responses, as well as the exact signals that are regulated by Smad2 versus Smad3 are still unclear [333].

In our previous work (Chapter 2) we show that a miRNA downregulated in PE, miR-218-5p, promotes trophoblast invasion and differentiation into enEVT through the suppression of TGFβ2. Furthermore, our data suggest that Smad2 also plays a role in miR-218-5p-regulated enEVT differentiation. In the current study, we investigate the differential function of Smad2 and Smad3 in first trimester trophoblasts and discuss their potential role in regulating EVT differentiation. Furthermore, we characterize the expression and activity of Smad2 and Smad3 across gestation in healthy placenta tissues as well as placentas from patients diagnosed with PE.

MATERIALS AND METHODS

Patients and Placental Tissue Collection

All fresh and frozen human placenta tissues used in this study are described in Chapter 2. For the evaluation of Smad2 and Smad3 expression across gestation, 20 placentas were used. Specifically, 10 from 6-20 weeks and 10 from 25-40 weeks were analyzed. To assess if there is dysregulation of Smad2/3 in PE, we used 6 placentas from PE patients delivered between 28-39 weeks.

Protein Extraction and Immunoblot Analysis

Snap frozen tissues were lysed in five volumes of HEPES lysis buffer (10 mM HEPES, 10 mM NaCl, 0.1 mM EDTA, 0.1 mM EGTA, 1.0 mM DTT, 0.1% NP-40, pH 7.9) with a Pierce Protease and Phosphatase inhibitor (Thermo Scientific) and homogenized for 30 s twice while kept on ice. Protein was quantified using the Pierce BCA Protein Assay Kit (Thermo Fisher). Equal amounts of protein were separated by SDS-polyacrylamide gel electrophoresis and transferred to a polyvinylidene difluoride membrane (Immobilon-P, Millipore Corp.). Membranes were blocked in 5% blocking buffer (5% skim milk in Tris-buffered Saline and Tween-20) for 1h at room temperature, then incubated overnight in primary antibody at 4°C (Table 3.1). Membranes were subsequently probed using horseradish peroxidase–conjugated secondary antibody (1:5000) at room temperature for 2h. Signals were detected using the ECL Plus Kit (Amersham Biosciences).

Table 3.1 Primary Antibodies and Staining Reagents

Antibody	Company	Cat No.	Species	Dilution	Diluent
pSmad2	Cell Signaling	3101S	Rabbit	1:500	5% Milk-TBST
pSmad3	Cell Signaling	9520S	Rabbit	1:500	5% BSA-TBST
Smad3	Invitrogen	511500	Rabbit	1:150	5% Milk-TBST
Smad2/3	Cell Signaling	3102S	Rabbit	1:1000	5% BSA-TBST
Smad4	Santa Cruz	sc-7966	Mouse	1:100	5% Milk-TBST
GAPDH	Santa Cruz	sc-47724	Mouse	1:5000	5% Milk-TBST
Calcein AM	Corning	354217	N/A	1µM	Serum-free media

Cell Culture

An immortalized human first trimester trophoblast cell line, HTR8/SVneo, was obtained from Charles Graham (Queen's University, Kingston, ON, Canada), and was cultured as previously described [279]. Briefly, cells were maintained in HyClone™ Classical Liquid Media RPMI 1640 (Fisher Scientific) supplemented with 10% Fetal Bovine Serum (FBS) (GIBCO), Streptomycin (100 µg/ml), and Penicillin (100 IU/ml), in an atmosphere of 5% CO_2 at 37°C. Cells were periodically checked for mycoplasma contamination using a Mycoplasma Detection Kit-QuickTest (BioTools), and when needed, treated with MycoSmash Mycoplasm Removal Kit (BioTools), following the manufacturer's directions. All experiments were carried out on cells in between passages 73 and 85.

Transfections and Recombinant Protein Treatment

Transient transfection of siRNA oligomers (100 nM) was carried out using Lipofectamine RNAiMax (Invitrogen). All plasmid transfections (1 ug) were carried out using Lipofectamine 2000 (Invitrogen). A modified protocol was used to optimize for transfection efficiency and cell survival. Transfections were carried out in 6-well plates on 70% confluent cultures. For each transfection reaction, 2 µl of Lipofectamine reagent was used and incubated with nucleotides for 15min at room temperature in Opti-MEM media (GIBCO). Transfections were carried out for 5h, then recovered with 10% FBS containing media for 16hr. Cells used for marker analysis were recovered for an additional 24h in serum-free media. SiSmad2, siSmad3 and non-targeting controls were purchased from GenePharma Co. (Shanghai, China) (Table 3.2). The Smad2 and Smad3 wild type constructs were a kind gift from Dr. Yan Chen (Indiana University School of Medicine, Department of Medical and Molecular Genetics).

Table 3.2 Primers and Oligomers

Name	Sequence: 5' → 3'	NCBI BLAST
Cyc1	**F:** CAGATAGCCAAGGATGTGTG **R:** CATCATCAACATCTTGAGCC	Cytochrome c1
VE-cad	**F:** GCCAGTTCTTCCGAGTCACA **R:** TTTCCTGTGGGGGTTCCAGT	Cadherin 5
MMP1	**F:** GTCTCACAGCTTCCCAGCGA **R:** ATGGCATGGTCCACATCTGC	Matrix Metallopeptidase 1
IL1b	**F:** AATCTGTACCTGTCCTGCGTGTT **R:** TGGGTAATTTTTGGGATCTACACTCT	Interleukin 1 beta
IL8	**F:** CAGAGACAGCAGAGCACACA **R:** GGCAAAACTGCACCTTCACA	C-X-C motif chemokine ligand 8
ECSCR	**F:** ACAACTCCCAGCCCACAATG **R:** GTGGTCAGACTTAGACCGCC	Endothelial Cell-Specific Chemotaxis Regulator
siSmad2	**Sense:** GUCCCAUGAAAAGACUUAAtt **Anti-sense:** UUAAGUCUUUUCAUGGGACtt	SMAD family member 2
siSmad3	**Sense:** CUGUGUGAGUUCGCCUUCAtt **Anti-sense:** UGAAGGCGAACUCACACAGtt	SMAD family member 3
siSmad4	**Sense:** GGUCUUUGAUUUGCGUCAGtt **Anti-sense:** CUGACGCAAAUCAAAGACCtt	SMAD family member 4
NC	UUCUCCGAACGUGUCACGUtt ACGUGACACGUUCGGAGAAtt	No match

RNA Extraction, Reverse Transcription and qRT-PCR

Total RNA from cells was extracted using TRIzol reagent (Invitrogen) as per manufacturer's protocol. Reverse transcription was performed on 1.5 µg total RNA with M-MuLV Reverse Transcriptase (New England Biolabs). Quantitative Real Time PCR was carried out with EvaGreen qPCR Master Mix (ABM), following the manufacturer's directions, on a RotorGene Q thermocycler (QIAGEN). All target genes were normalized to cytochrome c1 (Cyc1). The relative mRNA level was calculated using the $2^{-\Delta\Delta ct}$ method. All primers (Table 3.2) used in this study were validated for specificity with primer-BLAST (NCBI), and amplified products were run on an agarose gel to ensure a single band product.

Transwell Invasion Assay

Transwell inserts with 8 µm pores (Costar, Corning Inc.) were coated with Celtrex Reduced Growth Factor BM extract-PathClear (1:100 in Serum Free media, Trevigen) and allowed to polymerize overnight at 37°C. Cells were gently removed from culture plates using Accutase (Innovative Cell Technologies), and seeded at a density of 20,000 cells per well in serum-free RMPI1640 media. As a chemotactic agent, 10% serum containing medium was seeded on the outside of the transwell. After 24h, membranes were fixed for 2min in 100% methanol and stained using Harleco Hemacolor Staining Kit (EMD Chemicals). Invaded cells were counted with ImageJ [280] and the invasion index was calculated as a fold of invaded cells in the treated groups compared to the control group.

First-Trimester Human Placental Explant Culture

Explant cultures were performed as previously described [21,235]. Briefly, villous explants with potential EVT columns were carefully dissected and positioned on Transwell inserts (Millipore,

Billerica, MA) pre-coated with 200 µL of undiluted phenol red-free Matrigel (BD Biosciences, Bedford, MA). Explants were left overnight to attach to the matrigel, at 37°C with 3% O_2 and 5% CO_2, before adding serum-free DMEM-F12 medium supplemented with 100 U/mL of penicillin, 100 U/mL of streptomycin, 100 µg/mL Normacin™. After two days of culture, villous tips were examined under the dissecting microscope for successful EVT outgrowths. All successful explants were selected for treatment with 200 nM oligomers (Table 3.2). Explants were photographed immediately after adding treatment, and subsequently at 48hr, using a Leica DFC400 camera attached to a dissecting microscope. ImageJ was used to measure the area of EVT outgrowth. Specifically, total outgrowth area was calculated by subtracting the area at the end point with the initial area upon treatment. Each experiment was designed with a minimum of four replicates, and was repeated on three individual placental samples.

Endothelial-like Network Formation Assay

On ice, 96-well plates were quickly coated with 50 µl of Celtrex Reduced Growth Factor BM extract-PathClear (Trevigen), and allowed to polymerize at 37°C for 30min. HTR8/SVneo cells were seeded at 25,000 cells per well in 100 µl of 10% FBS containing RPMI1640. After 16-20h of culture, cells were stained with 1 µM Calcein AM (Corning) for 15min, and pictures were taken at 20X magnification on a fluorescence microscope. Total network length was quantified in ImageJ using the NeuronJ plugin [285].

Statistical Analysis

Statistical analysis was performed using Graphpad Prism 7 ($p<0.05$, 95% CI). Unpaired, two-tailed, Student *t* test was used for comparison between two groups. One-way ANOVA followed by a Dunnett's multiple comparisons test determined differences among several groups.

RESULTS

Smad2 and Smad3 have opposing patterns of activity in placenta across gestation

To explore the roles of Smad2 and Smad3 in placenta development we first assessed their expression pattern across gestation. Healthy placentas from patients at Mount Sinai Hospital undergoing elective termination or Caesarean section were chosen at random from available Biobank samples. Total Smad2 and total Smad3 levels were normalized to their respective loading control, GAPDH. We found no significant difference in total Smad2 (Figure 3.1A) or Smad3 (Figure 3.1B) protein expression across gestation. To assess if the active forms of Smad2 or Smad3 differed between the two halves of pregnancy we used anti-phospho antibodies. Quantification of p-Smad2 and p-Smad3 levels was normalized to the total Smad2 or Smad3 protein levels, respectively. A significant increase ($p<0.01$) in phosphorylated Smad2 (pSmad2) was observed between 25-40 weeks of gestation compared to 6-20 weeks of gestation (Figure 3.1A). Conversely, a significant decrease ($p<0.01$) in phosphorylated Smad3 (pSmad3) was observed in 6-20 weeks of gestation compared to 25-40 weeks of gestation (Figure 3.1B).

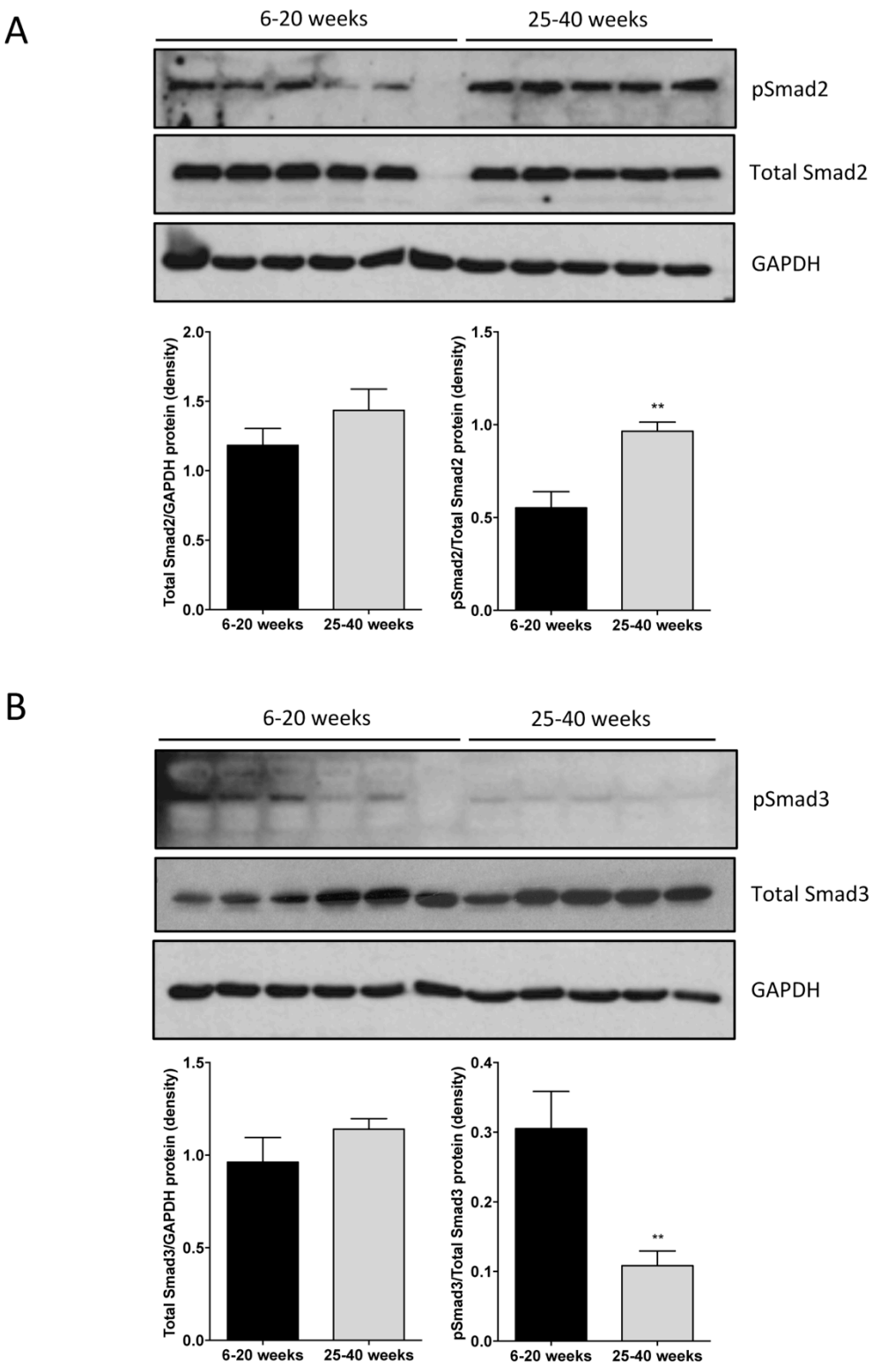

Figure 3.1 Legend found on next page

Figure 3.1 Smad2 and Smad3 activity has opposing patterns in placenta across gestation.
Healthy placentas from patients at Mount Sinai Hospital undergoing elective termination or Caesarean section were assessed for **(A)** pSmad2/Total Smad2 or **(B)** pSmad3/Total Smad3 with Western Blotting. Band density was quantified using ImageJ from two separate blots. A total of ten placentas were used for each gestation period and a representative blot is shown. Total Smad2 and Smad3 levels were normalized to corresponding GAPDH signal and no significant difference was found. P-Smad2 and p-Smad3 were normalized to Total Smad2 or Smad3 protein, respectively. **(A)** A significant increase ($p<0.01$) in pSmad2 was observed in the 25-40 week group compared to the 6-20 weeks of gestation. **(B)** A significant decrease ($p<0.01$) in pSmad3 was observed in the 25-40 week group relative to the 6-20 weeks of gestation. Statistical analysis was performed on GraphPad Prism using an unpaired t-test ($p<0.05$, 95% CI). Error bars represent SEM.

Smad2 and Smad3 have differential roles in EVT differentiation

To investigate the functional roles of Smad2 and Smad3 we used a siRNA knockdown approach. We used an established first trimester trophoblast cell line, HTR8/SVneo, with a confirmed functioning TGFβ signaling pathway. First we validated the siRNA used in our study. Quantitative-Real Time PCR showed a significant downregulation ($p<0.005$) of Smad2 mRNA with siSmad2 transfection, and Smad3 mRNA with siSmad3 transfection (Figure 3.2A and 3.2B, respectively). Furthermore, Western blotting with the Total Smad2/3 antibody showed a clear downregulation of total Smad2 protein by siSmad2 and total Smad3 protein by siSmad3 (Figure 3.2C). HTR8/SVneo transfected with siSmad2 showed a significant upregulation of major markers of EVT differentiation previously shown to be upregulated by miR-218-5p (Chapter 2). Specifically, siSmad2 transfected cells significantly upregulated VE-cadherin by 4 fold ($p<0.01$), MMP1 by 14 fold ($p<0.01$), ECSCR by 2.5 fold ($p<0.01$), IL1b by 5 fold ($p<0.05$), and IL8 by 5 fold ($p<0.001$) (Figure 3.3A). In contrast, siSmad3 transfected cells showed a significant downregulation of all of these markers. Specifically, a significant downregulation of VE-cadherin by 4 fold ($p<0.0001$), MMP1 by 2 fold ($p<0.005$), ECSCR by 1.5 fold ($p<0.001$), IL1b by 6 fold ($p<0.0001$), and IL8 by 23 fold ($p<0.01$) was observed in siSmad3 transfected cells compared to the control (Figure 3.3B).

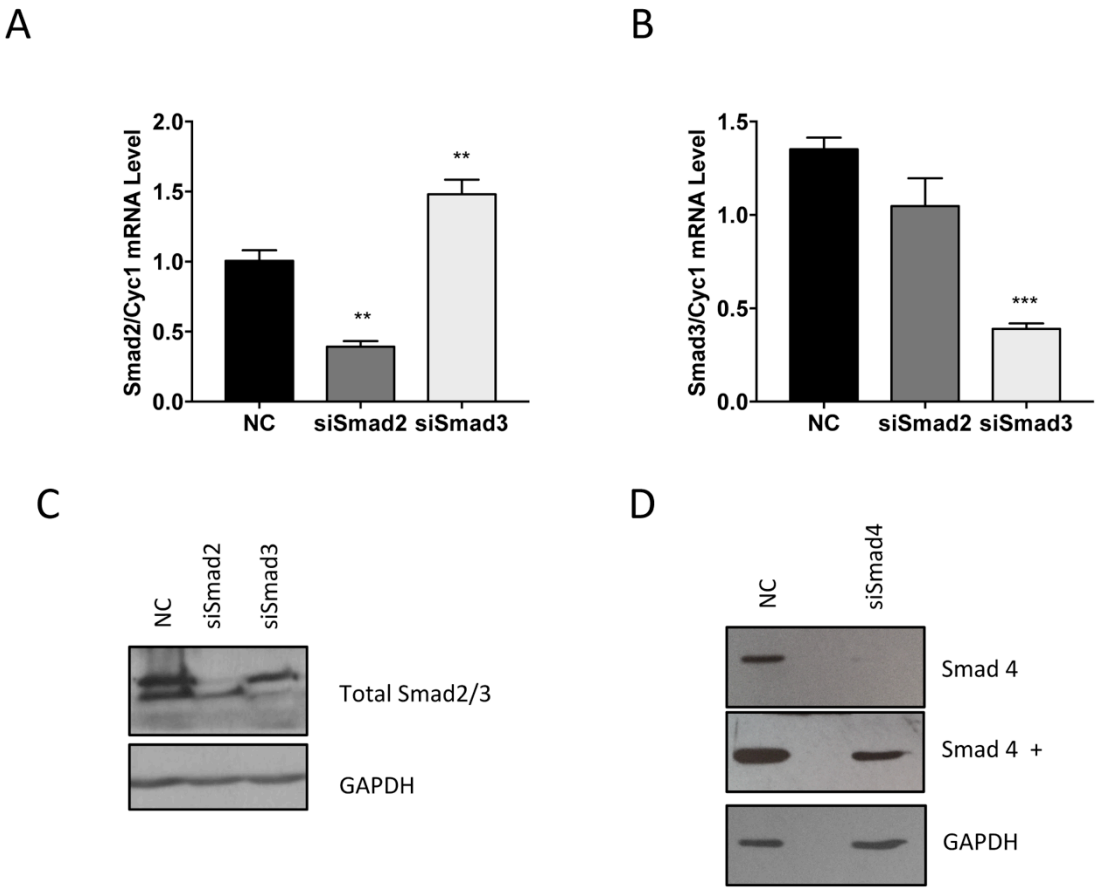

Figure 3.2 Validation of Smad siRNAs.
To investigate the functional roles of Smad2 and Smad3 we used a siRNA knockdown approach. **(A)** Using q-RT-PCR we validated that siSmad2 significantly downregulated ($p<0.01$) Smad2 mRNA, without reducing Smad3 levels. **(B)** siSmad3 significantly reduced ($p<0.001$) Smad3 mRNA without reducing Smad2 levels. **(C)** Western blotting with a Total Smad2/3 antibody further validated the downregulation of Smad2 with siSmad2 and Smad3 with siSmad3. **(D)** Western blotting with Total Smad4 antibody confirmed the knockdown of Smad4 by siSmad4. "+" indicates longer exposure time. Level of GAPDH was used as a loading control for Western blotting.

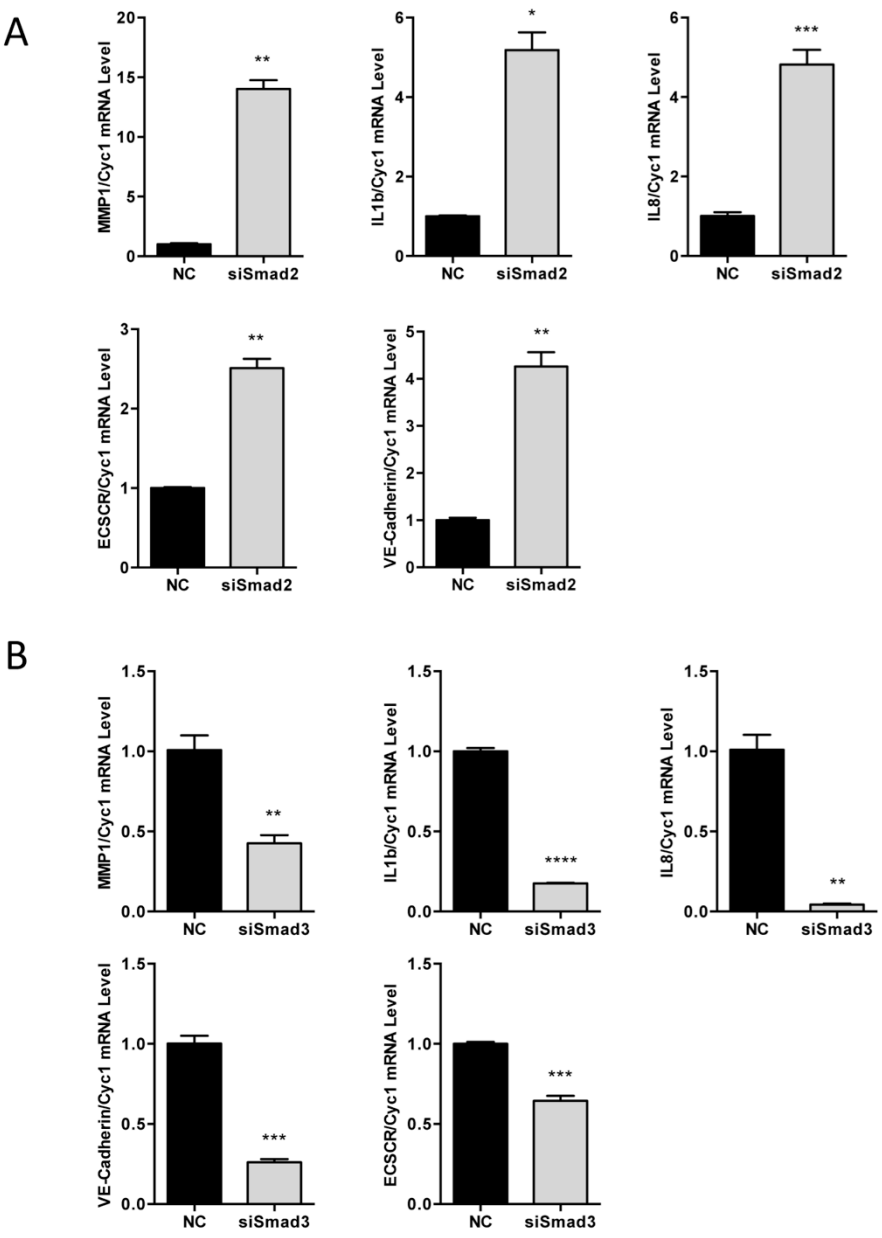

Figure 3.3 Smad2 and Smad3 have differential roles in EVT differentiation.
(A) First trimester cell line, HTR8/SVneo, was transfected with 100nM siSmad2 and total RNA was extracted and used for qRT-PCR. A significant upregulation of major markers of EVT differentiation were observed. **(B)** HTR8/SVneo was transfected with siSmad3 and total RNA was used for qRT-PCR. A significant downregulation of key markers involved in EVT differentiation were observed. Statistical analysis was performed on GraphPad Prism using an unpaired t-test ($p<0.05$, 95% CI). Error bars represent SEM. *$p<0.05$, **$p<0.01$, ***$p<0.001$, ****$p<0.0001$

Next, we investigated the effect of Smad2 or Smad3 knockdown on trophoblast cell invasion. In our first model we used HTR8/SVneo transfected cells seeded on matrigel-coated transwells. Cells transfected with siSmad2 invaded significantly higher ($p<0.01$) than control cells (Figure 3.4A). HTR8/SVneo cells transfected with siSmad3 showed a significant reduction ($p<0.01$) in invasion compared to control cells (Figure 3.4B). In our second model we used first trimester placental explants attached to a matrigel substrate. Tissues treated with siSmad2 showed a significantly higher ($p<0.05$) 48h EVT outgrowth area compared to control tissues (Figure 3.4C). Whereas, first trimester placental explants treated with siSmad3 showed a significant reduction ($p<0.05$) in EVT outgrowth at 48h compared to control treated tissues (Figure 3.4D).

Since many of the upregulated gene markers suggest a switch from the epithelial to endovascular phenotype, we assessed the role of Smad2 and Smad3 using an endothelial-like network formation assay. HTR8/SVneo cells were transfected, seeded on matrigel-coated wells, and after 16h were stained with Calcein AM. Total network length was measured with ImageJ. Cells transfected with siSmad2 had a significantly larger ($p<0.0001$) network formed compared to the scramble control. Interestingly, siSmad2 co-transfected with siSmad4 increased the total network length even further (Figure 3.5A). Conversely, siSmad3 transfected cells formed overall a significantly smaller ($p<0.0001$) network structure compared to scramble control cells. Similarly, co-transfection of siSmad3 and siSmad4 enhanced the effect further, with nearly no network formation.

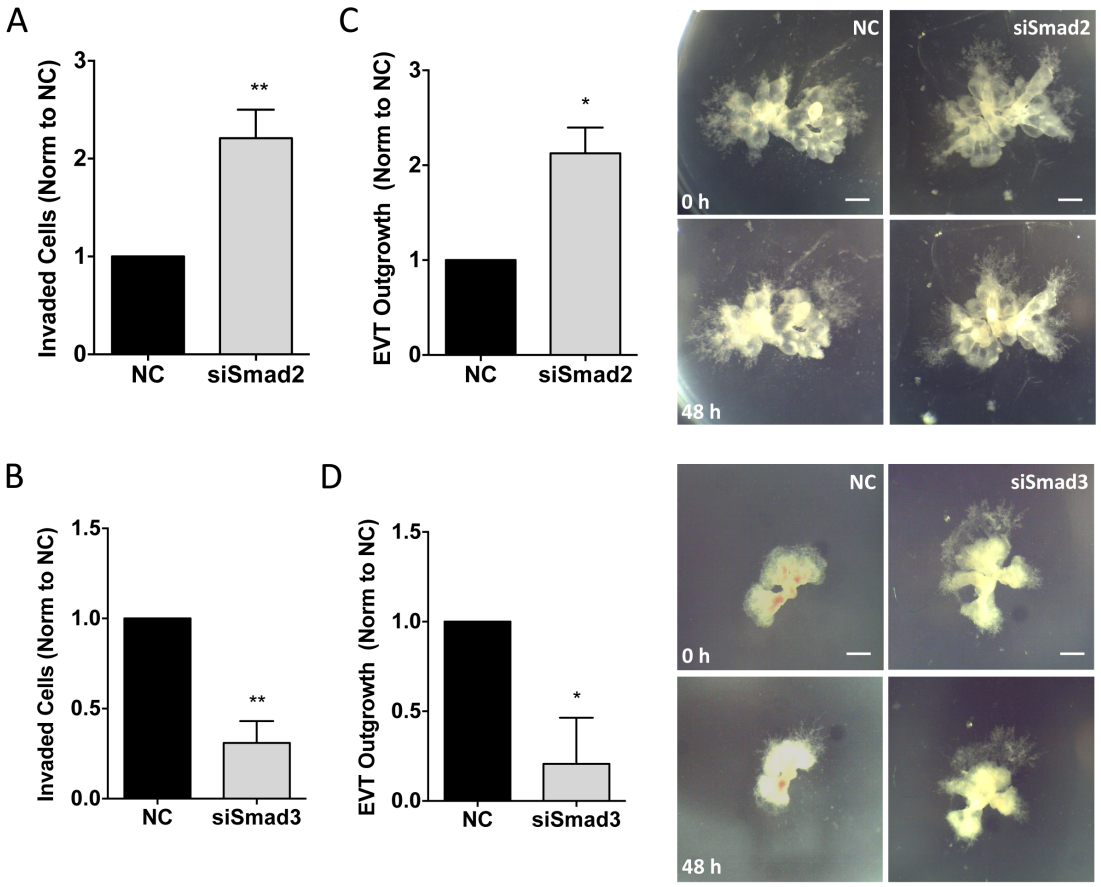

Figure 3.4 Smad2 represses and Smad3 promotes invasion and EVT outgrowth.
(A) HTR8/SVneo cells transfected with siSmad2 and seeded on matrigel-coated transwells invaded significantly higher ($p<0.01$) than control cells. **(B)** HTR8/SVneo cells transfected with siSmad3 showed a significant reduction ($p<0.01$) in invasion compared to control cells. **(C)** SiSmad2 treated first trimester placenta explants showed a significantly higher ($p<0.05$) 48h outgrowth area compared to control tissues. **(D)** First trimester placental explants treated with siSmad3 showed a significant reduction ($p<0.05$) in EVT outgrowth at 48h compared to control treated tissues. Image quantifications were performed using ImageJ software. Statistical analysis was performed on GraphPad Prism using an unpaired t-test ($p<0.05$, 95% CI).
Scale bar: 500 µm. Error bars represent SEM.

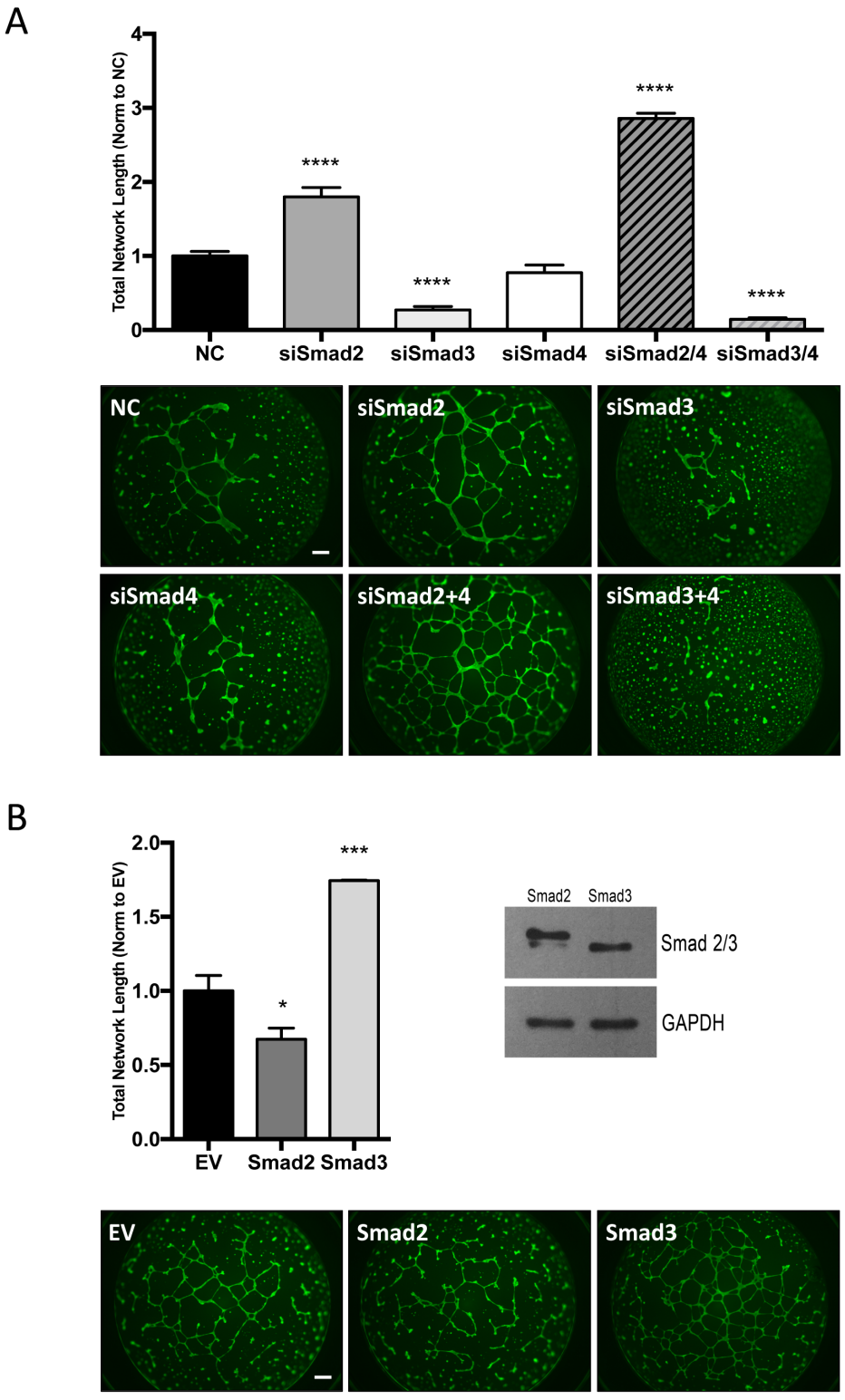

Figure 3.5 Legend found on next page

Figure 3.5 Smad2 represses, while Smad3 promotes trophoblast network formation.
HTR8/SVneo cells transfected with 100 nM oligomers **(A)** or 1 µg plasmid **(B)** were seeded on matrigel-coated wells. After 16h cells were stained with Calcein AM and total network length was measured with ImageJ. **(A)** siSmad2 and siSmad2/4 transfected cells formed more intricate network structures with significantly larger ($p<0.0001$) total length compared to scramble control. Conversely, siSmad3 and siSmad3/4 transfected cells formed significantly smaller ($p<0.0001$) network structures compared to scramble control cells. SiSmad4 transfected cells formed structures similar to scramble control cells. **(B)** Overexpression of Smad2 significantly suppressed ($p<0.05$) the network size, while Smad3 significantly increased ($p<0.001$) total network length compared to the empty vector control. Western Blot indicates levels of Smad2 or Smad3 after indicated construct transfection. Statistical analysis was performed on GraphPad Prism using an unpaired t-test ($p<0.05$, 95% CI). Scale bar: 500 µm. Error bars represent SEM.

On the other hand, cells transfected with only siSmad4 formed networks similar to the control cells (Figure 3.5A). To support these findings further, we overexpressed wild type Smad2 or Smad3 into HTR8/SVneo cells. Overexpression of Smad2 significantly suppressed ($p<0.05$), while Smad3 significantly increased ($p<0.001$) the total network length compared to the empty vector control (Figure 3.5B).

Smad2 and Smad3 activity in PE placenta

Healthy placentas and placentas from PE diagnosed patients at Mount Sinai Hospital undergoing Caesarean section were processed. Total Smad2 and Smad3 protein levels were normalized to their GAPDH loading control. No significant difference in total levels of Smad2 and Smad3 were found in either healthy or PE tissues (Figure 3.6A and B, respectively). P-Smad2 and p-Smad3 were normalized to Total Smad2 or Smad3 protein, respectively. The expression of pSmad2 was slightly elevated in PE samples compared to gestation age-matched controls (Figure 3.6A). Whereas the level of p-Smad3 was significantly decreased ($p<0.0001$) in PE placentas relative to healthy gestation age-matched controls (Figure 3.6B). Interestingly, the expression of p-Smad3 in all PE tissues analyzed was nearly undetectable even with longer ECL exposure (data not shown).

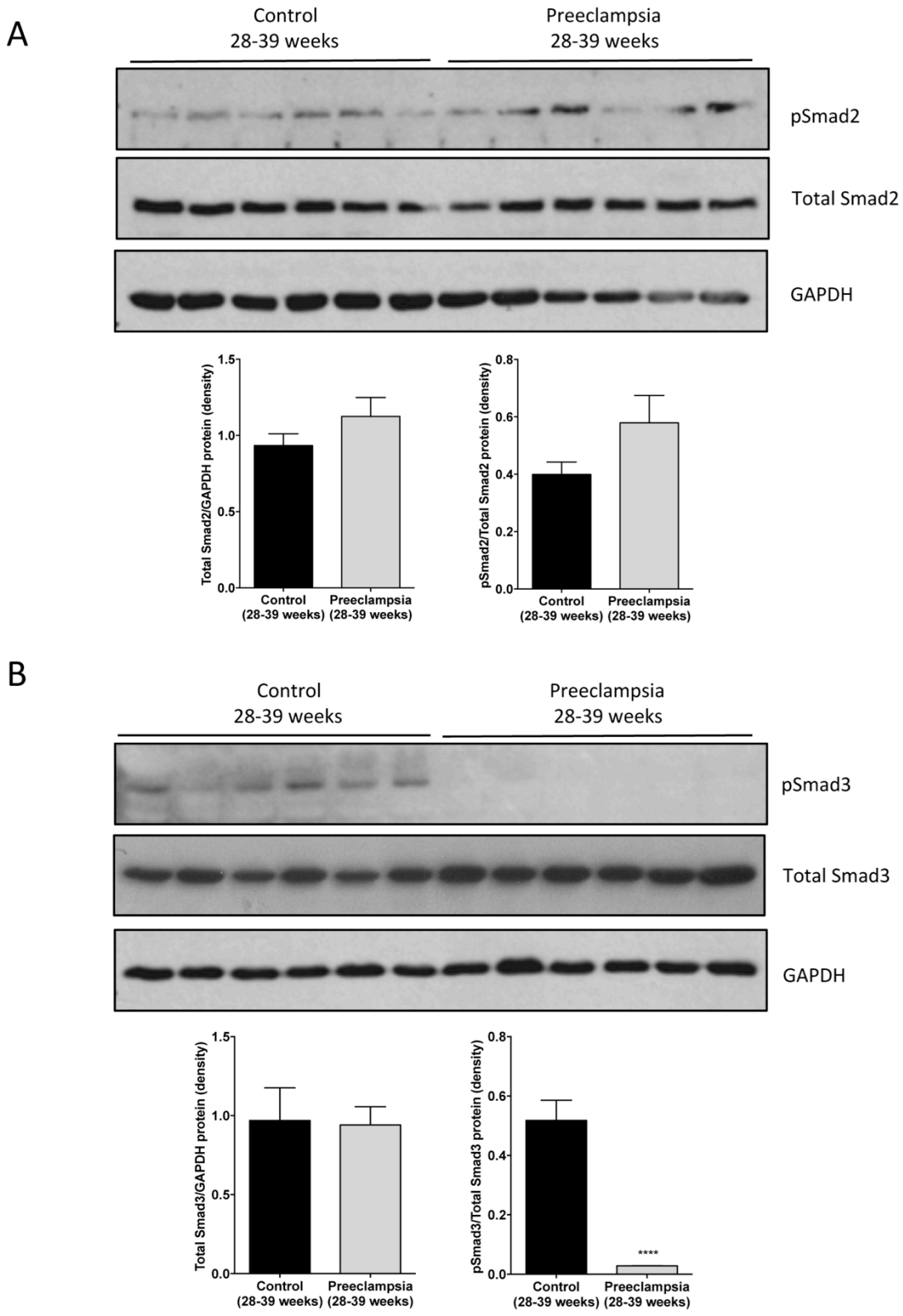

Figure 3.6 Legend found on next page

Figure 3.6 p-Smad3 is downregulated in PE tissues.
Healthy placentas and placentas from PE diagnosed patients at Mount Sinai Hospital undergoing Caesarean section were assessed for **(A)** pSmad2/Total Smad2 or **(B)** p-Smad3/Total Smad3 with Western Blotting. Band density was quantified using ImageJ. Each group consisted of six unique patient placenta samples. Total Smad2 and Smad3 levels were normalized to corresponding GAPDH signal and no significant difference was found. P-Smad2 and p-Smad3 were normalized to Total Smad2 or Smad3 protein, respectively. **(A)** p-Smad2 was slightly elevated in PE samples compared to gestation age-matched controls **(B)** A significant decrease ($p<0.0001$) in p-Smad3 was observed in PE placenta relative to healthy gestation age-matched controls. Statistical analysis was performed on GraphPad Prism using an unpaired t-test ($p<0.05$, 95% CI). Error bars represent SEM.

DISCUSSION

In this study, we provide the first evidence that Smad2 and Smad3 may have distinct roles in EVT invasion and endovascular differentiation. Specifically, we show that Smad2 inhibits, while Smad3 promotes trophoblast invasion and differentiation into enEVTs. Our expression data indicate that while total Smad2/3 levels are consistent across gestation, their phosphorylated (p-Smad) levels have differential expression. P-Smad3 was relatively higher in the first 20 weeks of gestation compared to later in gestation. Where as p-Smad2 levels were relatively lower in the first 20 weeks of gestation compare to later in gestation. Furthermore, we are first to show that pSmad3 levels are significantly downregulated in placenta from PE patients.

Knockdown of Smad2 promoted, while knockdown of Smad3 inhibited, several important genes that promote the invasive capacity of trophoblasts. Matrix metallopeptidase 1 (MMP1) is a collagenase important for deep placental invasion and is downregulated in EVTs from PE placentas [334]. Interleukin-1b (IL1b) upregulates trophoblast proteases essential in EVT invasion [230]. Likewise, Interleukin-8 (IL8) promotes trophoblast migration and invasion through the upregulation of MMP2/9 [335]. Additionally, we report that Smad2 suppressed, while Smad3 promoted, the epithelial to endovascular marker switch involved in enEVT differentiation, such as the VE-cadherin and Endothelial Cell-Specific Chemotaxis Regulator (ECSCR). VE-cadherin upregulation is essential in the trophoblast-mediated endothelial replacement during spiral artery remodeling [336]. Although no known function of ECSCR has been reported in placenta, the enEVT of decidua basalis have shown strong immunostaining [337]. Despite their sequence similarity, Smad2 and Smad3 have shown distinct transcriptional activities [338,339]. Furthermore,

their distinct roles in regulating cell differentiation have been reported in other systems. For example, Smad3 has been identified as a key promoter of neuronal differentiation and cell fate specification, independent of Smad2 [340]. While Smad2 signaling, and not Smad3, was indispensible for normal epiblast development [339].

As suggested by the gene expression data, Smad2-depletion promoted trophoblast cell invasion through matrigel-coated transwells and EVT outgrowth of first trimester placenta tissues. These data are in line with previous findings that Smad2 inhibits trophoblast invasion [160]. Previous studies also identified p-Smad2 positive EVTs to be located in the proximal anchoring column, which is composed of proliferating, non-invasive trophoblasts [332]. P-Smad2 expression also decreased along the distal ends of the column as the cells entered the invasive pathway [332]. In contrast, our findings from Smad3 knockdown experiments suggest that Smad3 promotes trophoblast invasion. The role of Smad3 in trophoblast function has not been directly studied. However, previous studies have suggested the involvement of both Smad2 and Smad3 as mediators of invasive and pro-angiogenic signals from TGF-β family proteins. Pro-invasive effects of Activins, by the upregulation of N-Cadherin, were mediated by both Smad2 and Smad3 [238]. Similarly, pro-invasive effects of Activin by MMP2 upregulation were mediated through an ALK4/Smad2/3/Snail mechanism [237]. Conversely, the anti-invasive effect of TGF-β1 through VE-cadherin downregulation was also mediated through Smad2/3 [312]. The reason for these discrepancies is not clear; however, the siRNAs used between these studies and ours may target different regions of Smad2 or Smad3. Alternatively, the relative expression level of Smad2 and Smad3 may determine their functions in trophoblasts. Additional siRNAs will be

used in the future to rule out potential off-target effects of the siRNAs. In addition, different doses of siSmad2 and Smad3, either alone or in combination, will also be used to further characterize the functions of Smad2 and Smad3 in trophoblast invasion and enEVT differentiation.

Consistent with the increased endovascular gene expression, we observed that the knockdown of Smad2 promoted the endothelial network-forming ability of trophoblasts, while depletion of Smad3 significantly reduced the total network length. Previously, Activin A was shown to promote trophoblast endothelial-like network formation through Smad2/3/4 mediated VEGF-A upregulation [240]. Lastly, our data show that additional knockdown of Smad4 in the network formation assay further enhanced the differential phenotypes of Smad2 and Smad3. This suggests that Smad4 is involved in both the Smad2 suppression and Smad3 promotion of EVT differentiation.

In this study, we show that the total levels of Smad2 and Smad3 proteins across gestation do not change significantly. However, their activities, reflected by the levels of the phosphorylated forms (Ser465/467 and Ser423/425, respectively), varied during different stages of pregnancy. Specifically, we found that the relative activity of Smad3 is higher in the period between 6 and 20 weeks compared to late gestation, while the opposite is true for p-Smad2 protein levels. Placental expression of active Smad2 and Smad3 has not been closely examined. The cytoplasmic expression of total Smad2/3 has been reported in both STBs and CTBs, decreasing in expression with gestational age [341]. However, the antibody used detected the total protein

level of both Smads concurrently. A recent study has reported that active Smad2 has been detected in both STBs and proliferating EVTs of first trimester placentas. Furthermore, they show that the p-Smad2 protein levels decrease with advancing gestational age [332]. In general, Smad2 and Smad3 are activated by signals from TGFβs, Nodal, and Activins [342]. The expression pattern of TGF-β/Nodal/Activin signaling components suggests a complex autocrine/paracrine role in both the fusion and invasive trophoblast pathway [343]. All three isoforms of TGF-β and their receptors, ALK-5 and TGFβ-RII, have been localized to the STBs and EVTs, decreasing in intensity with gestational age [341,344]. Similarly, Nodal and its Type I receptor, ALK-7, have been localized to the STBs, CTBs and EVTs, staining highest in the first trimester and disappearing by term [277]. Activin A was detected in the STBs and EVTs of term placentas [345]. Expression patterns of ALK-4 have not been reported in humans. Although Activin signaling through ALK-4 promotes trophoblast invasion, suggesting it is expressed in invasive trophoblasts [237]. Furthermore, conditional knockout of ALK-4 in mice causes subfertility in females due to inadequate trophoblast action in establishing the maternal-fetal interface [346]. Together, these studies suggest that the TGF-β/Nodal/Activin-Smad2/3 pathway plays important roles in placental development.

The differential activity of Smads depends on many factors; all centered around the phosphorylation of Smad2 or Smad3 C-terminal Serines by their cognate Type I receptors. Upon ligand binding, the differential recruitment of Smad2 versus Smad3 to the receptor is complex [333,347]. Several accessory proteins have high affinity for non-phosphorylated Smad2/3 and are responsible for recruiting them to the Type I receptor for activation. For example, Smad Anchor

for Receptor Activation (SARA) is able to bind to both Smad2 and Smad3 [213]. Interestingly, preferential selection by SARA has been reported [348,349]. Furthermore, cytoplasmic pro-myelocytic leukemia (cPML) and disabled-2 (DAB-2) adaptor proteins are also important for the specific recruitment of Smad2 and Smad3 for activation [350,351]. Expression of these adaptor proteins has been reported in the placenta, although their exact cellular localization remains to be fully characterized [352-354]. Conversely, availability of inhibitory Smads, Smad6 and Smad7, influences the accessibility of the Type I receptor activation site to Smad2 or Smad3. For example, Smad7 was shown to block only Smad3 signaling in mesangial cells, while Smad6 enhanced Smad3 signaling [355]. Both Smad6 and Smad7 expression have been reported in trophoblasts [356]. Furthermore, Smad7 expression was shown to increase with gestation and shift to the STB layer towards term [332]. Crosstalk of Smad2/3 with other signaling pathways also influences their relative activity. For example, ERK (Extracellular signal–regulated kinases) phosphorylation of the Smad linker region positively regulates the Smad2 pathway [357] while negatively regulating Smad3 signaling [358]. Furthermore, Akt (RAC-alpha serine/threonine-protein kinase; PKB) was shown to sequester Smad3, making it unavailable for Type I receptor phosphorylation [359]. While we show that the relative phosphorylation levels of Smad2 and Smad3 differ across gestation, it is important to note that both signaling mediators are active at the same time. The formation of Smad2 or Smad3 homodimers, as well as the formation of Smad2/3 heterodimers has been reported [195]. The possibility that a specific ratio of active Smad2 and Smad3 proteins available for transcription complex formation could be responsible to mediate genes required in first and second trimester tissues versus later in gestation.

Additionally, Smad2 and Smad3 cooperation and antagonism have been reported to occur simultaneously in the same cellular context [360].

Furthermore, we show that the total protein levels of Smad2 and Smad3 are not dysregulated in PE. Although in our PE tissues the increase in the level of p-Smad2 is minor, the upregulation of p-Smad2 in PE has been previously reported [332]. Likewise, the upregulation of total Smad2 in severe PE has been reported [160]. On the other hand, we are the first to show that p-Smad3 levels were significantly downregulated in PE. We can only speculate as to whether the dysregulation of Smad2/3 observed in PE is a picture of an early event that contributes to the etiology of the disease, or if this is a result of this gestational complication. It is possible that the prolonged hypoxic status of PE can selectively inactivate Smad3 without altering p-Smad2 levels as reported in some cancers [361]. Alternatively, it is possible that the elevated p-Smad2 levels contribute to the maternal dysfunction of PE by the Smad2-dependent upregulation of sFlt-1 [362].

In conclusion, our study provides evidence for specific roles of Smad2 and Smad3 in TGF-β signaling in placenta. It demonstrates the importance of investigating the roles of Smad2 and Smad3 independently, as well as together. Since siRNA are known to have off-target effects, validation of these findings with additional siRNA sequences would strengthen our conclusion. From our findings and those reported by others, we postulate that a delicate balance of Smad2 versus Smad3 expression exists at the anchoring column that drives the proliferative phenotype at the proximal end, while promoting the pro-invasive and pro-angiogenic phenotype at the distal end. However, the exact expression of both p-Smad2 and p-Smad3 across EVT columns

needs to be validated. The mechanisms of Smad2 and Smad3 differential activation remain unclear. It is most likely a spatially and temporally regulated mechanism dependent on availability of ligands, receptors, and accessory proteins [333]. Our study is the first to explore the differential role of Smad2 and Smad3 in the Invasive EVT pathway. Furthermore, our findings highlight the importance of further characterizing key proteins involved in the regulation of Smad2/3 phosphorylation states across the feto-placental interface in order to better understand these intricate processes essential to healthy pregnancy outcomes.

CHAPTER 4: SUMMARY AND FUTURE DIRECTIONS

SUMMARY

In this dissertation, I have investigated the function and mechanism of miR-218-5p in human placenta development. Specifically, the overall objectives of this study were to 1) determine miR-218-5p function in EVT differentiation; 2) investigate how the TGFβ pathway is involved in miR-218-5p-induced EVT differentiation; and 3) further characterize the role of the TGFβ pathway in EVT differentiation.

I. miR-218-5p promotes trophoblast invasion and enEVT differentiation.

The function of miR-218-5p in placenta development was investigating using both an immortalized first trimester trophoblast cell line and human placenta tissues (Chapter 2). We confirm earlier reports of miR-218-5p downregulation in PE [160]. Furthermore, we report that miR-218-5p is upregulated during second trimester and promotes trophoblast cell migration, invasion, and differentiation into enEVTs. In addition, we show that miR-218-5p accelerated the process of spiral artery remodelling. Together, our findings suggest that miR-218-5p is an important regulator of placental development where it promotes the processes of EVT differentiation, invasion and spiral artery remodelling. Dysregulation of miR-218-5p, and consequently these key developmental processes, may contribute to the etiology of PE.

Overexpression of miR-218-5p upregulated genes known to promote trophoblast invasion and that are involved in enEVT differentiation, such as: *MMP1, VE-cad, PECAM1, IL-1b, and IL8*. These data were confirmed with first trimester EVT treated with miR-218-5p or anti-miR-218-

5p. Migration and invasion assays revealed that cells overexpressing miR-218-5p migrated and invaded in greater number across the transwells compared to controls. The opposite was observed with anti-miR-218-5p transfection. These data were validated in a first trimester explant model. Overexpression of miR-218-5p promoted trophoblast endothelial-like network formation on matrigel, while anti-miR-218-5p inhibited this process. Similarly, miR-218-5p overexpressing cells promoted network formation in co-culture with HUVEC and exhibited the ability to replace endothelial cells. These data were confirmed in an *in vitro* model of trophoblast-mediate decidua vessel remodelling where miR-218-5p accelerated the remodelling process.

Starting from late first trimester the remodelling of spiral arteries is actively occurring until ~20 weeks of gestation [54]. As such, a spike in miR-218-5p during this stage of development is inline with our observations that miR-218-5p promotes EVT differentiation, invasion and spiral artery remodeling. Furthermore, we hypothesize that the upregulation of miR-218-5p in second trimester is specific to the trophoblasts at the anchoring column that are entering the invasive pathway. However, since these data were obtained from placental tissues that consist of multiple cell types, future studies are required to identify which cell type(s) in the placenta expresses miR-218-5p. Specifically *in situ* hybridization using first trimester EVT columns and decidua basalis can be conducted to determine if miR-218-5p is expressed in the EVT population that is actively invading and remodelling spiral arteries.

In the future we are interested in investigating the possible use of miR-218-5p as a predictive biomarker of PE. As previously discussed, miRNA show great potential as stable, non-invasive biomarkers [262]. Furthermore, miR-218-5p has already shown great promise as a predictive biomarker in certain types of cancers [272,273]. Currently, in collaboration with Dr. Lye's group at Mount Sinai Hospital, we have obtained approval from the research ethics board to begin processing plasma samples collected from asymptomatic women at 10-14 weeks of gestation, that later developed PE. In order to compare miR-218-5p levels from patients destined to develop PE, we have a control group that is matched for race, gestational age, and maternal age. I have conducted a pilot experiment with a small group of these samples to verify the successful isolation and amplification of miR-218-5p.

II. miR-218-5p exerts its effect through suppression of TGF-β2.

The mechanism of miR-218-5p action was examined in the miR-218-5p overexpressing first trimester trophoblast cell line (Chapter 2). We found that miR-218-5p suppressed TGF-β2 expression. TGF-β2 is a predicted target of miR-218-5p and a luciferase reporter assay using a construct that contains a portion of the wild type TGF-β2 3'UTR confirms that TGF-β2 is a direct target of miR-218-5p. To further validate this interaction we will repeat the luciferase reporter assay using a construct containing point mutations in the miR-218-5p predicted binding region. Treatment with recombinant TGF-β2 protein was able to rescue the pro-invasive, and pro-enEVT differentiation effects observed with miR-218-5p overexpression. These results suggest that miR-218-5p exerts its effects on placenta in part via the suppression of TGF-β2 expression.

Furthermore, we showed miR-218-5p suppressed TGF-β signaling using pAR3-Lux reporter assay. Interestingly, treatment with TGF-β2 was not able to rescue the reporter activity in miR-218-5p overexpressing cells. These data suggest that TGF-β2 downstream signaling components were also downregulated in our system. Since pAR3-Lux is mainly Smad2 responsive, and Smad2 had a potential miR-218-5p binding site, we checked for Smad2 involvement in the miR-218-5p/TGF-β2 mechanism. As suspected, Smad2 was downregulated in miR-218-5p overexpressing cells. Furthermore, the knockdown of Smad2 mimicked the miR-218-5p phenotype. Interestingly, the overexpression of Smad2 did not suppress enEVT markers, suggesting that TGF-β2 was needed for the activation of specific Smad2 co-repressors (data not shown).

In addition to TGF-β2, miR-218-5p has two predicted targets in the 3'UTR of Nodal. Previous studies from our lab reported the Nodal was upregulated in PE and inhibited trophoblast proliferation, migration, and invasion [221,235]. We confirmed that Nodal was downregulated in miR-218-5p overexpressing cells (Figure 4.1A and 4.1B). Furthermore, we confirmed that miR-218-5p suppressed Nodal expression through binding to both its targets in the 3'UTR (Figure 4.1C). Future studies are needed to determine if Nodal mediates some of the effects of miR-218-5p on enEVT differentiation and spiral artery remodelling.

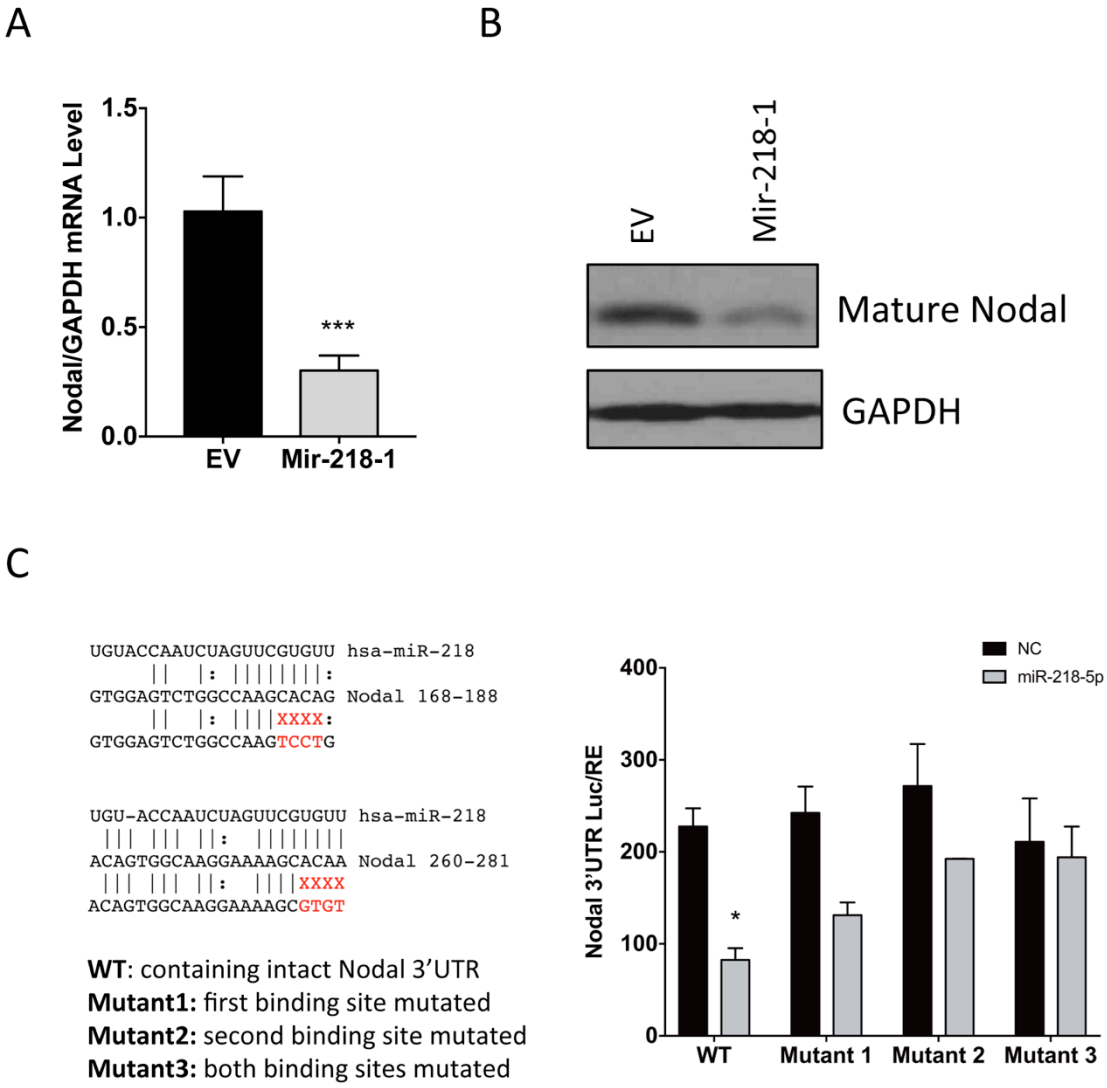

Figure 4.1 miR-218-5p downregulates Nodal through its 3'UTR.
(A) Nodal mRNA expression was significantly ($p<0.001$) reduced in mir-218-1 overexpressing cells compared to control cells. **(B)** Mir-218-1 suppressed levels of mature nodal protein compared to control. **(C)** A fragment of the Nodal 3'UTR containing the two predicted miR-218-5p target sites was cloned upstream of a luciferase gene. Transfection with miR-218-5p significantly ($p<0.05$) suppressed luciferase activity of the wild type (WT) 3'UTR. Mutation of the first or second binding site partially reversed the miR-218-5p effect. Mutation of both binding sites fully rescued the miR-218-5p suppression.

III. Smad2 and Smad3 have distinct roles in enEVT differentiation.

In Chapter 2 of this dissertation I report that the miR-218-5p/TGF-β2 mechanism is in part mediated through Smad2, and not Smad3. The distinct roles of Smad2 and Smad3 prompted us to further characterize these R-Smads in placenta development (Chapter 3). Specifically, we show that Smad2 acts as a suppressor, while Smad3 acts as a promoter, of trophoblast invasion and differentiation into invasive, endovascular EVTs. Furthermore, we report that the total level of Smad2 and Smad3 protein does not change across gestation, but the phosphorylated states of these proteins show opposite patterns. P-Smad2 was higher in later gestation, while p-Smad3 was higher in the first twenty weeks when the invasive pathway is most active. Lastly, for the first time we report a complete loss of p-Smad3 in PE placenta tissues.

Our findings, that Smad2 and Smad3 have differential roles in EVT differentiation, can be further strengthened through several methods. First, we can repeat our key findings with two additional siRNAs targeting different regions of Smad2 or Smad3 to ensure the observed effects are not a result of off-target genes. However, our Smad2 or Smad3 overexpression data is in support of our endothelial-like network formation in the siRNA knockdown approach. I have already confirmed the suppression of endothelial-like network formation for two additional siSmad3 siRNAs. Second, our phosphorylation Smad data is based on protein lysates from pieces of whole placenta. As such, the relative Smad2 or Smad3 expression may be confounded by the presence of cell types other than trophoblasts. I have performed preliminary immunohistochemistry experiments on first trimester placenta, and observed strong staining for both Smad2 and Smad3 in EVT columns. We have obtained histological sections of healthy

placenta across gestation, and PE tissues. These sections can be used to validate our findings with p-Smad2 or p-Smad3 specific antibodies.

Furthermore, our Smad2 and Smad3 functional findings focus on the invasive trophoblast pathway. As previously mentioned, the expression of TGF-β/Nodal/Activin pathway signaling components in STBs have been reported [235,363,364]. TGF-β1 was shown to promote trophoblast fusion into STBs and hCG production in part through a Smad-dependent mechanism [228,365]. On the other hand, TGF-β1 inhibition of hCG production was also reported [224]. TGF-β1 inhibition on progesterone and estradiol production by trophoblast has also been reported [226,366], while Activin signals have shown to have a promoting effect on progesterone and estradiol [225]. In the future, we can investigate the role of Smad2 versus Smad3, or their combined action, in the trophoblast fusion and hormone production pathway.

FUTURE DIRECTIONS

In Chapter 2 of this dissertation, we report that miR-218-5p promotes trophoblast invasion and enEVT differentiation in part through the suppression of TGF-β2/Smad2 signaling. The Gene Ontology enrichment analysis from our mir-218-1 overexpressing cell line showed a significant enrichment of genes belonging to the nuclear factor kappa-light-chain-enhancer of activated B cells (NF-κB) pathway. The NF-κB pathway is important in the expression of many proinflammatory cytokines and adhesion molecules [367]. The upregulation of NF-κB in first trimester trophoblasts resulted in increased migration [368]. Furthermore, IL1b expression is upregulated by the NF-κB transcription heterodimer, p50/p65 [369]. I performed several preliminary experiments to elucidate the possible role of NFκB in the miR-218-5p upregulation of invasion and enEVT differentiation.

To confirm the upregulation of NF-κB signaling in our mir-218 stable cell lines I performed a nuclear fractionation in order to check for p50 and p65 nuclear accumulation. In line with our microarray findings, we observed the nuclear accumulation of both p50 and p65, which was reversed upon treatment with a NF-κB inhibitor, ACHP (2-Amino-6-[2-(cyclopropylmethoxy)-6-hydroxyphenyl]-4-(4-piperidinyl)-3-pyridinecarbonitrile) (Figure 4.2A). Next we wanted to test if the miR-218-5p upregulation of IL1b was positively regulated through the NF-κB pathway. Transfection of primary EVT with miR-218-5p upregulated IL1b as reported in Chapter2, and this effect was inhibited with ACHP treatment (Figure 4.2B).

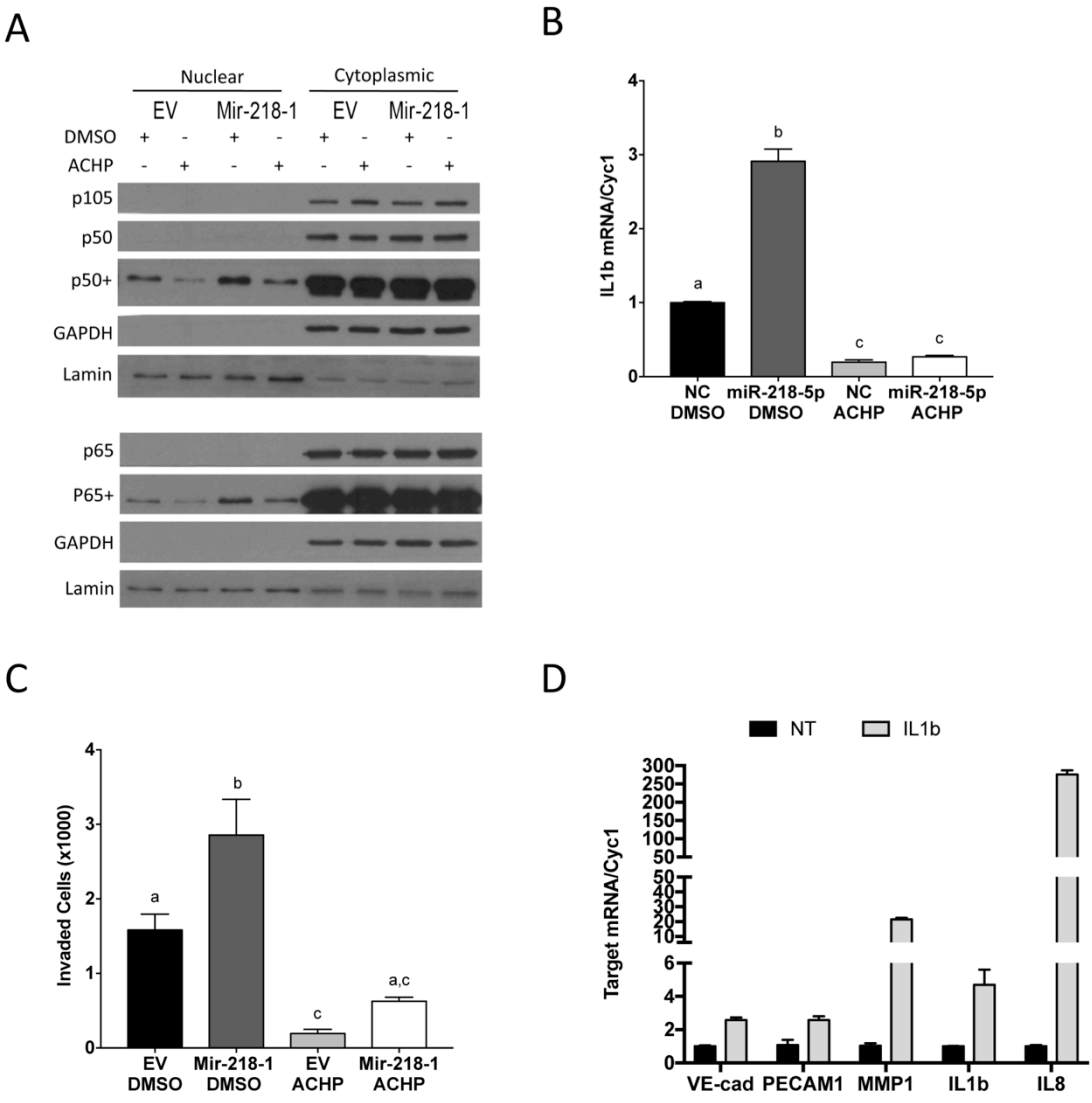

Figure 4.2 Mir-218-1 promotes invasion and enEVT differentiation through IL1b/NFkB.
(A) Mir-218 overexpressing cells had an increase of p50 and p65 nuclear accumulation than control cells. The nuclear accumulation was reversed with a NF-κB pathway inhibitor, ACHP (10μM). The "+" indicated a longer exposure time during development. NB: GAPDH blot was stripped and re-blotted with Lamin B (nuclear marker) **(B)** Mir-218 upregulation of IL1b was inhibited with the NF-κB pathway inhibitor **(C)** The mir-218 pro-invasive effect was reversed with inhibition of the NF-κB pathway. **(D)** Treatment with recombinant IL1b (10ng/mL) upregulated genes involved in trophoblast invasion and enEVT differentiation.

The pro-invasive role of IL1b in primary first trimester trophoblasts has been reported [370]. To investigate if the NF-κB pathway mediated the pro-invasive effect of miR-218-5p we treated our stable cells with and without the NF-κB inhibitor. Our data report that miR-218-5p upregulated invasion through the upregulation of NFkB signaling (Figure 4.2C). Next, we wanted to test the possible role of NF-κB/IL1b signaling in enEVT differentiation. Treatment of HTR8/SVneo cells with recombinant IL1b resulted in the upregulation of the same genes involved in trophoblast invasion and enEVT differentiation that we observed with miR-218-5p overexpression. Specifically, IL1b upregulated VE-cadherin, PECAM1, MMP1, IL8, and had positive feedback on its own expression (Figure 4.2D). To our knowledge, the role of IL1b or NFkB on enEVT differentiation has not been reported. However, IL1b has been reported to upregulate MMP1, IL8, and to form a positive feedback with NF-κB in other systems [371-373]. These preliminary findings suggest that miR-218-5p exerts its effect through the upregulation of NF-κB in addition to its suppression of TGF-β2.

In the future, we can investigate the potential mechanisms by which miR-218-5p upregulates NFkB signaling. Since the TGF-β-Smad pathway has been reported to inhibit NFkB signaling [374,375], one possible mechanism to explore is to determine if miR-218-5p activates NFkB signaling via the inhibition of TGF-β/Smad. Furthermore, we can further characterize the role of NF-κB in the invasive and enEVT pathway by investigating another NF-κB regulated cytokine, IL8. IL8 has been reported to promote trophoblast invasion, but its direct role in enEVT differentiation has not been well characterized.

CONCLUSION

Despite the downregulation of miR-218-5p in PE, its role in placenta has never been investigated. The present study provides the first evidence that miR-218-5p promotes trophoblast migration, invasion, differentiation into enEVT, and spiral artery remodelling. Identifying the mechanisms involved in establishing the feto-maternal perfusion are important to our understanding of the critical processes that are dysregulated in gestational hypertensive disorders like PE. To our knowledge, this is the first study to implicate the involvement of miRNAs in these vital processes. Specifically, this study has highlighted the importance of investigating the role of miRNAs further than their implication on trophoblast invasion and migration, which is the predeominant focus of research currently published. In addition, this is the first study to implement the *in vitro* model of trophoblast-mediated decidua vessel remodelling and will hopefully contribute to future utilization of this novel and useful tool.

Furthermore, this study identifies TGF-β2-Smad2 as a key pathway that mediates the action of miR-218-5p. In addition, we report a differential role of Smad2 and Smad3 in placenta development. Our data suggest that Smad2 acts to suppress, while Smad3 acts to promote, trophoblast invasion and enEVT differentiation. These data highlight the role of miR-218-5p and TGF-β signaling in key events that are dysregulated in PE. While the involvement of the TGF-β pathway in PE is not novel, we have added to the current understanding of this mechanism through the involvement of miRNA regulation. In addition, our preliminary findings that Smad2 and Smad3 have distinct function in trophoblast development introduce a new aspect of the TGF-β signaling pathway that may elucidate some conflicting reports in literature.

Taken together, our study suggests the dysregulation of the miR-218-5p/TGF-β mechanism contributes to the etiology of PE (Figure 4.3). The use of microRNAs as potential plasma biomarkers has been investigated [223,316], and a significant increase in serum TGFβ-2 was reported in cases of severe PE and eclampsia compared to control [254]. These data, taken together with our findings, suggest great potential of investigating the utilization of miR-218-5p as part of a predictive biomarker panel of PE. The effectiveness of managing clinical symptoms greatly depends on implementing therapeutic intervation early. Having a collection of predictive and accurate biomarkers can ultimately help in reducing severity of symptons and subseqntly the frequency of premature deliveries and other complications thereby improving the health and quality of life in pregnant women and infants.

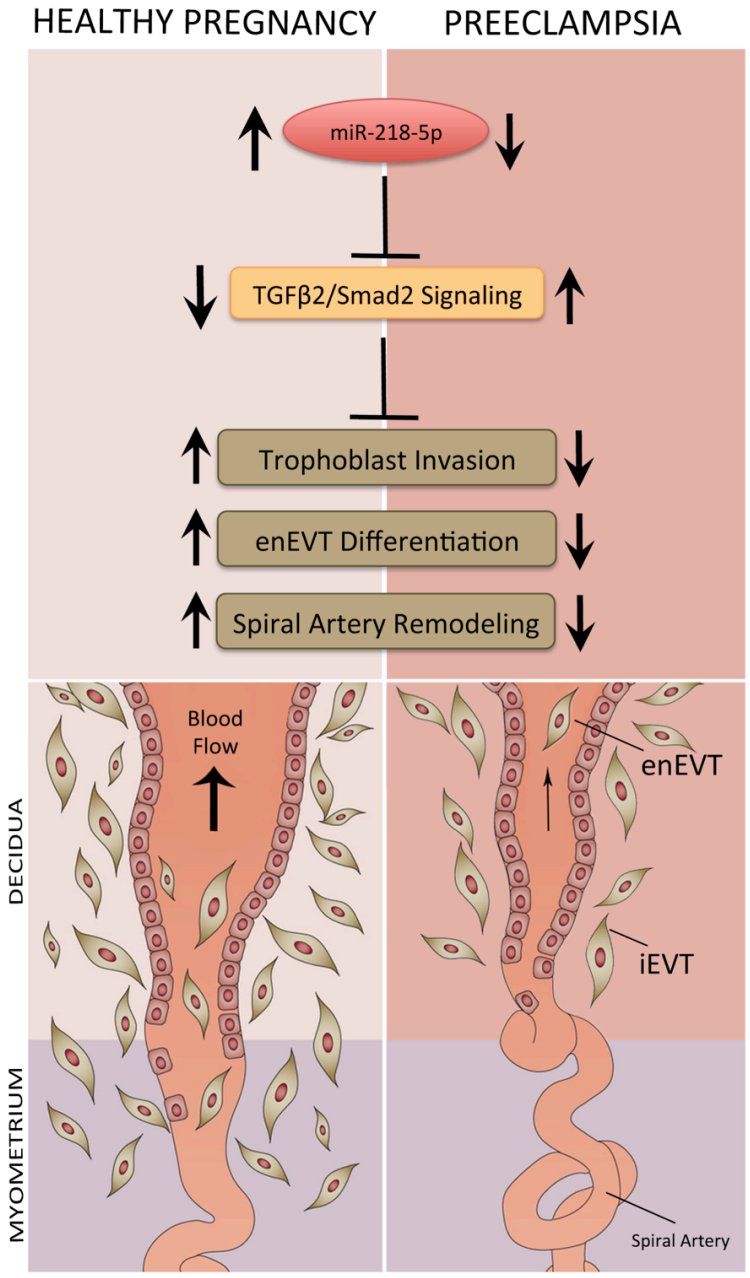

Figure 4.3 Proposed mechanism of miR-218-5p in healthy and PE placentas.
Mir-218-5p promotes trophoblast invasion, enEVT differentiation, and spiral artery remodeling partially by the suppression of TGFβ2/Smad2 signaling. We postulate that the downregulation of miR-218-5p, and the subsequent upregulation of TGFβ signaling, contribute to poor trophoblast invasion, reduced enEVT pool, and shallow spiral artery remodelling resulting in variable blood flow with high velocity to the intervillous space that are observed in preeclampsia. iEVT- interstitial extravillous trophoblast, enEVT- endovascular EVT. Bottom panel used with permission from Chaiworapongsa T., et al. (2014) [60].

REFERENCES

1. Rossant, J. & Cross, J. C. Placental development: lessons from mouse mutants. *Nat. Rev. Genet.* **2,** 538–548 (2001).
2. Wang, Y. & Zhao, S. Vascular Biology of the Placenta. (2010).
3. Clancy, K. B. Reproductive ecology and the endometrium: physiology, variation, and new directions. *Am J Phys Anthropol* **140 Suppl 49,** 137–154 (2009).
4. Evain-Brion, D. & Malassiné, A. Human placenta as an endocrine organ. *Growth Horm IGF Res* **13 Suppl A,** S34–7 (2003).
5. Paria, B. C., Reese, J., Das, S. K. & Dey, S. K. Deciphering the cross-talk of implantation: advances and challenges. *Science* **296,** 2185–2188 (2002).
6. Red-Horse, K. *et al.* Trophoblast differentiation during embryo implantation and formation of the maternal-fetal interface. *J. Clin. Invest.* **114,** 744–754 (2004).
7. Cartwright, J. E., Fraser, R., Leslie, K., Wallace, A. E. & James, J. L. Remodelling at the maternal-fetal interface: relevance to human pregnancy disorders. *Reproduction* **140,** 803–813 (2010).
8. Norwitz, E. R., Schust, D. J. & Fisher, S. J. Implantation and the Survival of Early Pregnancy. *New England Journal of Medicine* **345,** 1400–1408 (2001).
9. Norwitz, E. R. Defective implantation and placentation: laying the blueprint for pregnancy complications. *Reprod Biomed Online* **14 Spec No 1,** 101–109 (2007).
10. Fitzgerald, J. S., Poehlmann, T. G., Schleussner, E. & Markert, U. R. Trophoblast invasion: the role of intracellular cytokine signalling via signal transducer and activator of transcription 3 (STAT3). *Hum. Reprod. Update* **14,** 335–344 (2008).
11. Huppertz, B. The anatomy of the normal placenta. *J Clin Pathol* **61,** 1296–1302 (2008).
12. Benirschke, K. & Kaufmann, P. *Pathology of the human placenta*. (Springer, 2000).
13. Martini, F. H., Timmons, M. J. & Tallitsch, R. B. *Human Anatomy*. (Pearson Higher Ed, 2014).
14. Bárcena, A. *et al.* Human placenta and chorion: potential additional sources of hematopoietic stem cells for transplantation. *Transfusion* **51 Suppl 4,** 94S–105S (2011).
15. Standring, S. *Gray's Anatomy*. (Elsevier Health Sciences, 2015).
16. Reynolds, L. P. & Redmer, D. A. Angiogenesis in the Placenta. *Biol. Reprod.* **64,** 1033–1040 (2001).
17. Teasdale, F. & Jean-Jacques, G. Morphometric evaluation of the microvillous surface enlargement factor in the human placenta from mid-gestation to term. *Placenta* **6,** 375–381 (1985).
18. Nakamura, O. Children's immunology, what can we learn from animal studies (1): Decidual cells induce specific immune system of feto-maternal interface. *J Toxicol Sci* **34 Suppl 2,** SP331–9 (2009).
19. Kar, M., Ghosh, D. & Sengupta, J. Histochemical and morphological examination of proliferation and apoptosis in human first trimester villous trophoblast. *Hum. Reprod.* **22,** 2814–2823 (2007).
20. Hannan, N. J. The Chemokines, CX3CL1, CCL14, and CCL4, Promote Human Trophoblast Migration at the Feto-Maternal Interface. *Biol. Reprod.* **74,** 896–904 (2006).

21. Baczyk, D. *et al.* Glial cell missing-1 transcription factor is required for the differentiation of the human trophoblast. *Cell Death Differ.* **16,** 719–727 (2009).
22. Mi, S. *et al.* Syncytin is a captive retroviral envelope protein involved in human placental morphogenesis. *Nature* **403,** 785–789 (2000).
23. Okahara, G. *et al.* Expression analyses of human endogenous retroviruses (HERVs): tissue-specific and developmental stage-dependent expression of HERVs. *Genomics* **84,** 982–990 (2004).
24. Knerr, I. *et al.* Stimulation of GCMa and syncytin via cAMP mediated PKA signaling in human trophoblastic cells under normoxic and hypoxic conditions. *FEBS Lett.* **579,** 3991–3998 (2005).
25. Orendi, K., Gauster, M., Moser, G., Meiri, H. & Huppertz, B. The choriocarcinoma cell line BeWo: syncytial fusion and expression of syncytium-specific proteins. *Reproduction* **140,** 759–766 (2010).
26. Nelson, D. M. Apoptotic changes occur in syncytiotrophoblast of human placental villi where fibrin type fibrinoid is deposited at discontinuities in the villous trophoblast. *Placenta* **17,** 387–391 (1996).
27. Loukeris, K., Sela, R. & Baergen, R. N. Syncytial knots as a reflection of placental maturity: reference values for 20 to 40 weeks' gestational age. *Pediatr. Dev. Pathol.* **13,** 305–309 (2010).
28. Huppertz, B. & Kingdom, J. C. P. Apoptosis in the trophoblast--role of apoptosis in placental morphogenesis. *J. Soc. Gynecol. Investig.* **11,** 353–362 (2004).
29. Burton, G. J. & Jones, C. J. Syncytial knots, sprouts, apoptosis, and trophoblast deportation from the human placenta. *Taiwan J Obstet Gynecol* **48,** 28–37 (2009).
30. Vicovac, L., Jones, C. J. & Aplin, J. D. Trophoblast differentiation during formation of anchoring villi in a model of the early human placenta in vitro. *Placenta* **16,** 41–56 (1995).
31. Aplin, J. D., Haigh, T., Jones, C. J., Church, H. J. & Vicovac, L. Development of cytotrophoblast columns from explanted first-trimester human placental villi: role of fibronectin and integrin alpha5beta1. *Biol. Reprod.* **60,** 828–838 (1999).
32. Damsky, C. H., Fitzgerald, M. L. & Fisher, S. J. Distribution patterns of extracellular matrix components and adhesion receptors are intricately modulated during first trimester cytotrophoblast differentiation along the invasive pathway, in vivo. *J. Clin. Invest.* **89,** 210–222 (1992).
33. Prakobphol, A., Genbacev, O., Gormley, M., Kapidzic, M. & Fisher, S. J. A role for the L-selectin adhesion system in mediating cytotrophoblast emigration from the placenta. *Dev. Biol.* **298,** 107–117 (2006).
34. Kemp, B. *et al.* Invasive depth of extravillous trophoblast correlates with cellular phenotype: a comparison of intra- and extrauterine implantation sites. *Histochem. Cell Biol.* **117,** 401–414 (2002).
35. Knofler, M. & Pollheimer, J. IFPA Award in Placentology lecture: molecular regulation of human trophoblast invasion. *Placenta* **33 Suppl,** S55–62 (2012).
36. Huppertz, B. The feto-maternal interface: setting the stage for potential immune interactions. *Semin Immunopathol* **29,** 83–94 (2007).
37. Damsky, C. H. & Fisher, S. J. Trophoblast pseudo-vasculogenesis: faking it with

endothelial adhesion receptors. *Curr Opin Cell Biol* **10,** 660–666 (1998).
38. Zhou, Y. *et al.* Human cytotrophoblasts adopt a vascular phenotype as they differentiate. A strategy for successful endovascular invasion? *J. Clin. Invest.* **99,** 2139–2151 (1997).
39. Hofmann, G. E., Glatstein, I., Schatz, F., Heller, D. & Deligdisch, L. Immunohistochemical localization of urokinase-type plasminogen activator and the plasminogen activator inhibitors 1 and 2 in early human implantation sites. *International Journal of Gynecology & Obstetrics* **47,** 195 (1994).
40. Zhu, J.-Y., Pang, Z.-J. & Yu, Y.-H. Regulation of trophoblast invasion: the role of matrix metalloproteinases. *Rev Obstet Gynecol* **5,** e137–43 (2012).
41. Loke, Y. W. *et al.* Evaluation of trophoblast HLA-G antigen with a specific monoclonal antibody. **50,** 135–146 (1997).
42. Trowsdale, J. & Moffett, A. NK receptor interactions with MHC class I molecules in pregnancy. *Semin. Immunol.* **20,** 317–320 (2008).
43. Blaschitz, A., Hutter, H. & Dohr, G. HLA Class I protein expression in the human placenta. *Early Pregnancy* **5,** 67–69 (2001).
44. Hammer, A. Immunological regulation of trophoblast invasion. *J. Reprod. Immunol.* **90,** 21–28 (2011).
45. King, A. *et al.* HLA-E is expressed on trophoblast and interacts with CD94 / NKG2 receptors on decidual NK cells. **30,** 1623–1631 (2000).
46. Apps, R., Gardner, L., Sharkey, A. M., Holmes, N. & Moffett, A. A homodimeric complex of HLA-G on normal trophoblast cells modulates antigen-presenting cells via LILRB1. *Eur. J. Immunol.* **37,** 1924–1937 (2007).
47. al-Lamki, R. S., Skepper, J. N. & Burton, G. J. Are human placental bed giant cells merely aggregates of small mononuclear trophoblast cells? An ultrastructural and immunocytochemical study. *Hum. Reprod.* **14,** 496–504 (1999).
48. Lyall, F. Mechanisms regulating cytotrophoblast invasion in normal pregnancy and pre-eclampsia. *Aust N Z J Obstet Gynaecol* **46,** 266–273 (2006).
49. Burton, G. J., Woods, A. W., Jauniaux, E. & Kingdom, J. C. P. Rheological and physiological consequences of conversion of the maternal spiral arteries for uteroplacental blood flow during human pregnancy. *Placenta* **30,** 473–482 (2009).
50. Pijnenborg, R., Vercruysse, L. & Hanssens, M. The uterine spiral arteries in human pregnancy: facts and controversies. *Placenta* **27,** 939–958 (2006).
51. Harris, L. K. Review: Trophoblast-vascular cell interactions in early pregnancy: how to remodel a vessel. *Placenta* **31 Suppl,** S93–8 (2010).
52. Smith, S. D., Dunk, C. E., Aplin, J. D., Harris, L. K. & Jones, R. L. Evidence for immune cell involvement in decidual spiral arteriole remodeling in early human pregnancy. *Am. J. Pathol.* **174,** 1959–1971 (2009).
53. Whitley, G. S. J. & Cartwright, J. E. Cellular and molecular regulation of spiral artery remodelling: lessons from the cardiovascular field. *Placenta* **31,** 465–474 (2010).
54. Pijnenborg, R., Dixon, G., Robertson, W. B. & Brosens, I. Trophoblastic invasion of human decidua from 8 to 18 weeks of pregnancy. *Placenta* **1,** 3–19 (1980).
55. Khankin, E. V., Royle, C. & Karumanchi, S. A. Placental vasculature in health and disease. *Semin. Thromb. Hemost.* **36,** 309–320 (2010).

56. Anin, S., Vince, G. & Quenby, S. Trophoblast invasion. *Human Fertility* **7,** 169–174 (2004).
57. Kaufmann, P., Black, S. & Huppertz, B. Endovascular trophoblast invasion: implications for the pathogenesis of intrauterine growth retardation and preeclampsia. *Biol. Reprod.* **69,** 1–7 (2003).
58. Kam, E. P. Y., Gardner, L., Loke, Y. W. & King, A. The role of trophoblast in the physiological change in decidual spiral arteries. *Human Reproduction* **14,** 2131–2138 (1999).
59. Duley, L. The global impact of pre-eclampsia and eclampsia. *Semin. Perinatol.* **33,** 130–137 (2009).
60. Chaiworapongsa, T., Chaemsaithong, P., Yeo, L. & Romero, R. Pre-eclampsia part 1: current understanding of its pathophysiology. *Nat Rev Nephrol* **10,** 466–480 (2014).
61. Gaiser, R. Preeclampsia: What's New? *Advances in Anesthesia* **26,** 103–119 (2008).
62. Noris, M., Perico, N. & Remuzzi, G. Mechanisms of disease: Pre-eclampsia. *Nat Clin Pract Nephrol* **1,** 98–114– quiz 120 (2005).
63. Silasi, M., Cohen, B., Karumanchi, S. A. & Rana, S. Abnormal placentation, angiogenic factors, and the pathogenesis of preeclampsia. *Obstet. Gynecol. Clin. North Am.* **37,** 239–253 (2010).
64. Wang, A., Rana, S. & Karumanchi, S. A. Preeclampsia: the role of angiogenic factors in its pathogenesis. *Physiology (Bethesda)* **24,** 147–158 (2009).
65. Zhou, Y., Damsky, C. H. & Fisher, S. J. Preeclampsia is associated with failure of human cytotrophoblasts to mimic a vascular adhesion phenotype. One cause of defective endovascular invasion in this syndrome? *J. Clin. Invest.* **99,** 2152–2164 (1997).
66. Lala, P. K. & Chakraborty, C. Factors Regulating Trophoblast Migration and Invasiveness: Possible Derangements Contributing to Pre-eclampsia and Fetal Injury. *Placenta* **24,** 575–587 (2003).
67. Cheng, M. H. & Wang, P. H. Placentation abnormalities in the pathophysiology of preeclampsia. *Expert Rev Mol Diagn* **9,** 37–49 (2009).
68. Lockwood, C. J. *et al.* Decidual hemostasis, inflammation, and angiogenesis in pre-eclampsia. *Semin. Thromb. Hemost.* **37,** 158–164 (2011).
69. Pennington, K. A., Schlitt, J. M., Jackson, D. L., Schulz, L. C. & Schust, D. J. Preeclampsia: multiple approaches for a multifactorial disease. *Dis Model Mech* **5,** 9–18 (2012).
70. Redman, C. W. & Sargent, I. L. Latest advances in understanding preeclampsia. *Science* **308,** 1592–1594 (2005).
71. Aksornphusitaphong, A. & Phupong, V. Risk factors of early and late onset pre-eclampsia. *Journal of Obstetrics and Gynaecology Research* **39,** 627–631 (2012).
72. Valensise, H., Vasapollo, B., Gagliardi, G. & Novelli, G. P. Early and Late Preeclampsia: Two Different Maternal Hemodynamic States in the Latent Phase of the Disease. *Hypertension* **52,** 873–880 (2008).
73. Van der Merwe, J. O965 Do early and late pre-eclampsia share the same aetiology? What does the placenta reveal? Comparison of histopathological features in placentas from pregnancies complicated by early and late onset pre-eclampsia. *International Journal of Gynecology & Obstetrics* **107,** S368 (2009).
74. Khodzhaeva, Z. S. *et al.* Clinical and pathogenetic features of early- and late-onset pre-

eclampsia. *J. Matern. Fetal. Neonatal. Med.* **29,** 2980–2986 (2016).
75. Snydal, S. Major Changes in Diagnosis and Management of Preeclampsia. *Journal of Midwifery & Women's Health* **60,** 226–226 (2015).
76. Leavey, K. *et al.* Unsupervised Placental Gene Expression Profiling Identifies Clinically Relevant Subclasses of Human Preeclampsia. *Hypertension* **68,** 137–147 (2016).
77. Polliotti, B. M. *et al.* Second-trimester maternal serum placental growth factor and vascular endothelial growth factor for predicting severe, early-onset preeclampsia. *Obstet Gynecol* **101,** 1266–1274 (2003).
78. Levine, R. J. *et al.* Circulating angiogenic factors and the risk of preeclampsia. *N. Engl. J. Med.* **350,** 672–683 (2004).
79. Hertig, A. *et al.* Maternal serum sFlt1 concentration is an early and reliable predictive marker of preeclampsia. *Clinical Chemistry* **50,** 1702–1703 (2004).
80. Chaiworapongsa, T. *et al.* Plasma soluble vascular endothelial growth factor receptor-1 concentration is elevated prior to the clinical diagnosis of pre-eclampsia. *J. Matern. Fetal. Neonatal. Med.* **17,** 3–18 (2005).
81. Levine, R. J. *et al.* Soluble endoglin and other circulating antiangiogenic factors in preeclampsia. *N. Engl. J. Med.* **355,** 992–1005 (2006).
82. De Vivo, A. *et al.* Endoglin, PlGF and sFlt-1 as markers for predicting pre-eclampsia. *Acta Obstet Gynecol Scand* **87,** 837–842 (2008).
83. O'Gorman, N. *et al.* Competing risks model in screening for preeclampsia by maternal factors and biomarkers at 11-13 weeks gestation. *Am. J. Obstet. Gynecol.* **214,** 103.e1–103.e12 (2016).
84. Huppertz, B. & Kawaguchi, R. Serum-Marker im ersten Trimenon zur Vorhersage der Präeklampsie. *Wiener Medizinische Wochenschrift* **162,** 191–195 (2012).
85. Than, N. G. *et al.* A primate subfamily of galectins expressed at the maternal-fetal interface that promote immune cell death. *Proc. Natl. Acad. Sci. U.S.A.* **106,** 9731–9736 (2009).
86. Huppertz, B. *et al.* Longitudinal determination of serum placental protein 13 during development of preeclampsia. *Fetal. Diagn. Ther.* **24,** 230–236 (2008).
87. Odibo, A. O. *et al.* First-trimester placental protein 13, PAPP-A, uterine artery Doppler and maternal characteristics in the prediction of pre-eclampsia. *Placenta* **32,** 598–602 (2011).
88. Chafetz, I. *et al.* First-trimester placental protein 13 screening for preeclampsia and intrauterine growth restriction. *Am. J. Obstet. Gynecol.* **197,** 35.e1–7 (2007).
89. Schneuer, F. J. *et al.* First trimester screening of maternal placental protein 13 for predicting preeclampsia and small for gestational age: in-house study and systematic review. *Placenta* **33,** 735–740 (2012).
90. Chim, S. S. *et al.* Detection and characterization of placental microRNAs in maternal plasma. *Clinical Chemistry* **54,** 482–490 (2008).
91. Pillar, N., Yoffe, L., Hod, M. & Shomron, N. The possible involvement of microRNAs in preeclampsia and gestational diabetes mellitus. *Best Pract Res Clin Obstet Gynaecol* **29,** 176–182 (2015).
92. Ura, B. *et al.* Potential role of circulating microRNAs as early markers of preeclampsia. *Taiwan J Obstet Gynecol* **53,** 232–234 (2014).

93. Luque, A. *et al.* Usefulness of circulating microRNAs for the prediction of early preeclampsia at first-trimester of pregnancy. *Sci Rep* **4,** 4882 (2014).
94. Lee, R. C., Feinbaum, R. L. & Ambros, V. The C. elegans heterochronic gene lin-4 encodes small RNAs with antisense complementarity to lin-14. *Cell* **75,** 843–854 (1993).
95. Wightman, B., Ha, I. & Ruvkun, G. Posttranscriptional regulation of the heterochronic gene lin-14 by lin-4 mediates temporal pattern formation in C. elegans. *Cell* **75,** 855–862 (1993).
96. Reinhart, B. J. *et al.* The 21-nucleotide let-7 RNA regulates developmental timing in Caenorhabditis elegans. *Nature* **403,** 901–906 (2000).
97. Lagos-Quintana, M., Rauhut, R., Lendeckel, W. & Tuschl, T. Identification of novel genes coding for small expressed RNAs. *Science* **294,** 853–858 (2001).
98. Li, L. & Liu, Y. in *Therapeutic Oligonucleotides* (ed. Goodchild, J.) **764,** 169–182 (Humana Press, 2011).
99. Vidigal, J. A. & Ventura, A. The biological functions of miRNAs: lessons from in vivo studies. *Trends Cell Biol.* **25,** 137–147 (2015).
100. Broderick, J. A. & Zamore, P. D. MicroRNA therapeutics. *Gene Therapy* **18,** 1104–1110 (2011).
101. Ling, H., Fabbri, M. & Calin, G. A. MicroRNAs and other non-coding RNAs as targets for anticancer drug development. *Nat Rev Drug Discov* **12,** 847–865 (2013).
102. Godnic, I. *et al.* Genome-wide and species-wide in silico screening for intragenic MicroRNAs in human, mouse and chicken. *PLoS ONE* **8,** e65165 (2013).
103. Ramalingam, P. *et al.* Biogenesis of intronic miRNAs located in clusters by independent transcription and alternative splicing. *RNA* **20,** 76–87 (2014).
104. Lee, Y., Jeon, K., Lee, J.-T., Kim, S. & Kim, V. N. MicroRNA maturation: stepwise processing and subcellular localization. *EMBO J.* **21,** 4663–4670 (2002).
105. Lee, Y. *et al.* The nuclear RNase III Drosha initiates microRNA processing. *Nature* **425,** 415–419 (2003).
106. Gregory, R. I. *et al.* The Microprocessor complex mediates the genesis of microRNAs. *Nature* **432,** 235–240 (2004).
107. Filipowicz, W., Bhattacharyya, S. N. & Sonenberg, N. Mechanisms of post-transcriptional regulation by microRNAs: are the answers in sight? *Nat. Rev. Genet.* **9,** 102–114 (2008).
108. Han, J. *et al.* Molecular basis for the recognition of primary microRNAs by the Drosha-DGCR8 complex. *Cell* **125,** 887–901 (2006).
109. Ma, H., Wu, Y., Choi, J.-G. & Wu, H. Lower and upper stem-single-stranded RNA junctions together determine the Drosha cleavage site. *Proc. Natl. Acad. Sci. U.S.A.* **110,** 20687–20692 (2013).
110. Nguyen, T. A. *et al.* Functional Anatomy of the Human Microprocessor. *Cell* **161,** 1374–1387 (2015).
111. Alarcón, C. R., Lee, H., Goodarzi, H., Halberg, N. & Tavazoie, S. F. N6-methyladenosine marks primary microRNAs for processing. *Nature* **519,** 482–485 (2015).
112. Kim, V. N., Han, J. & Siomi, M. C. Biogenesis of small RNAs in animals. *Nat. Rev. Mol. Cell Biol.* **10,** 126–139 (2009).
113. Haase, A. D. *et al.* TRBP, a regulator of cellular PKR and HIV-1 virus expression, interacts with Dicer and functions in RNA silencing. *EMBO Rep.* **6,** 961–967 (2005).

114. Meijer, H. A., Smith, E. M. & Bushell, M. Regulation of miRNA strand selection: follow the leader? *Biochem. Soc. Trans.* **42,** 1135–1140 (2014).
115. Su, H., Trombly, M. I., Chen, J. & Wang, X. Essential and overlapping functions for mammalian Argonautes in microRNA silencing. *Genes Dev.* **23,** 304–317 (2009).
116. Kobayashi, H. & Tomari, Y. RISC assembly: Coordination between small RNAs and Argonaute proteins. *Biochim. Biophys. Acta* **1859,** 71–81 (2016).
117. Iwasaki, S. *et al.* Hsc70/Hsp90 chaperone machinery mediates ATP-dependent RISC loading of small RNA duplexes. *Mol. Cell* **39,** 292–299 (2010).
118. Pfaff, J. & Meister, G. Argonaute and GW182 proteins: an effective alliance in gene silencing. *Biochem. Soc. Trans.* **41,** 855–860 (2013).
119. Ameres, S. L., Martinez, J. & Schroeder, R. Molecular basis for target RNA recognition and cleavage by human RISC. *Cell* **130,** 101–112 (2007).
120. Valencia-Sanchez, M. A., Liu, J., Hannon, G. J. & Parker, R. Control of translation and mRNA degradation by miRNAs and siRNAs. *Genes Dev.* **20,** 515–524 (2006).
121. Meister, G. *et al.* Human Argonaute2 mediates RNA cleavage targeted by miRNAs and siRNAs. *Mol. Cell* **15,** 185–197 (2004).
122. Inada, T. & Makino, S. Novel roles of the multi-functional CCR4-NOT complex in post-transcriptional regulation. *Front Genet* **5,** 135 (2014).
123. Wilczynska, A. & Bushell, M. The complexity of miRNA-mediated repression. *Cell Death Differ.* **22,** 22–33 (2015).
124. Vasudevan, S., Tong, Y. & Steitz, J. A. Switching from repression to activation: microRNAs can up-regulate translation. *Science* **318,** 1931–1934 (2007).
125. Truesdell, S. S. *et al.* MicroRNA-mediated mRNA translation activation in quiescent cells and oocytes involves recruitment of a nuclear microRNP. *Sci Rep* **2,** 842 (2012).
126. Lewis, B. P., Burge, C. B. & Bartel, D. P. Conserved seed pairing, often flanked by adenosines, indicates that thousands of human genes are microRNA targets. *Cell* **120,** 15–20 (2005).
127. Agarwal, V., Bell, G. W., Nam, J.-W. & Bartel, D. P. Predicting effective microRNA target sites in mammalian mRNAs. *Elife* **4,** 101 (2015).
128. Schirle, N. T., Sheu-Gruttadauria, J. & MacRae, I. J. Structural basis for microRNA targeting. *Science* **346,** 608–613 (2014).
129. Bartel, D. P. MicroRNAs: target recognition and regulatory functions. *Cell* **136,** 215–233 (2009).
130. Zheng, H. *et al.* Advances in the techniques for the prediction of microRNA targets. *Int J Mol Sci* **14,** 8179–8187 (2013).
131. Grimson, A. *et al.* MicroRNA targeting specificity in mammals: determinants beyond seed pairing. *Mol. Cell* **27,** 91–105 (2007).
132. Griffiths-Jones, S., Grocock, R. J., van Dongen, S., Bateman, A. & Enright, A. J. miRBase: microRNA sequences, targets and gene nomenclature. *Nucleic Acids Res.* **34,** D140–4 (2006).
133. Griffiths-Jones, S., Hui, J. H. L., Marco, A. & Ronshaugen, M. MicroRNA evolution by arm switching. *EMBO Rep.* **12,** 172–177 (2011).
134. Guo, L. *et al.* Evolutionary and expression analysis of miR-#-5p and miR-#-3p at the miRNAs/isomiRs levels. *Biomed Res Int* **2015,** 168358–14 (2015).

135. Sempere, L. F. *et al.* Expression profiling of mammalian microRNAs uncovers a subset of brain-expressed microRNAs with possible roles in murine and human neuronal differentiation. **5,** R13 (2004).
136. Thiebes, K. P. *et al.* miR-218 is essential to establish motor neuron fate as a downstream effector of Isl1-Lhx3. *Nat Commun* **6,** 7718 (2015).
137. Goossens, K. *et al.* Regulatory microRNA network identification in bovine blastocyst development. *Stem Cells Dev.* **22,** 1907–1920 (2013).
138. Wang, Y. *et al.* miR-294/miR-302 promotes proliferation, suppresses G1-S restriction point, and inhibits ESC differentiation through separable mechanisms. *Cell Rep* **4,** 99–109 (2013).
139. Zhang, W.-B., Zhong, W.-J. & Wang, L. A signal-amplification circuit between miR-218 and Wnt/β-catenin signal promotes human adipose tissue-derived stem cells osteogenic differentiation. *Bone* **58,** 59–66 (2014).
140. van Wijnen, A. J. *et al.* MicroRNA functions in osteogenesis and dysfunctions in osteoporosis. *Curr Osteoporos Rep* **11,** 72–82 (2013).
141. Gay, I. *et al.* Differentiation of human dental stem cells reveals a role for microRNA-218. *J. Periodont. Res.* **49,** 110–120 (2014).
142. Blockus, H. & Chédotal, A. Slit-Robo signaling. *Development* **143,** 3037–3044 (2016).
143. Fish, J. E. *et al.* A Slit/miR-218/Robo regulatory loop is required during heart tube formation in zebrafish. *Development* **138,** 1409–1419 (2011).
144. Small, E. M., Sutherland, L. B., Rajagopalan, K. N., Wang, S. & Olson, E. N. MicroRNA-218 regulates vascular patterning by modulation of Slit-Robo signaling. *Circ. Res.* **107,** 1336–1344 (2010).
145. Gara, R. K. *et al.* Slit/Robo pathway: a promising therapeutic target for cancer. *Drug Discov. Today* **20,** 156–164 (2015).
146. Dallol, A. *et al.* Frequent epigenetic inactivation of the SLIT2 gene in gliomas. *Oncogene* **22,** 4611–4616 (2003).
147. Dickinson, R. E. *et al.* Epigenetic inactivation of SLIT3 and SLIT1 genes in human cancers. *Br. J. Cancer* **91,** 2071–2078 (2004).
148. Uesugi, A. *et al.* The tumor suppressive microRNA miR-218 targets the mTOR component Rictor and inhibits AKT phosphorylation in oral cancer. *Cancer Res.* **71,** 5765–5778 (2011).
149. Yang, M. *et al.* Epigenetic Repression of miR-218 Promotes Esophageal Carcinogenesis by Targeting ROBO1. *Int J Mol Sci* **16,** 27781–27795 (2015).
150. Lu, Y.-F., Zhang, L., Waye, M. M. Y., Fu, W.-M. & Zhang, J.-F. MiR-218 Mediates tumorigenesis and metastasis: Perspectives and implications. *Exp. Cell Res.* **334,** 173–182 (2015).
151. Cheng, Y. *et al.* MicroRNA-218 inhibits bladder cancer cell proliferation, migration, and invasion by targeting BMI-1. *Tumour Biol.* **36,** 8015–8023 (2015).
152. Wang, T. *et al.* MicroRNA-218 inhibits the proliferation and metastasis of esophageal squamous cell carcinoma cells by targeting BMI1. *Int. J. Mol. Med.* **36,** 93–102 (2015).
153. Jiang, Z. *et al.* MicroRNA-218 inhibits EMT, migration and invasion by targeting SFMBT1 and DCUN1D1 in cervical cancer. *Oncotarget* **7,** 45622–45636 (2016).
154. Tu, Y. *et al.* MicroRNA-218 inhibits glioma invasion, migration, proliferation, and cancer

stem-like cell self-renewal by targeting the polycomb group gene Bmi1. *Cancer Res.* **73,** 6046–6055 (2013).
155. Gao, X. & Jin, W. The emerging role of tumor-suppressive microRNA-218 in targeting glioblastoma stemness. *Cancer Lett.* **353,** 25–31 (2014).
156. Wu, Z. *et al.* MiR-218-5p inhibits the stem cell properties and invasive ability of the A2B5^{+}CD133^{-} subgroup of human glioma stem cells. *Oncol. Rep.* **35,** 869–877 (2016).
157. Hu, Y., Xu, K. & Yagüe, E. miR-218 targets survivin and regulates resistance to chemotherapeutics in breast cancer. *Breast Cancer Res. Treat.* **151,** 269–280 (2015).
158. Zhang, X.-L., Shi, H.-J., Wang, J.-P., Tang, H.-S. & Cui, S.-Z. MiR-218 inhibits multidrug resistance (MDR) of gastric cancer cells by targeting Hedgehog/smoothened. *Int J Clin Exp Pathol* **8,** 6397–6406 (2015).
159. He, X. *et al.* MiR-218 regulates cisplatin chemosensitivity in breast cancer by targeting BRCA1. *Tumour Biol.* **36,** 2065–2075 (2015).
160. Xu, P. *et al.* Variations of microRNAs in human placentas and plasma from preeclamptic pregnancy. *Hypertension* **63,** 1276–1284 (2014).
161. Liao, W.-X., Wing, D. A., Geng, J.-G. & Chen, D.-B. Perspectives of SLIT/ROBO signaling in placental angiogenesis. *Histol. Histopathol.* **25,** 1181–1190 (2010).
162. Li, P. *et al.* Role of Slit2/Robo1 in trophoblast invasion and vascular remodeling during ectopic tubal pregnancy. *Placenta* **36,** 1087–1094 (2015).
163. Liao, W.-X., Laurent, L. C., Agent, S., Hodges, J. & Chen, D.-B. Human placental expression of SLIT/ROBO signaling cues: effects of preeclampsia and hypoxia. *Biol. Reprod.* **86,** 111–111 (2012).
164. Moses, H. L., Roberts, A. B. & Derynck, R. The Discovery and Early Days of TGF-β: A Historical Perspective. *Cold Spring Harb Perspect Biol* **8,** a021865 (2008).
165. Heldin, C.-H. TGF-β Signaling from Receptors to Smads. *Cold Spring Harbor Monograph Archive* **50,** 259–285 (2008).
166. Koinuma, D. *et al.* Chromatin immunoprecipitation on microarray analysis of Smad2/3 binding sites reveals roles of ETS1 and TFAP2A in transforming growth factor beta signaling. *Mol. Cell. Biol.* **29,** 172–186 (2009).
167. Derynck, R. & Zhang, Y. E. Smad-dependent and Smad-independent pathways in TGF-beta family signalling. *Nature* **425,** 577–584 (2003).
168. Zhang, Y. E. Non-Smad pathways in TGF-β signaling. *Cell Res.* **19,** 128–139 (2009).
169. Derynck, R. & Miyazono, K. TGF-β and the TGF-β Family. *Cold Spring Harbor Monograph Archive* **50,** 29–43–405 (2008).
170. Katagiri, T., Suda, T. & Miyazono, K. The Bone Morphogenetic Proteins. *Cold Spring Harbor Monograph Archive* **50,** 121–149 (2008).
171. Brennan, J., Norris, D. P. & Robertson, E. J. Nodal activity in the node governs left-right asymmetry. *Genes Dev.* **16,** 2339–2344 (2002).
172. McPherron, A. C., Lawler, A. M. & Lee, S. J. Regulation of skeletal muscle mass in mice by a new TGF-beta superfamily member. *Nature* **387,** 83–90 (1997).
173. Visser, J. A., de Jong, F. H., Laven, J. S. E. & Themmen, A. P. N. Anti-Müllerian hormone: a new marker for ovarian function. *Reproduction* **131,** 1–9 (2006).
174. Wiater, E. & Vale, W. Activins and Inhibins. *Cold Spring Harbor Monograph Archive* **50,** 79–120 (2008).

175. Daopin, S., Piez, K. A., Ogawa, Y. & Davies, D. R. Crystal structure of transforming growth factor-b2: an unusual fold for the superfamily. *Science* **257,** 369–373 (1992).
176. Dabovic, B. & Rifkin, D. B. TGF-β Bioavailability: Latency, Targeting, and Activation. *Cold Spring Harbor Monograph Archive* **50,** 179–202 (2008).
177. De Crescenzo, G., Grothe, S., Zwaagstra, J., Tsang, M. & O'Connor-McCourt, M. D. Real-time monitoring of the interactions of transforming growth factor-beta (TGF-beta) isoforms with latency-associated protein and the ectodomains of the TGF-beta type II and III receptors reveals different kinetic models and stoichiometries of binding. *Journal of Biological Chemistry* **276,** 29632–29643 (2001).
178. Davis, M. R. & Summers, K. M. Structure and function of the mammalian fibrillin gene family: implications for human connective tissue diseases. *Mol. Genet. Metab.* **107,** 635–647 (2012).
179. Hyytiäinen, M., Penttinen, C. & Keski-Oja, J. Latent TGF-beta binding proteins: extracellular matrix association and roles in TGF-beta activation. *Crit Rev Clin Lab Sci* **41,** 233–264 (2004).
180. Wrana, J. L., Ozdamar, B., Le Roy, C. & Benchabane, H. Signaling Receptors of the TGF-β Family. *Cold Spring Harbor Monograph Archive* **50,** 151–177 (2008).
181. Yamashita, H., Dijke, Ten, P., Franzen, P., Miyazono, K. & Heldin, C. H. Formation of hetero-oligomeric complexes of type I and type II receptors for transforming growth factor-beta. *Journal of Biological Chemistry* **269,** 20172–20178 (1994).
182. Wrana, J. L., Attisano, L., Wieser, R., Ventura, F. & Massagué, J. Mechanism of activation of the TGF-beta receptor. *Nature* **370,** 341–347 (1994).
183. Wieser, R., Attisano, L., Wrana, J. L. & Massagué, J. Signaling activity of transforming growth factor beta type II receptors lacking specific domains in the cytoplasmic region. *Mol. Cell. Biol.* **13,** 7239–7247 (1993).
184. Chen, R.-H., Moses, H. L., Maruoka, E. M., Derynck, R. & Kawabata, M. Phosphorylation-dependent Interaction of the Cytoplasmic Domains of the Type I and Type II Transforming Growth Factor- Receptors. *Journal of Biological Chemistry* **270,** 12235–12241 (1995).
185. Feng, X. H. & Derynck, R. Ligand-independent activation of transforming growth factor (TGF) beta signaling pathways by heteromeric cytoplasmic domains of TGF-beta receptors. *Journal of Biological Chemistry* **271,** 13123–13129 (1996).
186. Attisano, L., Wrana, J. L., Montalvo, E. & Massagué, J. Activation of signalling by the activin receptor complex. *Mol. Cell. Biol.* **16,** 1066–1073 (1996).
187. Dyson, S. & Gurdon, J. B. The Interpretation of Position in a Morphogen Gradient as Revealed by Occupancy of Activin Receptors. *Cell* **93,** 557–568 (1998).
188. Chen, W., Fu, X. & Sheng, Z. Review of current progress in the structure and function of Smad proteins. *Chin Med J (Engl)* **115,** 446–450 (2002).
189. Dennler, S., Huet, S. & Gauthier, J. M. A short amino-acid sequence in MH1 domain is responsible for functional differences between Smad2 and Smad3. (1999).
190. Hata, A. & Chen, Y.-G. TGF-β Signaling from Receptors to Smads. *Cold Spring Harb Perspect Biol* **8,** a022061 (2016).
191. Mochizuki, T. *et al.* Roles for the MH2 domain of Smad7 in the specific inhibition of transforming growth factor-beta superfamily signaling. *Journal of Biological Chemistry*

279, 31568–31574 (2004).
192. WB, T., GH, L., L, S. & FY, L. Smad anchor for receptor activation (SARA) in TGF-beta signaling. *Front Biosci (Elite Ed)* **2,** 857–860 (2010).
193. Fink, S. P., Mikkola, D., Willson, J. K. V. & Markowitz, S. TGF-|[beta]|-induced nuclear localization of Smad2 and Smad3 in Smad4 null cancer cell lines. *Oncogene* **22,** 1317–1323 (2003).
194. Kurisaki, A., Kose, S., Yoneda, Y., Heldin, C. H. & Moustakas, A. Transforming growth factor-beta induces nuclear import of Smad3 in an importin-beta1 and Ran-dependent manner. *Mol. Biol. Cell* **12,** 1079–1091 (2001).
195. Shi, Y. & Massagué, J. Mechanisms of TGF-beta signaling from cell membrane to the nucleus. *Cell* **113,** 685–700 (2003).
196. Feng, X.-H. & Derynck, R. SPECIFICITY AND VERSATILITY IN TGF-β SIGNALING THROUGH SMADS. *http://dx.doi.org/10.1146/annurev.cellbio.21.022404.142018* **21,** 659–693 (2005).
197. Shi, Y. *et al.* Crystal structure of a Smad MH1 domain bound to DNA: insights on DNA binding in TGF-beta signaling. *Cell* **94,** 585–594 (1998).
198. Lin, X., Chen, Y.-G. & Feng, X.-H. Transcriptional Control via Smads. *Cold Spring Harbor Monograph Archive* **50,** 287–332 (2008).
199. Chang, C. Agonists and Antagonists of the TGF-β Family Ligands. *Cold Spring Harbor Monograph Archive* **50,** 203–257 (2008).
200. Nakamura, T. *et al.* Activin-binding protein from rat ovary is follistatin. *Science* **247,** 836–838 (1990).
201. Zimmerman, L. B., De Jesús-Escobar, J. M. & Harland, R. M. The Spemann Organizer Signal noggin Binds and Inactivates Bone Morphogenetic Protein 4. *Cell* **86,** 599–606 (1996).
202. Neill, T., Schaefer, L. & Iozzo, R. V. Decorin. *Am. J. Pathol.* **181,** 380–387 (2012).
203. Meno, C. *et al.* lefty-1 is required for left-right determination as a regulator of lefty-2 and nodal. *Cell* **94,** 287–297 (1998).
204. Chen, C. & Shen, M. M. Two Modes by which Lefty Proteins Inhibit Nodal Signaling. *Curr Biol* **14,** 618–624 (2004).
205. Rotzer, D. *et al.* Type III TGF-beta receptor-independent signalling of TGF-beta2 via TbetaRII-B, an alternatively spliced TGF-beta type II receptor. *EMBO J.* **20,** 480–490 (2001).
206. Lewis, K. A. *et al.* Betaglycan binds inhibin and can mediate functional antagonism of activin signalling. *Nature* **404,** 411–414 (2000).
207. Lastres, P. *et al.* Endoglin modulates cellular responses to TGF-beta 1. *The Journal of Cell Biology* **133,** 1109–1121 (1996).
208. Arthur, H. M. *et al.* Endoglin, an Ancillary TGFβ Receptor, Is Required for Extraembryonic Angiogenesis and Plays a Key Role in Heart Development. *Developmental Biology* **217,** 42–53 (2000).
209. Lebrin, F. *et al.* Endoglin promotes endothelial cell proliferation and TGF-beta/ALK1 signal transduction. *EMBO J.* **23,** 4018–4028 (2004).
210. Gray, P. C., Harrison, C. A. & Vale, W. Cripto forms a complex with activin and type II activin receptors and can block activin signaling. *PNAS* **100,** 5193–5198 (2003).

211. Di Guglielmo, G. M., Le Roy, C., Goodfellow, A. F. & Wrana, J. L. Distinct endocytic pathways regulate TGF-|[beta]| receptor signalling and turnover. *Nature Cell Biology* **5,** 410–421 (2003).
212. Chen, Y.-G. Endocytic regulation of TGF-|[beta]| signaling. *Cell Res.* **19,** 58–70 (2009).
213. Tsukazaki, T., Chiang, T. A., Davison, A. F., Attisano, L. & Wrana, J. L. SARA, a FYVE domain protein that recruits Smad2 to the TGFbeta receptor. *Cell* **95,** 779–791 (1998).
214. Jones, R. L. *et al.* Expression of activin receptors, follistatin and betaglycan by human endometrial stromal cells; consistent with a role for activins during decidualization. *Mol. Hum. Reprod.* **8,** 363–374 (2002).
215. Jones, R. L., Salamonsen, L. A. & Findlay, J. K. Activin A Promotes Human Endometrial Stromal Cell Decidualization in Vitro. *J. Clin. Endocrinol. Metab.* **87,** 4001–4004 (2002).
216. Peng, J. *et al.* Uterine activin receptor-like kinase 5 is crucial for blastocyst implantation and placental development. *Proc. Natl. Acad. Sci. U.S.A.* **112,** E5098–107 (2015).
217. Monsivais, D. *et al.* Uterine ALK3 is essential during the window of implantation. *Proc. Natl. Acad. Sci. U.S.A.* **113,** E387–95 (2016).
218. Golos, T. G., Giakoumopoulos, M. & Gerami-Naini, B. Review: Trophoblast differentiation from human embryonic stem cells. *Placenta* **34,** S56–S61 (2013).
219. Sarkar, P. *et al.* Activin/nodal signaling switches the terminal fate of human embryonic stem cell-derived trophoblasts. *J. Biol. Chem.* **290,** 8834–8848 (2015).
220. Caniggia, I., Lye, S. J. & Cross, J. C. Activin is a local regulator of human cytotrophoblast cell differentiation. *Endocrinology* **138,** 3976–3986 (1997).
221. Munir, S. *et al.* Nodal and ALK7 inhibit proliferation and induce apoptosis in human trophoblast cells. *Journal of Biological Chemistry* **279,** 31277–31286 (2004).
222. Graham, C. H., Lysiak, J. J., McCrae, K. R. & Lala, P. K. Localization of transforming growth factor-beta at the human fetal-maternal interface: role in trophoblast growth and differentiation. *Biol. Reprod.* **46,** 561–572 (1992).
223. Fu, G. *et al.* MicroRNA-376c impairs transforming growth factor-β and nodal signaling to promote trophoblast cell proliferation and invasion. *Hypertension* **61,** 864–872 (2013).
224. Song, Y., Keelan, J. & France, J. T. Activin-A stimulates, while transforming growth factor β1 inhibits,chorionic gonadotrophin production and aromatase activity in cultured human placental trophoblasts. **17,** 603–610 (1996).
225. Ni, X., Luo, S., Minegishi, T. & Peng, C. Activin A in JEG-3 cells: potential role as an autocrine regulator of steroidogenesis in humans. *Biol. Reprod.* **62,** 1224–1230 (2000).
226. Luo, S., Yu, H., Wu, D. & Peng, C. Transforming growth factor-beta1 inhibits steroidogenesis in human trophoblast cells. *Mol. Hum. Reprod.* **8,** 318–325 (2002).
227. MORRISH, D. W., BHARDWAJ, D. & PARAS, M. T. Transforming Growth Factor β1 Inhibits Placental Differentiation and Human Chorionic Gonadotropin and Human Placental Lactogen Secretion. *Endocrinology* **129,** 22–26 (2009).
228. Cheng, J.-C., Chang, H.-M., Fang, L., Sun, Y.-P. & Leung, P. C. K. TGF-β1 up-regulates connexin43 expression: a potential mechanism for human trophoblast cell differentiation. *J. Cell. Physiol.* **230,** 1558–1566 (2015).
229. Graham, C. H. & Lala, P. K. Mechanisms of placental invasion of the uterus and their control. *Biochem. Cell Biol.* **70,** 867–874 (1992).
230. Karmakar, S. & Das, C. Regulation of trophoblast invasion by IL-1beta and TGF-beta1.

Am. J. Reprod. Immunol. **48,** 210–219 (2002).
231. Lash, G. E. *et al.* Inhibition of trophoblast cell invasion by TGFB1, 2, and 3 is associated with a decrease in active proteases. *Biol. Reprod.* **73,** 374–381 (2005).
232. Zhao, M.-R. *et al.* Dual effect of transforming growth factor beta1 on cell adhesion and invasion in human placenta trophoblast cells. *Reproduction* **132,** 333–341 (2006).
233. Prossler, J., Chen, Q., Chamley, L. & James, J. L. The relationship between TGFβ, low oxygen and the outgrowth of extravillous trophoblasts from anchoring villi during the first trimester of pregnancy. *Cytokine* **68,** 9–15 (2014).
234. Yang, Q. *et al.* Smurf2 participates in human trophoblast cell invasion by inhibiting TGF-beta type I receptor. *J. Histochem. Cytochem.* **57,** 605–612 (2009).
235. Nadeem, L. *et al.* Nodal signals through activin receptor-like kinase 7 to inhibit trophoblast migration and invasion: implication in the pathogenesis of preeclampsia. *Am. J. Pathol.* **178,** 1177–1189 (2011).
236. Law, J., Zhang, G., Dragan, M., Postovit, L.-M. & Bhattacharya, M. Nodal signals via β-arrestins and RalGTPases to regulate trophoblast invasion. *Cell. Signal.* **26,** 1935–1942 (2014).
237. Li, Y., Klausen, C., Zhu, H. & Leung, P. C. K. Activin A Increases Human Trophoblast Invasion by Inducing SNAIL-Mediated MMP2 Up-Regulation Through ALK4. *J. Clin. Endocrinol. Metab.* **100,** E1415–27 (2015).
238. Li, Y., Klausen, C., Cheng, J.-C., Zhu, H. & Leung, P. C. K. Activin A, B, and AB increase human trophoblast cell invasion by up-regulating N-cadherin. *J. Clin. Endocrinol. Metab.* **99,** E2216–25 (2014).
239. Peiris, H. N. *et al.* Myostatin is localized in extravillous trophoblast and up-regulates migration. *J. Clin. Endocrinol. Metab.* **99,** E2288–97 (2014).
240. Li, Y., Zhu, H., Klausen, C., Peng, B. & Leung, P. C. K. Vascular Endothelial Growth Factor-A (VEGF-A) Mediates Activin A-Induced Human Trophoblast Endothelial-Like Tube Formation. *Endocrinology* **156,** 4257–4268 (2015).
241. Oujo, B., Perez-Barriocanal, F., Bernabeu, C. & Lopez-Novoa, J. M. Membrane and soluble forms of endoglin in preeclampsia. *Curr. Mol. Med.* **13,** 1345–1357 (2013).
242. Silver, H. M., Lambert-Messerlian, G. M., Star, J. A., Hogan, J. & Canick, J. A. Comparison of maternal serum total activin A and inhibin A in normal, preeclamptic, and nonproteinuric gestationally hypertensive pregnancies. *Am. J. Obstet. Gynecol.* **180,** 1131–1137 (1999).
243. Ong, C. Y. T., Liao, A. W., Munim, S., Spencer, K. & Nicolaides, K. H. First-trimester maternal serum activin A in pre-eclampsia and fetal growth restriction. *J. Matern. Fetal. Neonatal. Med.* **15,** 176–180 (2004).
244. Lim, R. *et al.* Activin and NADPH-oxidase in preeclampsia: insights from in vitro and murine studies. *Am. J. Obstet. Gynecol.* **212,** 86.e1–12 (2015).
245. Hobson, S. R. *et al.* Role of activin A in the pathogenesis of endothelial cell dysfunction in preeclampsia. *Pregnancy Hypertens* **6,** 130–133 (2016).
246. Yu, L. *et al.* High levels of activin A detected in preeclamptic placenta induce trophoblast cell apoptosis by promoting nodal signaling. *J. Clin. Endocrinol. Metab.* **97,** E1370–9 (2012).
247. Moses, E. K. *et al.* Objective prioritization of positional candidate genes at a quantitative

trait locus for pre-eclampsia on 2q22. *Mol. Hum. Reprod.* **12,** 505–512 (2006).
248. Roten, L. T. *et al.* Association between the candidate susceptibility gene ACVR2A on chromosome 2q22 and pre-eclampsia in a large Norwegian population-based study (the HUNT study). *Eur. J. Hum. Genet.* **17,** 250–257 (2009).
249. Thulluru, H. K., Michel, O. J., Oudejans, C. B. M. & van Dijk, M. ACVR2A promoter polymorphism rs1424954 in the Activin-A signaling pathway in trophoblasts. *Placenta* **36,** 345–349 (2015).
250. Li, X., Shen, L. & Tan, H. Polymorphisms and plasma level of transforming growth factor-Beta 1 and risk for preeclampsia: a systematic review. *PLoS ONE* **9,** e97230 (2014).
251. Deepthi, G. *et al.* TGFB1 Functional Gene Polymorphisms (C-509T and T869C) in the Maternal Susceptibility to Pre-eclampsia in South Indian Women. *Scand. J. Immunol.* **82,** 390–397 (2015).
252. Khani, M. *et al.* Transforming growth factor beta-1 (TGF-β1) gene single nucleotide polymorphisms (SNPs) and susceptibility to pre-eclampsia in Iranian women: A case-control study. *Pregnancy Hypertens* **5,** 267–272 (2015).
253. Djurovic, S. *et al.* Plasma concentrations of Lp(a) lipoprotein and TGF-β1 are altered in preeclampsia. *Clinical Genetics* **52,** 371–376 (1997).
254. Shaarawy, M., Meleigy, El, M. & Rasheed, K. Maternal serum transforming growth factor beta-2 in preeclampsia and eclampsia, a potential biomarker for the assessment of disease severity and fetal outcome. *J. Soc. Gynecol. Investig.* **8,** 27–31 (2001).
255. Caniggia, I., Grisaru-Gravnosky, S., Kuliszewsky, M., Post, M. & Lye, S. J. Inhibition of TGF-beta 3 restores the invasive capability of extravillous trophoblasts in preeclamptic pregnancies. *J. Clin. Invest.* **103,** 1641–1650 (1999).
256. Zhu, X.-M., Han, T., Sargent, I. L., Yin, G.-W. & Yao, Y.-Q. Differential expression profile of microRNAs in human placentas from preeclamptic pregnancies vs normal pregnancies. *Am. J. Obstet. Gynecol.* **200,** 661.e1–661.e7 (2009).
257. Ji, L. *et al.* Placental trophoblast cell differentiation: physiological regulation and pathological relevance to preeclampsia. *Mol. Aspects Med.* **34,** 981–1023 (2013).
258. Velicky, P., Knöfler, M. & Pollheimer, J. Function and control of human invasive trophoblast subtypes: Intrinsic vs. maternal control. *Cell Adh Migr* **10,** 154–162 (2015).
259. Brosens, I., Pijnenborg, R., Vercruysse, L. & Romero, R. The 'Great Obstetrical Syndromes' are associated with disorders of deep placentation. *Am. J. Obstet. Gynecol.* **204,** 193–201 (2011).
260. Wallis, A. B., Saftlas, A. F., Hsia, J. & Atrash, H. K. Secular trends in the rates of preeclampsia, eclampsia, and gestational hypertension, United States, 1987-2004. *Am. J. Hypertens.* **21,** 521–526 (2008).
261. Redman, C. W., Sargent, I. L. & Staff, A. C. IFPA Senior Award Lecture: making sense of pre-eclampsia - two placental causes of preeclampsia? *Placenta* **35 Suppl,** S20–5 (2014).
262. Jadli, A. *et al.* Promising prognostic markers of preeclampsia: new avenues in waiting. *Thromb. Res.* **136,** 189–195 (2015).
263. Chen, D.-B. & Wang, W. Human Placental MicroRNAs and Preeclampsia. *Biol. Reprod.* **88,** 130–130 (2013).
264. Doridot, L. P., Miralles, F. P., Barbaux, S. P. & Vaiman, D. P. Trophoblasts, invasion, and microRNA. *Front Genet* **4,** (2013).

265. Small, E. M., Sutherland, L. B., Rajagopalan, K. N., Wang, S. & Olson, E. N. MicroRNA-218 regulates vascular patterning by modulation of Slit-Robo signaling. *Circ. Res.* **107,** 1336–1344 (2010).
266. Chiavacci, E. *et al.* MicroRNA 218 mediates the effects of Tbx5a over-expression on zebrafish heart development. *PLoS ONE* **7,** e50536 (2012).
267. Amin, N. D. *et al.* Loss of motoneuron-specific microRNA-218 causes systemic neuromuscular failure. *Science* **350,** 1525–1529 (2015).
268. Kong, Y. *et al.* Slit-miR-218-Robo axis regulates retinal neovascularization. *Int. J. Mol. Med.* **37,** 1139–1145 (2016).
269. Liao, W.-X., Wing, D. A., Geng, J.-G. & Chen, D.-B. Perspectives of SLIT/ROBO signaling in placental angiogenesis. *Histol. Histopathol.* **25,** 1181–1190 (2010).
270. Liao, W.-X., Zhang, H.-H., Feng, L., Zheng, J. & Chen, D. Placental Expression of Slit/Robo Signaling: Implication in Angiogenesis and Preeclampsia. *Biol. Reprod.* **78,** 126–126 (2008).
271. Kim, M., Kim, J.-H., Baek, S.-J., Kim, S.-Y. & Kim, Y. S. Specific expression and methylation of SLIT1, SLIT2, SLIT3, and miR-218 in gastric cancer subtypes. *Int. J. Oncol.* **48,** 2497–2507 (2016).
272. Jiang, Z. *et al.* Serum microRNA-218 is a potential biomarker for esophageal cancer. *Cancer Biomark* **15,** 381–389 (2015).
273. Taheriazam, A. *et al.* Up-regulation of miR-130b expression level and down-regulation of miR-218 serve as potential biomarker in the early detection of human osteosarcoma. *Diagn Pathol* **10,** 184 (2015).
274. Cheng, M.-W., Wang, L.-L. & Hu, G.-Y. Expression of microRNA-218 and its clinicopathological and prognostic significance in human glioma cases. *Asian Pac. J. Cancer Prev.* **16,** 1839–1843 (2015).
275. Zhu, X.-M., Han, T., Sargent, I. L., Yin, G.-W. & Yao, Y.-Q. Differential expression profile of microRNAs in human placentas from preeclamptic pregnancies vs normal pregnancies. *Am. J. Obstet. Gynecol.* **200,** 661.e1–7 (2009).
276. Peng, C. The TGF-beta superfamily and its roles in the human ovary and placenta. *J Obstet Gynaecol Can* **25,** 834–844 (2003).
277. Nadeem, L. *et al.* Nodal signals through activin receptor-like kinase 7 to inhibit trophoblast migration and invasion: implication in the pathogenesis of preeclampsia. *Am. J. Pathol.* **178,** 1177–1189 (2011).
278. Luo, L. *et al.* MicroRNA-378a-5p promotes trophoblast cell survival, migration and invasion by targeting Nodal. *J. Cell. Sci.* **125,** 3124–3132 (2012).
279. Graham, C. H. *et al.* Establishment and characterization of first trimester human trophoblast cells with extended lifespan. *Exp. Cell Res.* **206,** 204–211 (1993).
280. Schneider, C. A., Rasband, W. S. & Eliceiri, K. W. NIH Image to ImageJ: 25 years of image analysis. *Nat. Methods* **9,** 671–675 (2012).
281. Baczyk, D. *et al.* Glial cell missing-1 transcription factor is required for the differentiation of the human trophoblast. *Cell Death Differ.* **16,** 719–727 (2009).
282. Dunk, C. *et al.* A novel in vitro model of trophoblast-mediated decidual blood vessel remodeling. *Lab. Invest.* **83,** 1821–1828 (2003).
283. Wu, D. *et al.* Smads in human trophoblast cells: expression, regulation and role in TGF-

beta-induced transcriptional activity. *Mol. Cell. Endocrinol.* **175,** 111–121 (2001).
284. Crampton, S. P., Davis, J. & Hughes, C. C. W. Isolation of human umbilical vein endothelial cells (HUVEC). *J Vis Exp* 183–e183 (2007). doi:10.3791/183
285. Meijering, E. *et al.* Design and validation of a tool for neurite tracing and analysis in fluorescence microscopy images. *Cytometry A* **58,** 167–176 (2004).
286. Tie, J. *et al.* MiR-218 inhibits invasion and metastasis of gastric cancer by targeting the Robo1 receptor. *PLoS Genet.* **6,** e1000879 (2010).
287. Zhou, Y., Damsky, C. H. & Fisher, S. J. Preeclampsia is associated with failure of human cytotrophoblasts to mimic a vascular adhesion phenotype. One cause of defective endovascular invasion in this syndrome? *J. Clin. Invest.* **99,** 2152–2164 (1997).
288. Zhou, Y. *et al.* Human cytotrophoblasts adopt a vascular phenotype as they differentiate. A strategy for successful endovascular invasion? *J. Clin. Invest.* **99,** 2139–2151 (1997).
289. Pijnenborg, R. *et al.* Placental bed spiral arteries in the hypertensive disorders of pregnancy. *Br J Obstet Gynaecol* **98,** 648–655 (1991).
290. Pijnenborg, R., Dixon, G., Robertson, W. B. & Brosens, I. Trophoblastic invasion of human decidua from 8 to 18 weeks of pregnancy. *Placenta* **1,** 3–19 (1980).
291. Kemp, B. *et al.* Invasive depth of extravillous trophoblast correlates with cellular phenotype: a comparison of intra- and extrauterine implantation sites. *Histochem. Cell Biol.* **117,** 401–414 (2002).
292. Kaverina, I. & Straube, A. Regulation of cell migration by dynamic microtubules. *Semin. Cell Dev. Biol.* **22,** 968–974 (2011).
293. Highet, A. R. *et al.* First trimester trophoblasts forming endothelial-like tubes in vitro emulate a 'blood vessel development' gene expression profile. *Gene Expression Patterns* (2016). doi:10.1016/j.gep.2016.05.001
294. Jovanović, M., Stefanoska, I., Radojcić, L. & Vićovac, L. Interleukin-8 (CXCL8) stimulates trophoblast cell migration and invasion by increasing levels of matrix metalloproteinase (MMP)2 and MMP9 and integrins alpha5 and beta1. *Reproduction* **139,** 789–798 (2010).
295. Lian, I. A. *et al.* Matrix metalloproteinase 1 in pre-eclampsia and fetal growth restriction: reduced gene expression in decidual tissue and protein expression in extravillous trophoblasts. *Placenta* **31,** 615–620 (2010).
296. Karmakar, S. & Das, C. Regulation of trophoblast invasion by IL-1beta and TGF-beta1. *Am. J. Reprod. Immunol.* **48,** 210–219 (2002).
297. Hess, A. P. *et al.* Decidual stromal cell response to paracrine signals from the trophoblast: amplification of immune and angiogenic modulators. *Biol. Reprod.* **76,** 102–117 (2007).
298. Jovanović Krivokuća, M. *et al.* Pharmacological inhibition of MIF interferes with trophoblast cell migration and invasiveness. *Placenta* **36,** 150–159 (2015).
299. Craven, C. M., Morgan, T. & Ward, K. Decidual spiral artery remodelling begins before cellular interaction with cytotrophoblasts. *Placenta* **19,** 241–252 (1998).
300. Harris, L. K. Review: Trophoblast-vascular cell interactions in early pregnancy: how to remodel a vessel. *Placenta* **31 Suppl,** S93–8 (2010).
301. Smith, S. D., Dunk, C. E., Aplin, J. D., Harris, L. K. & Jones, R. L. Evidence for immune cell involvement in decidual spiral arteriole remodeling in early human pregnancy. *Am. J.*

Pathol. **174,** 1959–1971 (2009).
302. Bulla, R. *et al.* VE-cadherin is a critical molecule for trophoblast-endothelial cell interaction in decidual spiral arteries. *Exp. Cell Res.* **303,** 101–113 (2005).
303. Matsumura, T., Wolff, K. & Petzelbauer, P. Endothelial cell tube formation depends on cadherin 5 and CD31 interactions with filamentous actin. *J. Immunol.* **158,** 3408–3416 (1997).
304. Kilari, S. *et al.* Endothelial cell-specific chemotaxis receptor (ECSCR) enhances vascular endothelial growth factor (VEGF) receptor-2/kinase insert domain receptor (KDR) activation and promotes proteolysis of internalized KDR. *J. Biol. Chem.* **288,** 10265–10274 (2013).
305. Kervancioglu Demirci, E., Salamonsen, L. A. & Gauster, M. The role of CX3CL1 in fetal-maternal interaction during human gestation. *Cell Adh Migr* **10,** 189–196 (2016).
306. Shirasuna, K. *et al.* AGEs and HMGB1 Increase Inflammatory Cytokine Production from Human Placental Cells, Resulting in an Enhancement of Monocyte Migration. *Am. J. Reprod. Immunol.* **75,** 557–568 (2016).
307. Chen, S.-U. *et al.* Lysophosphatidic acid up-regulates expression of growth-regulated oncogene-alpha, interleukin-8, and monocyte chemoattractant protein-1 in human first-trimester trophoblasts: possible roles in angiogenesis and immune regulation. *Endocrinology* **151,** 369–379 (2010).
308. Gibson, D. A., Greaves, E., Critchley, H. O. D. & Saunders, P. T. K. Estrogen-dependent regulation of human uterine natural killer cells promotes vascular remodelling via secretion of CCL2. *Hum. Reprod.* **30,** 1290–1301 (2015).
309. Huang, Y., Zhu, X.-Y., Du, M.-R. & Li, D.-J. Human trophoblasts recruited T lymphocytes and monocytes into decidua by secretion of chemokine CXCL16 and interaction with CXCR6 in the first-trimester pregnancy. *J. Immunol.* **180,** 2367–2375 (2008).
310. Irving, J. A. & Lala, P. K. Functional role of cell surface integrins on human trophoblast cell migration: regulation by TGF-beta, IGF-II, and IGFBP-1. *Exp. Cell Res.* **217,** 419–427 (1995).
311. Lash, G. E. *et al.* Inhibition of trophoblast cell invasion by TGFB1, 2, and 3 is associated with a decrease in active proteases. *Biol. Reprod.* **73,** 374–381 (2005).
312. Cheng, J.-C., Chang, H.-M. & Leung, P. C. K. Transforming growth factor-β1 inhibits trophoblast cell invasion by inducing Snail-mediated down-regulation of vascular endothelial-cadherin protein. *J. Biol. Chem.* **288,** 33181–33192 (2013).
313. Zhou, X. *et al.* The aberrantly expressed miR-193b-3p contributes to preeclampsia through regulating transforming growth factor-β signaling. *Sci Rep* **6,** 19910 (2016).
314. Zuo, Y. *et al.* Effects of transforming growth factor-β1 on the proliferation and invasion of the HTR-8/SVneo cell line. *Oncol Lett* **8,** 2187–2192 (2014).
315. Lin, H.-Y. *et al.* Involvement of SMAD4, but not of SMAD2, in transforming growth factor-beta1-induced trophoblast expression of matrix metalloproteinase-2. *Front. Biosci.* **11,** 637–646 (2006).
316. Li, Q. *et al.* Quantification of preeclampsia-related microRNAs in maternal serum. *Biomed Rep* **3,** 792–796 (2015).
317. Palmer, S. K. *et al.* Quantitative estimation of human uterine artery blood flow and pelvic blood flow redistribution in pregnancy. *Obstet Gynecol* **80,** 1000–1006 (1992).

318. Noris, M., Perico, N. & Remuzzi, G. Mechanisms of disease: Pre-eclampsia. *Nat Clin Pract Nephrol* **1,** 98–114– quiz 120 (2005).
319. Lyall, F. Mechanisms regulating cytotrophoblast invasion in normal pregnancy and pre-eclampsia. *Aust N Z J Obstet Gynaecol* **46,** 266–273 (2006).
320. Cerdeira, A. S. & Karumanchi, S. A. Angiogenic factors in preeclampsia and related disorders. *Cold Spring Harb Perspect Med* **2,** a006585–a006585 (2012).
321. Verlohren, S. *et al.* An automated method for the determination of the sFlt-1/PIGF ratio in the assessment of preeclampsia. *Am. J. Obstet. Gynecol.* **202,** 161.e1–161.e11 (2010).
322. Martin, E. *et al.* Epigenetics and Preeclampsia: Defining Functional Epimutations in the Preeclamptic Placenta Related to the TGF-β Pathway. *PLoS ONE* **10,** e0141294 (2015).
323. Shi, Y. *et al.* Crystal structure of a Smad MH1 domain bound to DNA: insights on DNA binding in TGF-beta signaling. *Cell* **94,** 585–594 (1998).
324. Heyer, J. *et al.* Postgastrulation Smad2-deficient embryos show defects in embryo turning and anterior morphogenesis. *Proc. Natl. Acad. Sci. U.S.A.* **96,** 12595–12600 (1999).
325. Waldrip, W. R., Bikoff, E. K., Hoodless, P. A., Wrana, J. L. & Robertson, E. J. Smad2 signaling in extraembryonic tissues determines anterior-posterior polarity of the early mouse embryo. *Cell* **92,** 797–808 (1998).
326. Tremblay, K. D., Hoodless, P. A., Bikoff, E. K. & Robertson, E. J. Formation of the definitive endoderm in mouse is a Smad2-dependent process. *Development* **127,** 3079–3090 (2000).
327. Zhu, Y., Richardson, J. A., Parada, L. F. & Graff, J. M. Smad3 mutant mice develop metastatic colorectal cancer. *Cell* **94,** 703–714 (1998).
328. Datto, M. B. *et al.* Targeted disruption of Smad3 reveals an essential role in transforming growth factor beta-mediated signal transduction. *Mol. Cell. Biol.* **19,** 2495–2504 (1999).
329. Yang, X. *et al.* Targeted disruption of SMAD3 results in impaired mucosal immunity and diminished T cell responsiveness to TGF-beta. *EMBO J.* **18,** 1280–1291 (1999).
330. Morrish, D. W., Dakour, J. & Li, H. Functional regulation of human trophoblast differentiation. *J. Reprod. Immunol.* **39,** 179–195 (1998).
331. Caniggia, I., Grisaru-Gravnosky, S., Kuliszewsky, M., Post, M. & Lye, S. J. Inhibition of TGF-β3 restores the invasive capability of extravillous trophoblasts in preeclamptic pregnancies. *J. Clin. Invest.* **103,** 1641–1650 (1999).
332. Xu, J. *et al.* Aberrant TGFβ Signaling Contributes to Altered Trophoblast Differentiation in Preeclampsia. *Endocrinology* **157,** 883–899 (2016).
333. Brown, K. A., Pietenpol, J. A. & Moses, H. L. A tale of two proteins: differential roles and regulation of Smad2 and Smad3 in TGF-beta signaling. *J. Cell. Biochem.* **101,** 9–33 (2007).
334. Kim, M.-S. *et al.* Differential Expression of Extracellular Matrix and Adhesion Molecules in Fetal-Origin Amniotic Epithelial Cells of Preeclamptic Pregnancy. *PLoS ONE* **11,** e0156038 (2016).
335. Jovanović, M., Stefanoska, I., Radojcić, L. & Vićovac, L. Interleukin-8 (CXCL8) stimulates trophoblast cell migration and invasion by increasing levels of matrix metalloproteinase (MMP)2 and MMP9 and integrins alpha5 and beta1. *Reproduction* **139,** 789–798 (2010).

336. Bulla, R. *et al.* VE-cadherin is a critical molecule for trophoblast-endothelial cell interaction in decidual spiral arteries. *Exp. Cell Res.* **303,** 101–113 (2005).
337. Kilari, S. *et al.* Endothelial cell-specific chemotaxis receptor (ECSCR) enhances vascular endothelial growth factor (VEGF) receptor-2/kinase insert domain receptor (KDR) activation and promotes proteolysis of internalized KDR. *J. Biol. Chem.* **288,** 10265–10274 (2013).
338. Piek, E. *et al.* Functional characterization of transforming growth factor beta signaling in Smad2- and Smad3-deficient fibroblasts. *Journal of Biological Chemistry* **276,** 19945–19953 (2001).
339. Liu, L. *et al.* Smad2 and Smad3 have differential sensitivity in relaying TGFβ signaling and inversely regulate early lineage specification. *Sci Rep* **6,** 21602 (2016).
340. García-Campmany, L. & Martí, E. The TGFbeta intracellular effector Smad3 regulates neuronal differentiation and cell fate specification in the developing spinal cord. *Development* **134,** 65–75 (2007).
341. Xuan, Y. H. *et al.* Expression of TGF-beta signaling proteins in normal placenta and gestational trophoblastic disease. *Histol. Histopathol.* **22,** 227–234 (2007).
342. Gordon, K. J. & Blobe, G. C. Role of transforming growth factor-beta superfamily signaling pathways in human disease. *Biochim. Biophys. Acta* **1782,** 197–228 (2008).
343. Jones, R. L., Stoikos, C., Findlay, J. K. & Salamonsen, L. A. TGF-beta superfamily expression and actions in the endometrium and placenta. *Reproduction* **132,** 217–232 (2006).
344. Schilling, B. & Yeh, J. Transforming growth factor-beta(1), -beta(2), -beta(3) and their type I and II receptors in human term placenta. *Gynecol. Obstet. Invest.* **50,** 19–23 (2000).
345. Mylonas, I. *et al.* Expression of inhibin/activin subunits alpha (-alpha), beta A (-beta (A)) and beta B (-beta (B)) in placental tissue of normal and intrauterine growth restricted (IUGR) pregnancies. *J. Mol. Histol.* **37,** 43–52 (2006).
346. Peng, J. *et al.* Uterine Activin-Like Kinase 4 Regulates Trophoblast Development During Mouse Placentation. *Molecular Endocrinology* **29,** 1684–1693 (2015).
347. Yakymovych, I. & Souchelnytskyi, S. in *Smad Signal Transduction* **5,** 235–252 (Springer Netherlands, 2006).
348. Liu, C. *et al.* Smads 2 and 3 are differentially activated by transforming growth factor-beta (TGF-beta) in quiescent and activated hepatic stellate cells. Constitutive nuclear localization of Smads in activated cells is TGF-beta-independent. *Journal of Biological Chemistry* **278,** 11721–11728 (2003).
349. Runyan, C. E., Schnaper, H. W. & Poncelet, A.-C. The role of internalization in transforming growth factor beta1-induced Smad2 association with Smad anchor for receptor activation (SARA) and Smad2-dependent signaling in human mesangial cells. *Journal of Biological Chemistry* **280,** 8300–8308 (2005).
350. Faresse, N. *et al.* Identification of PCTA, a TGIF antagonist that promotes PML function in TGF-beta signalling. *EMBO J.* **27,** 1804–1815 (2008).
351. Hocevar, B. A., Smine, A., Xu, X. X. & Howe, P. H. The adaptor molecule Disabled-2 links the transforming growth factor beta receptors to the Smad pathway. *EMBO J.* **20,** 2789–2801 (2001).

352. Davison, A. F. Characterization of the Smad anchor for receptor activation in TGFß signal transduction. (University of Toronto, 2000).
353. Liu, F. PCTA: a new player in TGF-beta signaling. *Sci Signal* **1,** pe49–pe49 (2008).
354. Lybbert, J. *et al.* Abundance of megalin and Dab2 is reduced in syncytiotrophoblast during placental malaria, which may contribute to low birth weight. *Sci Rep* **6,** 24508 (2016).
355. Schiffer, M. *et al.* Inhibitory smads and tgf-Beta signaling in glomerular cells. *J. Am. Soc. Nephrol.* **13,** 2657–2666 (2002).
356. Xu, G., Chakraborty, C. & Lala, P. K. Expression of TGF-beta signaling genes in the normal, premalignant, and malignant human trophoblast: loss of smad3 in choriocarcinoma cells. *Biochem. Biophys. Res. Commun.* **287,** 47–55 (2001).
357. Funaba, M., Zimmerman, C. M. & Mathews, L. S. Modulation of Smad2-mediated signaling by extracellular signal-regulated kinase. *Journal of Biological Chemistry* **277,** 41361–41368 (2002).
358. Kretzschmar, M., Doody, J., Timokhina, I. & Massagué, J. A mechanism of repression of TGFbeta/ Smad signaling by oncogenic Ras. *Genes Dev.* **13,** 804–816 (1999).
359. Conery, A. R. *et al.* Akt interacts directly with Smad3 to regulate the sensitivity to TGF-beta induced apoptosis. *Nature Cell Biology* **6,** 366–372 (2004).
360. Míguez, D. G., Gil-Guiñón, E., Pons, S. & Martí, E. Smad2 and Smad3 cooperate and antagonize simultaneously in vertebrate neurogenesis. *J. Cell. Sci.* **126,** 5335–5343 (2013).
361. Heikkinen, P. T. *et al.* Hypoxia-activated Smad3-specific dephosphorylation by PP2A. *J. Biol. Chem.* **285,** 3740–3749 (2010).
362. Nakagawa, T. *et al.* TGF-beta induces proangiogenic and antiangiogenic factors via parallel but distinct Smad pathways. *Kidney Int.* **66,** 605–613 (2004).
363. Xuan, Y. H. *et al.* Expression of TGF-beta signaling proteins in normal placenta and gestational trophoblastic disease. *Histol. Histopathol.* **22,** 227–234 (2007).
364. Schilling, B. & Yeh, J. Transforming Growth Factor-β1, -β2, -β3 and Their Type I and II Receptors in Human Term Placenta. *Gynecol. Obstet. Invest.* **50,** 19–23 (2000).
365. Getsios, S., Chen, G. T., Huang, D. T. & MacCalman, C. D. Regulated expression of cadherin-11 in human extravillous cytotrophoblasts undergoing aggregation and fusion in response to transforming growth factor beta 1. *J. Reprod. Fertil.* **114,** 357–363 (1998).
366. Zhou, H., Fu, G., Yu, H. & Peng, C. Transforming growth factor-beta inhibits aromatase gene transcription in human trophoblast cells via the Smad2 signaling pathway. *Reprod. Biol. Endocrinol.* **7,** 146 (2009).
367. Lawrence, T. The nuclear factor NF-kappaB pathway in inflammation. *Cold Spring Harb Perspect Biol* **1,** a001651–a001651 (2009).
368. Wang, S.-C. *et al.* Cyclosporine A promotes in vitro migration of human first-trimester trophoblasts via MAPK/ERK1/2-mediated NF-κB and Ca2+/calcineurin/NFAT signaling. *Placenta* **34,** 374–380 (2013).
369. Goto, M., Katayama, K.-I., Shirakawa, F. & Tanaka, I. INVOLVEMENT OF NF-κB p50/p65 HETERODIMER IN ACTIVATION OF THE HUMAN PRO-INTERLEUKIN-1β GENE AT TWO SUBREGIONS OF THE UPSTREAM ENHANCER ELEMENT. *Cytokine* **11,** 16–28 (1999).
370. Prutsch, N. *et al.* The role of interleukin-1β in human trophoblast motility. *Placenta* **33,**

696–703 (2012).
371. Guo, P., Zhang, S.-Z., He, H., Zhu, Y.-T. & Tseng, S. C. G. PTX3 controls activation of matrix metalloproteinase 1 and apoptosis in conjunctivochalasis fibroblasts. *Invest. Ophthalmol. Vis. Sci.* **53,** 3414–3423 (2012).
372. Kim, G.-Y. *et al.* Proinflammatory cytokine IL-1beta stimulates IL-8 synthesis in mast cells via a leukotriene B4 receptor 2-linked pathway, contributing to angiogenesis. *J. Immunol.* **184,** 3946–3954 (2010).
373. Streicher, K. L. *et al.* Activation of a nuclear factor kappaB/interleukin-1 positive feedback loop by amphiregulin in human breast cancer cells. *Mol. Cancer Res.* **5,** 847–861 (2007).
374. Arsura, M., Wu, M. & Sonenshein, G. E. TGFβ1 Inhibits NF-κB/Rel Activity Inducing Apoptosis of B Cells: Transcriptional Activation of IκBα. *Immunity* **5,** 31–40 (1996).
375. DiChiara, M. R. *et al.* Inhibition of E-selectin gene expression by transforming growth factor beta in endothelial cells involves coactivator integration of Smad and nuclear factor kappaB-mediated signals. *J. Exp. Med.* **192,** 695–704 (2000).

APPENDIX A: EXTENDED PROTOCOLS

Isolation of Primary Human Umbilical Vein Endothelial Cells (HUVEC)

Protocol modified from Davis, J., Crampton, S. P., Hughes, C. C. Isolation of Human Umbilical Vein Endothelial Cells (HUVEC). J. Vis. Exp. (3), e183, doi:10.3791/183 (2007).

Day 1

1. After cesarean delivery, if the placenta is not needed, sever the umbilical cord from the placenta with a fresh razor blade.
   N.B: If cord blood was banked ensure to ask the nurse to retrieve the umbilical cord that was removed during this procedure. Otherwise the cord remaining attached to the placenta may not be sufficient for the isolation procedure.

2. Transport the umbilical cord in a clean container or ziplock bag on ice and transfer to 4°C refrigerator for a minimum of 2 and a maximum of 4 days.
   N.B: For successful isolation the cord needs to be aged in order for the coagulation process to finish. Leaving for longer may result in a contamination due to bacterial growth.

Day 2

3. Take the umbilical cord out of the refrigerator and lay it down onto a clean diaper pad inside the cell culture hood.

4. With gauze dab off excess blood and make fresh cuts on both ends of the cord with sterile scissors or razor blade. You should see two arteries (protruding out) and one vein (largest opening).

5. Gently insert the 21g butterfly needle with sheath on (BD Vacutainer No. 367296) into the vein. If you feel any resistance, just twist the cord as you gently push the needle (with sheath on) until the wings of the butterfly needle are flush with the cord. At this point clasp the needle in place with a sterile hemostat.

6. Fill a 20mL syringe with Hank's Buffered Salt Solution (1X -Mg^{2+}, -Ca^{2+}, and 10,000 I.U./mL Penicillin, 10,000 (µg/mL) Streptomycin) and attach to the butterfly needle tubing. Gently push the fluid through the cord allowing it to pass out the open-end one drip at a time into a waste container filled with bleach.

7. Repeat the wash with an additional 20mL of HBSS. Before the last 5mL are pushed through, lay the cord down and clasp the open end of the cord closed with a second haemostat. Slowly fill the vein with the remaining HBSS to check for any leaks.

N.B: This is especially important if cord blood was banked. In the case of holes you need to locate them and see if they can be closed off with a third haemostat during the enzymatic step. If not, the cord will not be usable for the remainder of the protocol and can be discarded.

8. Remove the haemostat from the open end and slowly push the remaining HBSS into the waste collection container.

9. Place 10mL of sterile Dulbecco's Phosphate-Buffered Saline (1X +D-Glucose, + Sodium Pyruvate; GIBCO 14287) into a sterile 15mL falcon tube. Weigh out 10mg of Collagenase Type I (Worthington), then add it to the DPSB and invert until dissolved.

10. Once the 0.1% collagenase solution is fully dissolved, filter it with a syringe filter (0.22 micron) and warm in 37°C in water bath for 15min.

11. In a 1L glass beaker place ~500mL of DPBS, cover with aluminum foil, and place into 37°C water bath.

12. Take out a new 25mL syringe and remove the plunger. Attach 25mL syringe to the needle tubing and pour in the 10ml of collagenase and replace the plunger.

13. Slowly push the collagenase into the vein until you see the first amount exit the open end. This is to wash out the residual HBSS. Then quickly re-clamp the open end and fill with collagenase until there is moderate distention of vein.

14. Once the cord is filled with collagenase you want to gently massage it starting from left to right. Using the pads of three fingers apply moderate pressure to the cord. The pressure and motion is similar to that of rolling bread dough. Spend about 5-6 seconds on each portion of the cord. The pressure and length need to be strong/long enough to dislodge the HUVECs but not to get smooth muscle contamination.

15. After massaging incubate the cord (with hemostats, needle and syringe attached) in DPBS at 37°C for 15 min.
    N.B: Collagenase activity varies, therefore will need to optimize the incubation time (10min-20min) for each lot. Keep in mind the HUVEC readily proliferate so it is safer to incubate for shorter time than risk contamination of smooth muscle cells or fibroblasts.

16. After incubation, remove cord from DPBS. Place a 50mL falcon tube filled with 5mL of plating media in a rack. While holding the cord over the 50mL tube cut the end above the line of the bottom clamp creating a fresh cut. Push the remaining collagenase through the cord slowly, same as before with the HBSS.
17. Remove the syringe from the tubing. Place a fresh 25mL syringe filled with 20mL of HBSS and slowly push through the vein into the collection tube with the same pace as during the washing step.

N.B: In this step you are dislodging any HUVEC that didn't come out during the previous step.

18. Spin the collection tube at 1200 rpm for 5min (as with other cells).
    N.B: There will be a big pellet that appears to be made of red blood cells, debris, etc. After the HUVEC attach overnight all of these components will be washed off.

19. Aspirate the supernatant and resuspend in 10% FBS containing M199 media supplemented with 10,000 I.U./mL Penicillin, 10,000 (µg/mL) Streptomycin, and 50 µg/mL of Endothelial Cell Growth Supplement (ECGS; Corning 356006) on a 10cm cell culture dish. Incubate overnight at 37°C with 5% CO_2.
    N.B: Cells can be grown in 20% FBS containing media to speed up their initial recovery after isolation. Alternatively, the cells can be grown in Lonza Endothelial Cell Basal Media -2 + Bullet Kit (No.CC-3156) media. However, if you are testing the effect of certain molecules on their pro- or anti-angiogenic capacity, using a very rich media may confound your findings. In this case using the M199 media supplemented with ECGS is more appropriate.

Day 3

20. Aspirate the media from the attached cells, and wash several times with warmed 1x PBS. Replenish with fresh growth media and allow cells to proliferate until 80% confluent refreshing the media every 2 days.
    N.B: HUVEC will begin to senes after 10-15 passages. It is best to allow freshly isolated cells to grow in 10cm dish then split the one plate onto four additional 10cm plates (if cells are fast growing can split 1:6) and freeze them down for future use at the early passage. Cells can be frozen down as usual in 10% DMSO containing full growth media (ECGS not needed).

<u>Preparation of ECGS (Corning 356006)</u>

100mg ECGS
100mg Heparan Sulfate Salt

1. Dissolve in 20mL of serum free M199 media
2. Filter with 0.22 micron syringe filter
3. Store in 200ul aliquots in -80°C
4. Use 100ul of the 5mg/mL solution per 10mL of media.

First Trimester Human Placental Explant Culture

Protocol adapted from Dr. Lye Lab at Lunenfeld-TaneN.Baum Research Institute

Day 1

1. Thaw phenol red-free growth factor containing matrigel (BD Biosciences 354262) on ice. *N.B: Matrigel will polymerize at room temperature, ensure it is kept on ice at all times until needed.*

2. Place all placenta tissues for processing on ice. Each patient's placenta will be contained in a numbered 50mL falcon tube in PBS (without Ca^{++} and Mg^{++}). One placenta at a time, empty contents of falcon tube into a clean 10cm petri dish. Keep sample ID and gestation age in notes for future reference.

3. Clean fine tweezers and dissecting scissors with 70% Ethanol.

4. Under sterile conditions place the Millicell™ Culture Plate Inserts (Millipore; PICM01250) into a 24-well cell culture plate. One insert per villi tree will be needed. Pipette 200 µl of ice-cold matrigel into each insert ensuring to cover the whole bottom and not create any bubbles. Pipette 600 µl of DMEM/F12 Phenol-red free media around each insert. Let the matrigel polymerize at 37°C for 20 minutes.

5. Examine the tissue under a dissecting microscope (preferably in a sterile environment eg. Class II fume hood). Depending on gestation age, a healthy placenta will have these key features:
    i. Intact villi with little/no shredding and debris
    ii. 5-6 week placentas have shorter villi that lack elaborate vascularization. Many villi contain EVT columns, however overall tissue size is small.
    iii. 7-9 week placentas have longer villi that are progressively more vascularized. With advancing gestation EVT containing villi decrease and are often found in clusters of very bright and vascularized villi. The placenta will contain more floating villi than in younger tissues.
    iv. EVT containing villi will often have white fuzzy caps that consist of the trophoblast-derived matrix.

6. Once an EVT column containing villi is identified, carefully cut the villi tree at its base where it connects to the chorionic plate. Place the cut villi in fresh PBS on ice. *N.B: To ensure enough tissue will be successfully attached for experimental set up always process more tissue than needed.*

7. Process one villi at a time to ensure tissue does not dry out. Hold the base of the villi with tweezers while gently separating the villi tips from one another with a sterile needle. Very carefully loosen the matrix on the tip of the EVT columns.

N.B: Gently scratching the matrix will allow the EVT located beneath to grow out on to the matrigel. Completely removing the matrix can risk removing all EVT cells in the tip with them.

8. Transfer the prepared villi tri onto the polymerized matrigel. Pull the base of the villi tri (where it was cut) to one side and with a needle, ensuring not to damage the matrigel, spread out the remaining villi branches giving them each room to grow out on to the matrigel.

9. Once all villi are spaced out onto the matrigel-coated inserts, place the plate into a 37°C incubator at 3% O_2 and 5% CO_2 to allow the tissues to attach overnight.

Day 2

10. Cover each tissue gently with 200 µl pre-warmed, serum-free, phenol-red free DMEM/F12 media supplemented with Normacin (1:100).

11. Place the plate back into the 37°C incubator at 3% O_2 and 5% CO_2 to allow for the EVT columns to form sprouts.

Day 3

12. Under a bright field microscope check each villi tip for EVT sprouts. Transfer all inserts with villi that have successfully attached to the matrigel into a new 24-well plate. Place fresh media around each insert like before.
    N.B: if a villus tree has no successful sprouts formed it need to be excluded from experiment and discarded.

13. Depending on the speed of growth the tissues can be allowed to incubate another day prior to treatment.
    N.B: if we anticipate a promoting effect starting treatment with small outgrowths will allow for the induction of outgrowth in treatment group to be easily visualized. Alternatively, allowing EVT to grow up abundantly will make observing an inhibition of outgrowth more clear.

Day 4

14. With a 200 µl pipette carefully remove the media and replace with fresh media containing desired treatment (oligomers were used at 200 nM).

15. Using a camera attached to a dissecting microscope, take a 0h picture of each villi tree.

16. Place the plate back into the 37°C incubator at 3% O_2 and 5% CO_2 to allow for the EVT columns to grow out for 24h.

Day 5

17. Using the same microscope settings take a 24h picture of each villi tree.

18. If 48h time point id desired place the plate back into the 37°C incubator at 3% O_2 and 5% CO_2 to allow for the EVT columns to grow out for another 24h.

Day 6

19. Using the same microscope settings take a 48h picture of each villi tree.

20. Dispose of tissues in proper biohazard. Alternatively tissues can be fixed in 4% PFA for 1h and embedded for downstream histology procedure.
    N.B: Ensure to submerge the whole insert with the tissue into a well filled with fixative and not only fill the middle. This will ensure the matrigel doesn't curl during the dehydration process.

21. Area of EVT outgrowth is quantified using ImageJ by drawing around the EVT outgrowth at 0h and subtracting it from the area of EVT outgrowth at 24h or 48h.

Human First Trimester Extravillous Column Dissection

N.B: Early tissues (5-6 week) are primarily proliferative. For differentiation markers, ie. enEVT, later tissues respond better to treatment (7.5-9 weeks).

1. Empty the first trimester tissue into a 10cm petri dish containing PBS (without Ca^{++} and Mg^{++}).

2. Under the dissecting microscope locate and remove all villi trees that contain potential EVT columns (see First Trimester Human Placental Explant Culture protocol for more details) and place in new falcon tube with PBS.

3. One at a time, remove the tissue from PBS and hold the villus base with tweezers and touch the tips of the villi to the dry, inside lid of a 10cm dish. Essentially you want to let the tips of the villi stick to the surface of the dish and carefully with fine dissecting scissors trim those tips off. You should be left with very fine tissues on the lid and the majority of the villi tissue left over held by the tweezers. You can discard the large villi tree tissue and gently gather the fine tissues containing EVT columns into a pile on the dish cover. If you feel the trimmed tissue is drying up you can add a tiny drop (<10 µl) of PBS.
   N.B: This is one method of trimming the tissues. The goal is to enrich the tissues containing EVT cells, reducing the remaining tissue that is not of interest.

4. Once all of the villi have been trimmed (at least 25 villi per treatment group) you want to divide the trimmed tissues into equal groups depending on the number of treatments.

5. Place 500 µl pre-warmed serum-free DMEM/F12 media supplemented with ITS Liquid Media Supplement (1:100, I3146 SIGMA) and your treatment (oligomers were used at 200 nM) in a 24 well plate.

6. Transfer approximately equal amount of cut tissue into each treatment. Place the plate to incubate at 37°C, 3% O_2 and 5% CO_2 for 48h.

7. After 48h, carefully remove the conditioned media and place in freezing vials labeled with Tissue ID, gestation age, and treatment. Subsequently, collect the tissue into a separate labeled freezing vial.

8. Drop all vials into a thermos with liquid nitrogen to snap freeze and transfer tubes to dry ice for transportation or place in -80°C for future processing.

N.B: Tissues can be homogenized in either 1mL Trizol for RNA processing, or in 300-500 µl lysis buffer + protease and phosphatase inhibitors for protein work.

Human First Trimester Placenta-Decidua Explant Co-culture

Protocol modified from Dunk C, Petkovic L, Baczyk D, Rossant J, Winterhager E, Lye S. A novel in vitro model of trophoblast-mediated decidual blood vessel remodeling. Lab Invest. 2003 Dec;83(12):1821–8.

N.B: For highest success need to use tissues 9-10 weeks of gestation.

Day 1

1. Thaw phenol red-free growth factor containing matrigel (BD Biosciences 354262) on ice.
   N.B: Matrigel will polymerize at room temperature, ensure it is kept on ice at all times until needed.

2. Clean fine tweezers and dissecting scissors with 70% Ethanol.

3. Place all placenta and decidua tissues for processing on ice. Each patient's tissue will be contained in a numbered 50mL falcon tube in PBS (without Ca^{++} and Mg^{++}). One patient ID at a time, empty the decidua tissue into a clean 10cm petri dish. Keep sample ID and gestation age in notes for future reference. Examine the decidua to assess if usable, keeping in mind the following points:
   i. The tissue should feel thick, you can check by pressing gently down on the tissue with tweezers and checking if you can tap on the dish through it. Tissue should not be scrappy and be a minimum of 5mm thickness.
   ii. Ensure the tissue is intact by checking for the epithelial layer (will be smooth and shiny under the dissecting microscope).
   iii. Any large bloody vessels/clots may indicate this is decidua basalis (we want decidua parietalis) and should be avoided if possible. However, nice blood vessels along the surface are desired.

4. With dissecting scissors cut a minimum of 3 squares/rectangles of decidua tissue per treatment group. The tissue should be approximately 4-6 mm^3 with the epithelial layer on one side and a thick spongy decidua mesenchyme on the other.
   N.B: Keep in mind that an additional 3 squares of decidua are needed for the decidua-only control.

5. If the patient's decidua is usable next you need to examine the matched placental tissue. Empty the contents of the falcon tube on a clean 10cm dish. As for other EVT protocols, identify villi with intact EVT columns. A villus tree with several anchoring villi is preferred. Once identified, cut the villus tree off the chorionic plate and transfer it to a fresh falcon tube with PBS.

6. Under sterile conditions place the Millicell™ Culture Plate Inserts (Millipore; PICM01250) into a 24-well cell culture plate. One insert per decidua square-villi tree will be needed. Pipette 150 µl of ice-cold matrigel into each insert ensuring to cover the whole bottom

and not create any bubbles.

7. Before the matrigel can polymerize, transfer one cut decidua at a time into the matrigel. Ensure to place the tissue with the luminal epithelial side facing up at a 45° angle by resting it on one side of the insert. Pipette 600 µl of DMEM/F12 Phenol-red free media around each insert. Let the matrigel polymerize at 37°C for 20 minutes.

8. While waiting for the matrigel to set, prepare the treatments for the placental explants. Place 500 µl phenol-red free, serum-free DMEM/F12 media into a 24-well plate and add treatment (eg. 200 nM oligomers). To each treatment add three-four dissected placental explants with intact EVT columns. Place the plate in 37°C, 3% O_2 and 5% CO_2 for 24h.

9. After the matrigel has set, add 200 µl of phenol-red free, serum-free, DMEM/F12 media supplemented with Normacin (1:100), Estrodiol (0.3 ng/mL) and Progesterone (20ng/mL) on top of each decidua square. Return to 37°C, 3% O_2 and 5% CO_2 for 24h.

10. Aliquot some matrigel (100 µl per insert plus extra) into a 1.5 mL epitube to use on Day 3.

Day 2

11. Remove placental explants from treatments and wash three times in PBS or HBSS (without Ca^{++} and Mg^{++}) using fresh wash buffer for each wash.

12. Place on villus tree at a time onto a dish and gently separate the villi and scrape the fuzzy caps on the villi tips.
    N.B: A good way to check for EVT is if the villi sticks to the bottom of the 10cm dish when you gently shake the PBS around. This is due to EVT columns being very sticky.

13. Take the decidua tissues out of the incubator and carefully remove the media with a pipette.

14. Gently place one villi tree per decidua ensuring the villi tips are laying flat against the epithelial surface of the decidua. Adjust the tissue carefully with a needle tip if necessary.

15. Return the plate to 37°C, 3% O_2 and 5% CO_2 for another 24h.

Day 3

16. Place the small aliquot of matrigel on ice to thaw.

17. Remove the tissues from the incubator and at the base of each placental villus gently add 50-100 µl of matrigel. Return the tissues to 37°C for 10min.
    N.B: This step will secure the placenta to the decidua further, which is essential during the fixation and dehydration step as to not lose the tissue for downstream histology work.

18. Once matrigel is polymerized, to each insert add 200 µl of media as before (supplemented with Normacin, P4 and E2).

19. Return the plates to incubate at 37°C, 3% O_2 and 5% CO_2 for 3-6 days.
    N.B: This is Day 1 of spiral arteriole remodelling.

20. Once the incubation is done continue to Fixation, Dehydration, and Embedding of Tissues followed by H&E staining and IHC.

Fixation, Dehydration, Embedding, and Sectioning of Tissues

1. Gently remove the media from the well and insert using a low suction or pipette taking care not to disturb the tissues.

2. To each well add 1mL of freshly prepared 4% Paraformaldehyde (PFA) in PBS. Holding the plate on an angle, tip each insert using tweezers to allow for the PFA to flood the inside of the insert.

3. Fix the tissues for 1h at room temperature.

4. Remove the PFA slowly and replace with PBS. Repeat the wash three times to ensure all PFA residue is removed before continuing.
   N.B: If not able to continue to the embedding procedure, leave the tissue in the last PBS wash and keep in 4°C fridge for up to 3 days.

5. Prepare ethanol solutions diluting with distilled water: 100%, 95%, 90%, 80%, and 70%.

6. Remove the PBS from each well and replace with 1mL of stock ethanol submerging the insert to fill the inside as before. Start with 70% ethanol for 15min (increase to 20min if tissue is bigger >5mm^3).

7. Repeat the dehydration with 80%, 90%, 95%, and 3x 100%.

8. During the dehydration process label the embedding cassettes with pencil. Each treatment n=3 or 4 will be embedded in one block ie. one cassette per treatment. Label the tissue ID and treatment on the bottom of each cassette (yellow cassettes are a good size for co-culture, Fisher Tissue Path Cassettes IV).

9. Prepare a 500mL-1L beaker with Xylene (cover with aluminum foil if not working in fume hood) filled enough to accommodate all of the cassettes that will be cleared.

10. One treatment at a time, take all the inserts and place them into a 10cm dish filled with 100% ethanol. Holding the insert with one hand score the backside of the insert with a razor without cutting the matrigel. With fine tip tweezers remove the insert membrane from the underside of the matrigel. Next, gently push the edges of the matrigel from the underside and guide the matrigel disk (wish tissue) to the top of the insert and remove it from the insert. Place the matrigel/tissue disk into the ethanol-containing dish until the remaining inserts are processed for that treatment.

11. Transfer all the matrigel/tissues removed from the inserts into the appropriately labeled cassette (one cassette per treatment group). Leave the cassette laying in the ethanol dish while you process the remaining treatment groups in the same fashion.

12. Once all groups have been processed, transfer all of the cassettes containing tissues into the xylene at the same time. Clear the tissues for 20min.

13. Drain the cassettes from xylene and transfer to the first paraffin wax beaker in a 60°C oven for 30 min.

14. Transfer the cassettes from the first wax beaker to the second for another 20 min.

15. Again, transfer the cassettes from the second wax beaker to the third for another 20 min.

16. Submerge the metal trays for embedding into the wax reservoir of the embedding machine.

17. Transfer all of the cassettes from the third beaker to the embedding station wax reservoir once ready for embedding.

18. Embed one cassette at a time. Take one metal embedding tray from the wax reservoir and place on the hot plate of embedding station and pour in some wax from the spout. Remove one cassette from the wax reservoir and open it. Evenly space out all of the tissues in the wax-filled metal tray with the tissue facing up and matrigel touching the bottom of the metal tray. Quickly transfer the metal tray to a cool portion of the embedding station and with tweezers press down the tissues while the wax starts to cool. Then quickly return the metal tray under the wax spout and place the bottom part of the cassette (with the label) on top of the wax tray and pour more wax on top. Transfer everything to the cooling table of the embedding station.

19. Once the wax has fully cooled, remove the wax block from the metal embedding tray. Store the blocks at room temperature until ready for sectioning.

20. To section tissue place the block into the microtome and align the blade.

21. Label positively charged slides with tissue ID, treatment, and slide number. Depending on depth of tissue you will need roughly 40-60 slides per block.

22. Trim the block until you begin to cut into tissue and then reduce the thickness to 5 µm.
23. Cut strips of tissue and check every 10^{th} section under the light microscope to catch when you have started cutting across the placenta.
    N.B: The decidua portion will be visible much sooner than the placenta since it was embedded into the matrigel while the placenta lays on top of the matrigel.

24. Once you have reached a portion of the tissue where both the decidua and placenta are visible begin to collect the tissues. Cut tissue into strips long enough for you to handle.
    N.B: It is important that serial sections be preserved so do not handle long strips that can

result in losing large portions of the tissue.

25. Transfer the strip carefully to a warm water bath ensuring you don't form any bubbles or folds in the tissue.

26. Using flat tipped tweezers separate the tissue sections into two-three section pieces (depending on how many can fit on a slide).

27. Dip the labelled slide into the water bath and place under the floating section. Align the first section with the top of the slide, allow it to come into contact with the wax section, and slowly pull the slide out of the water bath at a 45° angle as the section lays across the slide.

28. Place the slide upright to allow to dry and repeat this process with all of the remaining tissue. You want to stop cutting when you feel that the region where the placenta is in contact with the decidua (where we would observe remodelling of vessels) is out of view.
N.B: Ensure to not mess up the order of the sections. Serial sections are vital to successfully investigating a region of the remodelling process after a part is selected for Immunohistochemistry.

Haematoxylin and Eosin Staining of Paraffin Embedded Tissue

Protocol adapted from Dr. Lye Lab at Lunenfeld-TaneN.Baum Research Institute

1. After sectioned tissues have fully dried select several slides for H&E staining to decide on which slides should be used for IHC (1st, 10th etc, last).

2. Dewax in consecutive Xylene (Leica Surgipath 3803665) solutions for 5min/each
    - 1st xylene = most wax
    - 3rd xylene = least wax

3. Clear the Xylene in three solutions of 100% Ethanol 1min/each
    - 1st EtOH= most Xylene
    - 3rd EtOH=least Xylene

4. Rehydrate the tissue by submerging the slides in a series of EtOH solutions for 30s/each starting with
    - 95%, 90%, 80%, 70%, 50% (diluted in tap water)

5. Wash sections in tap water for 2min

6. Stain in Harris Haematoxylin (Sigma HH532) for 2min (return to bottle, can reuse stain)

7. Dip 5 times in Acid Alcohol (recipe below) → dispose in Ethanol waste

8. Wash slides in tap water until they run clear (at least 3min)

9. Stain slides in Eosin (Sigma HT110316) for 1min 20sec (return to bottle, can reuse stain)

10. Wash in tap water until runs clear (at least 3min)

11. Dehydrate slides for 5s/each in ethanol
    - 90%, 95%, 100% Ethanol 2, 100% Ethanol 1 (1min)

12. Clear in Xylene for 1min/each
    - Xylene 2nd
    - Xylene 3rd

13. Mount slides with coverslip straight from Xylene (don't let them dry out). Place two small dabs of Paramount onto cover slip and place slide with tissue down on top. Let dry overnight before handling.

Immunohistochemistry of Paraffin Embedded Tissues

Protocol adapted from Dr. Lye Lab at Lunenfeld-TaneN.Baum Research Institute

Day 1

1. After looking at the H&E stained slides the corresponding tissue of interest in the surrounding area is placed in a rack and baked overnight at 60°C.

2. Deparaffinization in Xylene for 5min/each
    - Xylene 1 = most wax
    - Xylene 3 = least wax

3. Rehydration for 2min/each ethanol
    - 100% EtOH 1, 100% EtOH 2, 100% EtOH 3, 95%

4. Quench endogenous peroxidase activity in 3% Hydorgen Peroxide solution in Methanol (30% solution diluted 1:10 in methanol. 25ml H_2O_2 + 225 MeOH). Normally for 30min *modified to 50 min with decidua.
   N.B. H_2O_2 should be stored at -20°C, it goes off at room temp or 4°C. If slides (including negative control) turn brown, buy a new bottle.

5. Continue Rehydration for 2min/each ethanol
    - 90%, 80%, 70%

6. Wash in 1X PBS two times, 5min/each

7. Fix slides in 4% PFA (in PBS) for 15min

8. Wash in 1X PBS two times, 5min/each

9. Antigen retrieval will depend on antibody – for these antibodies use Sodium citrate boiling

    i. Triton 0.01-0.02% in PBS 10min at room temperature. This will permeabilise the cell membrane to allow the Ab to go in.
    ii. Trypsin (50ul of 5%Trypsin in 1.9ml PBS pH7.4) at 37°C for 10min
    iii. Proteinase K (5-40ug/ml in PBS at 37°C for 10min)
    iv. Microwave pretreatment, 10mM sodium citrate: bring to a boil (5 min, power 6, lid on) cool for 20min, boil again (3 min, power 6, lid off), cool for 15min. Solutions A and B in 4°C
        - Solution A: Citric Acid 4.5ml in 250ml of water
        - Solution B: Sodium Citrate 20.5ml in 250ml of water

10. Wash in 1X PBS two times, 5min/each

11. One by one, take slide out of PBS, make circle around each tissue with IHC pen and add one drop of blocking buffer- 10% Goat Serum 2% Rabbit serum (Dako X0909) for 1h at RT in a covered humidified tray.

12. Place 1°Ab (50ul in PBS) at a time by vacuum suctioning off the blocking buffer and replacing as follows:
    - CK7 (Dako M7018) 1:100
    - CD31 (Dako M0823) 1:50
    - SMA (Dako M0851) 1:100
    - CD45 (Dako M0701) 1:100
    - HLAG (ExBio 11-499) 1:500 *modified to 1:300
    - Ki67 1:100
    - Cleaved Caspase 3 1:300
    - Mouse IGG (X0931) 1:100

13. Incubate overnight in 4°C cold room in a closer humidified box.

Day 2

14. Wash in 1X PBS two times, 5min/each

15. Add Secondary Antibody (1:300 in PBS) for 1hour at RT in a covered humidified tray.
    - Polyclonal Rabbit anti Mouse Biotinylated Ref:E0464

16. Wash in 1X PBS two times, 5min/each

17. Add tertiary reagent Invitrogen Streptavidin HRPO Conjugated (SA1007) 1:2000 PBS for 1h at room temperature.

18. Wash in 1X PBS two times, 5min/each

19. Add DAB (DiAminoBenzidene) and observe for precipitate formation on a white piece of paper. Double check under the light microscope for appropriate signal intensity and once reached place slides in new rack in distilled water.
    - DAB + Substrate Ref K3468
    - 2ml Buffer + 1 drop substrate * modified to 3ml Buffer + 1 drop substrate to try and remove the unspecific glandular stain
    - Use only for specific antibodies

20. Counter stain with Haematoxylin diluted Harris 1:2 with tap water for 15s

21. Rinse slides in tap water until runs clear.

22. Dehydrate the tissue for 2min each in Ethanol
    - 70%, 80%, 90%, 95%, 100% – Ethanol 2, 100% - Ethanol 3

23. Clear in xylene for 2 min each
    - Xylene 2
    - Xylene 3

    N.B. If there is a lot of wax pen left, prolong the xylene.

24. Mount slides with coverslips using Peramount, let dry in hood overnight.

25. Image slides on a bright field microscope.

APPENDIX B: ADDITIONAL PUBLICATIONS

1. Cytoplasmic mislocalization of p27 and CDK2 mediates the anti-migratory and anti-proliferative effects of Nodal in human trophoblast cells.

Nadeem L, **Brkic J**, Chen YF, Bui T, Munir S, Peng C.

Journal of Cell Science 2013 Jan 15;126(Pt 2):445-53.

I contributed to this paper during the revision processes. I performed experiments that addressed several reviewer questions. First, I performed the qRT-PCR to measure p27 mRNA levels after Nodal treatment (Figure 1A). Additionally, I addressed the concerns of establishing a causal link between Nodal, stathmin inactivation, and inhibition of cell migration. I performed many experiments to characterize the effects of Stathmin siRNA, HDAC6, and Nocadazol on microtubule acetylation and trophoblast migration. These findings were not included into the final manuscript, and instead I used them in writing a response to the reviewers concerns.

2. MicroRNAs in Human Placental Development and Pregnancy Complications.

Fu G, **Brkić J**, Hayder H, Peng C.

International Journal of Molecular Sciences 2013 Mar 8;14(3):5519-44.

I contributed to this review by writing section 2 (Key Processes in Human Placenta Development) and section 4.3 (MicroRNAs and Placental Angiogenesis). I also created Figure 1 used, and in the editing the final draft for submission.

3. Placental trophoblast cell differentiation: physiological regulation and pathological relevance to preeclampsia.

Ji L*, **Brkić J***, Liu M*, Fu G, Peng C, Wang YL.

* Contributed equally

Molecular Aspects of Medicine 2013 Oct;34(5):981-1023.

I contributed to this special edition review by writing section 1 (Introduction) and Section 2 (Pathways of Human Placental Trophoblast Cell Differentiation). I also contributed information used in generating Figure 1. I was closely involved in editing the review to the final version. In addition, I addressed the requested revisions and drafted the response to reviewers.

4. Activated NK cells cause placental dysfunction and miscarriages in fetal alloimmune thrombocytopenia

Issaka Yougbaré, Wei-She Tai, Darko Zdravic, Brigitta Elaine Oswald, Sean Lang, Guangheng Zhu, Howard Leong-Poi, Qu Dawei, Yu Lisa, Caroline Dunk, Jianhong Zhang, John G. Sled, Stephen J. Lye, **Jelena Brkić**, Chun Peng, Petter Höglund, Anne Croy, S. Lee Adamson, Duncan J. Stewart, John Freedman, and Heyu Ni

Currently submitted to Nature Medicine for review

I contributed to this manuscript by validating the effect of Integrin β3 antibodies on trophoblast migration and invasion. I used sera from immunized mice provided by Yougbaré on transwell migration and invasion assays with human first trimester trophoblast cell line, HTR8/SVneo. Additionally, I used these sera in the human first trimester EVT outgrowth model. Furthermore, I processed these EVT outgrowths for sectioning and provided first trimester tissues processed for protein and RNA work.